The University of Nottingham

UNITED KINGDOM · CHINA · MALAYSIA

UNIVERSITY OF BIRMINGHAM

Molecular investigation of *Bdellovibrio bacteriovorus* envelope processes associated with bacterial predation

A thesis submitted by

Emma J. Banks

As part of the requirement for the degree of:

MRes. Antimicrobials and Antimicrobial Resistance (AAMR)

This research was carried out under the supervision of Professor Liz Sockett & Dr Andrew Lovering

Supported by wellcome trust

Date: 25.7.18
Word count: 24,367

Abstract

Antibiotics have been used to treat bacterial infections for nearly 80 years, however, the increasing emergence of antibiotic-resistant bacteria has now led to a significant global burden of antimicrobial resistance (AMR) and a worldwide healthcare crisis. Combatting AMR requires the complementary development of novel therapeutics. *Bdellovibrio bacteriovorus* is a small predatory bacterium that invades Gram-negative prey, replicates within the periplasm and then lyses the host cell. This predatory ability presents *B. bacteriovorus* as a potential novel antimicrobial therapeutic. In this thesis, I describe two short research projects which investigate the predatory envelope processes of gliding motility and cell wall-modification in *B. bacteriovorus*.

B. bacteriovorus uses gliding motility on surfaces to both scout for prey and to ultimately facilitate exit from the dead host. Cyclic-di-GMP (c-di-GMP) positively regulates gliding motility in *B. bacteriovorus* and c-di-GMP signals are transduced through PilZ domains of receptor proteins. Some *B. bacteriovorus* PilZ proteins contain an additional putative GYF domain. We hypothesised that PilZ: GYF hybrid proteins may bind c-di-GMP (via the PilZ domain) and interact with the gliding motor (via the GYF domain) to regulate gliding motility. We aimed to test this hypothesis by crystallising the PilZ: GYF protein Bd1996. Bd1996 homologues from two different *B. bacteriovorus* strains were successfully expressed and purified. Bd1996 bound c-di-GMP *in vitro*, however, neither protein homologue could be crystallised.

Modification of predator and prey cell walls is an important predatory process that involves a repertoire of different enzymes. In my second project, I investigated the function of the two cell wall-modifying enzymes Bd1402 and Bd1075. Bd1402 was secreted into the periplasm of the prey in which it may modify the prey cell wall. In contrast, Bd1075 localised to the *B. bacteriovorus* predator itself and an unmarked deletion of *bd1075* resulted in the formation of predator cells that were straight rods, in comparison to vibroid wild-type cells. Together, these data suggest that Bd1075 is the curvature-determinant of *B. bacteriovorus* HD100.

Acknowledgements

I would firstly like to thank everyone in the Lovering lab at the University of Birmingham, particularly Mr Christopher Harding and Dr Ian Cadby for their guidance and training. I must also thank my fantastic supervisor, Dr Andy Lovering, for introducing a newcomer to the world of structural biology with such enthusiasm.

I'd also like to thank all the members of the Sockett group at the University of Nottingham for being so lovely and welcoming. Special thanks go out to Dr Carey Lambert and Mr Paul Radford for their teaching and advice throughout my project. I'd especially like to thank Prof Liz Sockett for her excellent supervision and inspiring me both professionally and personally.

I feel incredibly fortunate to have had the opportunity to work in two great collaborating groups and thank both universities for hosting me during my rotation projects and the Wellcome Trust for funding me on this 4-year AAMR doctoral training programme.

List of abbreviations

AMR	Antimicrobial resistance or antimicrobial-resistant
AP	Attack-phase
bp	Base pair
Cyclic-di-GMP	Bis-(3´-5´)-cyclic dimeric guanosine monophosphate
CPase	Carboxypeptidase
EPase	Endopeptidase
DNA	Deoxyribonucleic acid
dNTPs	Deoxynucleotide triphosphates
EDTA	Ethylenediaminetetraacetic acid
EPS	Exopolysaccharide
ESBL	Extended-spectrum β-lactamase
FDA	Food and Drug Administration
gDNA	Genomic DNA
GTase	Glycosyltransferase
HEPES	N-(2-Hydroxyethyl) piperazine-N'-(2-ethanesulphonic acid)
HD	Host-dependent
HI	Host-independent
IM	Inner membrane
IPTG	Isopropyl-β-D-thiogalactopyranoside
Kan	Kanamycin
Kb	Kilobase, 1,000 base pairs
kDa	Kilodalton
KO	knockout
LDTP	L,D-transpeptidase
LPS	Lipopolysaccharide
Mb	Megabase, 1,000,000 base pairs
mCherry	Monomeric cherry fluorescent protein
m-DAP	*meso*-diaminopimelic acid
MDR	Multi-drug-resistant
NAG	N-acetyl-glucosamine
NAM	N-acetyl-muramic acid
NEB	New England Biolabs
OM	Outer membrane
PBP	Penicillin-binding-protein
PCR	Polymerase chain reaction
PDB	Protein Data Bank
Pfam	Protein Families Database
PG	Peptidoglycan
RNA	Ribonucleic acid
rRNA	Ribosomal RNA
RT-PCR	Reverse-transcriptase polymerase chain reaction
SDS	Sodium dodecyl sulphate
SDS-PAGE	Sodium dodecyl sulphate polyacrylamide gel electrophoresis
TPase	Transpeptidase
UV	Ultraviolet
WHO	World Health Organisation
WT	Wild type
XDR	Extensively drug-resistant
X-gal	5-bromo-4-chloro-3-indolyl-β-D-galactopyranoside

List of tables and figures

Table of Contents

CHAPTER 1: Introduction

1. Introduction to antimicrobial resistance

1.1 The antibiotic era

Antimicrobial discovery began in the early 20th century with the development of chemicals which contained antimicrobial properties. These chemicals included Salvarsan, which was used to treat the aetiological agent of syphilis, *Treponema pallidum*, and sulphonamides which were active against a wide range of bacteria (Jansen *et al.*, 2018). Antibiotics were originally defined as antibacterial substances that are produced by a microorganism, therefore the first 'true' antibiotic to be discovered was penicillin (Waksman, 1947). Penicillin was used to treat bacterial wound infections in the 1940s to widespread success, and in the following decades, numerous antibiotics were discovered, marking a golden era of antibiotic development (Lobanovska and Pilla, 2017). Over 20 classes of antibiotic have been discovered, each with a particular mechanism of action that targets a cellular process critical to bacterial viability (Figure 1A). Mechanisms that target cellular structural integrity include the inhibition of cell wall synthesis by β-lactam antibiotics such as penicillin, and disruption of the cytoplasmic membrane by polymyxins (Bush, 2012). These antibiotics are described as bactericidal as their action directly results in bacterial cell lysis. Antibiotics can alternatively inhibit bacterial protein synthesis by targeting 50S (macrolides, chloramphenicol) or 30S (tetracyclines, kanamycin) ribosomal subunits, preventing translation of bacterial proteins (Poehlsgaard and Douthwaite, 2005). Additional cellular targets include DNA replication/transcription (via the inhibition of DNA gyrase by fluoroquinolones (Collin *et al.*, 2011)), and folic acid metabolism (inhibited by sulphonamides and trimethoprim (Bourne, 2014; Collin *et al.*, 2011)). Antibiotics that limit protein synthesis or metabolism are generally said to be bacteriostatic as their action results in cellular growth arrest instead of lysis. Despite the existence of a wide range of commercially available antibiotics, by the late 1980s, research had entered a 'discovery void' and very few new classes of antibiotic have since been identified, despite an urgent

demand for discovery due to the rise of antimicrobial resistance.

1.2 Antimicrobial resistance

1.2.1. An overview of antimicrobial resistance

Antimicrobial resistance (AMR) is a naturally occurring phenomenon which has been observed since the discovery and use of the first antibiotics, however, the rapid increase in the spread of AMR and severity of AMR infections in recent decades has prompted a global healthcare crisis. In the USA, 2 million AMR infections are reported each year (Centers for Disease Control and Prevention, 2013), costing the US government $20 billion annually (Smith and Coast, 2013). It has been estimated that at least 700,000 people globally die of AMR infections every year and this number is predicted to increase to up to 10 million annual deaths by 2050. AMR can arise in many classes of microorganism including fungi (*Candida* spp. to antifungal drugs, (Wiederhold, 2017)), parasites (*Plasmodium falciparum* to antimalarial drugs, (Cui *et al.*, 2015)) and viruses (HIV to antiretroviral therapy, (Strasfeld and Chou, 2010)), however, the focus of this thesis will be on antimicrobial-resistant bacteria.

In 2017, the World Health Organisation (WHO) released a global priority list of pathogens for which new antimicrobial drugs are urgently required (The World Health Organisation, 2017a). Prioritised pathogens are classified by urgency as critical (e.g. carbapenem-resistant *Enterobacteriaceae*), high (e.g. methicillin-resistant *Staphylococcus aureus*) or medium (e.g. fluoroquinolone-resistant *Shigella* spp.). *Mycobacterium tuberculosis* was not included in the report as it is ‘already a globally established priority’ (The World Health Organisation, 2017a). In 2016, multi-drug-resistant tuberculosis (MDR-TB) was reported in 490,000 people, of which an estimated 9.7% of patients harboured extensively drug-resistant tuberculosis (XDR-TB), defined by resistance to at least 4 of the critical anti-TB drugs (The World Health Organisation, 2017b).

1.2.2. Mechanisms of antimicrobial resistance

AMR can be either intrinsic or acquired. Bacteria can be intrinsically resistant to

a particular class of antibiotic if a resistance mechanism is naturally encoded (in the chromosome or on a plasmid) in the normal structure of a bacterial cell type (Arzanlou *et al.*, 2017). Acquired resistance, in contrast, occurs via genetic mutation in response to an antimicrobial selection pressure and is capable of transfer between bacterial cells (Arzanlou *et al.*, 2017). Acquired AMR can arise through several different mechanisms (Figure 1B). One mechanism involves the inactivation or complete degradation of the antibiotic by bacterial enzymes. Antibiotics can be modified and ultimately inactivated via numerous chemical reactions including acetylation, phosphorylation or adenylation (Munita and Arias, 2016). The most scientifically well-known enzymes that degrade antibiotics are Gram-negative β-lactamases which hydrolyse the amide bond in the β-lactam ring of β-lactam antibiotics like penicillins (Bush and Bradford, 2016). β-lactamases were first discovered during the commercialisation of penicillin in the 1930s (Abraham and Chain, 1940), and although β-lactam antibiotics have been continually developed since then, that development has occurred concurrently with the natural evolution by targeted bacteria of additional β-lactamases specific for these new drugs (Hall and Barlow, 2004). Over 1000 β-lactamase enzymes have now been identified, including extended-spectrum β-lactamases (ESBLs) (Paterson and Bonomo, 2005) capable of hydrolysing cephalosporins and monobactams, and carbapenemases which can additionally hydrolyse carbapenems (often referred to as an antibiotic of last resort) (Queenan and Bush, 2007).

Another common resistance mechanism is antibiotic efflux from the bacterial cell. Drug efflux can be specific to one antibiotic class or demonstrate broad specificity towards a range of antibiotics (Sun *et al.*, 2014). Furthermore, efflux genes can either be encoded on the chromosome on carried on mobile genetic elements (Poole, 2007). Removal of tetracyclines is arguably the best-described mechanism of antibiotic efflux and there are at least 23 genes that encode diverse tetracycline efflux pumps in both Gram-positive and Gram-negative bacteria (Roberts, 2005). Efflux pumps are comprised of cytoplasmic membrane proteins that exchange an antibiotic cation complex for a proton against a concentration gradient, consequently lowering the cytoplasmic concentration of the antibiotic (Piddock, 2006). Drug efflux pumps are classified into different

groups which include the resistance-nodulation-cell division (RND) family, the ATP-binding cassette (ABC) family, the small multidrug resistance (SMR) family, and the major facilitator superfamily (MFS) (Borges-Walmsley *et al.*, 2003).

Resistance can alternatively occur via modification, protection or bypass of the cellular antibiotic target (Munita and Arias, 2016). Target modification could involve mutations in the gene encoding the antibiotic target - for example mutations in the genes *gyrA-gyrB* of DNA gyrase or *parC-parE* of topoisomerase IV confer protection against fluoroquinolone antibiotics (Aldred *et al.*, 2014). A well-described example of antibiotic target protection is that of ribosomal protection which is mediated by ribosomal protection proteins (RPPs) (Connell *et al.*, 2003). RPPs are cytoplasmic proteins that mimic the elongation factors EF-Tu and EF-G which are involved in protein translation (Sanchez-Pescador *et al.*, 1988). This mimicry allows RPPs to bind to the ribosome and induce a conformational change in the ribosome structure which causes the antibiotic to dislodge from the targeted subunit (Dönhöfer *et al.*, 2012). The RPP then dissociates from the ribosome but the conformational change remains, preventing the antibiotic from re-binding to the ribosome (Dönhöfer *et al.*, 2012).

In contrast to the Gram-negative production of β-lactamases to hydrolyse β-lactam antibiotics, Gram-positive bacteria instead modify the penicillin-binding protein (PBP) targets (Tomasz and Munoz, 1995). However, the Gram-positive and methicillin-resistant *S. aureus* can employ an alternative mechanism to bypass the normal PBP targets via the acquisition of *mecA* which encodes PBP2a, a PBP with low affinity for β-lactams (Wielders *et al.*, 2002). Further resistance mechanisms include reduced uptake of the drug which can arise through mutations in outer membrane porins (e.g. a mutation in *oprD* of *Pseudomonas aeruginosa* reduces imipenem uptake (Quinn *et al.*, 1986). Reduction in antibiotic uptake generally confers a low-level of resistance, although this resistance can be increased through combination with drug expulsion mediated by efflux pumps (Kumar and Schweizer, 2005; Spidlova *et al.*, 2018).

1.2.3. Rise and mobility of antimicrobial resistance

AMR determinants can be carried chromosomally or on mobile genetic elements. Resistance is spread between cells by mechanisms of horizontal gene transfer including natural transformation of extracellular DNA, transduction of DNA via bacteriophages, and transfer of plasmids by conjugative pili (Barlow, 2009). These mechanisms contribute towards a natural level of AMR within bacterial populations, however the emergence of AMR has been dramatically accelerated by both the general use (e.g. occupational exposure to antibiotics) but also misuse of antibiotics in clinical and industrial settings (Ventola, 2015). Clinical antibiotic misuse could involve incorrect prescription by the clinician or non-adherence of the patient towards the prescribed antibiotic course such as incompletion of the course (Pechère, 2001). The greatest clinical misuse of antibiotics arguably results from the general over-consumption of antibiotics. This is facilitated both by the over-prescription of antibiotics when an alternative treatment could suffice, and access to non-prescribed antibiotics that may be purchased over the counter in pharmacies in certain parts of the world including the USA and developing countries (Morgan *et al.*, 2011). Industrial antibiotic misuse has greatly contributed to the rise of AMR and occurs through the prophylactic administration of antibiotics to animal growth feed in order to reduce the risk of infection and increase growth yields (Wegener, 2003). Although this practice has been banned in the EU (European Commission, 2005) and new rules have begun to emerge in the USA (Food and Drug Administration, 2013), previous antibiotic use in animals in the USA has accounted for 80% of total antibiotic consumption (Van Boeckel *et al.*, 2015) and in 2015, 62% of the antibiotics supplied in animal feed were medically-important antibiotics also used to treat human infections (Food and Drug Administration, 2015). Collectively, clinical and industrial misuse of antibiotics has led to a substantial burden of AMR, the combating of which will require the employment of multiple different strategies.

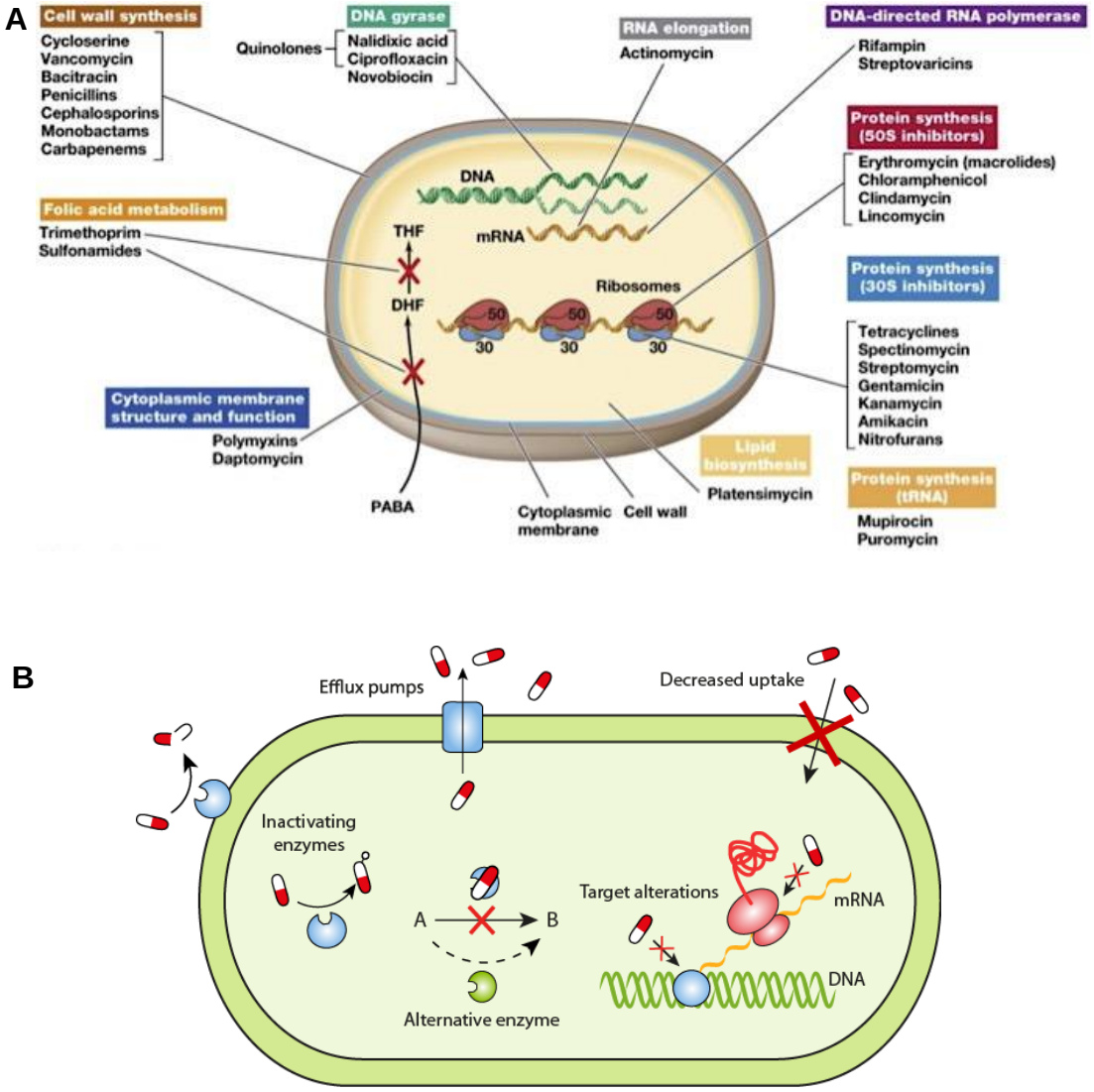

Figure 1. Traditional antibiotic targets and common mechanisms of resistance

A. Illustration of a bacterial cell depicting common cellular targets of antibiotics such as cell wall synthesis. Examples of antibiotics that are active against these targets are listed below the target heading. (Madigan *et al.*, 2015). **B.** Illustration of several antibiotic resistance mechanisms such as efflux pumps and inactivating enzymes. (Blair *et al.*, 2015; Gullberg, 2014).

1.3. Strategies to combat antimicrobial resistance

To tackle the issue of AMR, we must improve antimicrobial stewardship and conservation of existing antibiotics. It is also imperative that a diversity of new antimicrobials are developed, however the discovery and development of new antibiotics is both challenging and expensive. The biotech company Achaogen has recently developed a powerful new antibiotic to treat complicated urinary tract infections (Achaeogen, 2018), however the Food and Drug Administration (FDA) rejected its use in the treatment of bloodstream infections and Achaogen stock has consequently dropped by 24% to a record-low (Campbell, 2018). New antibiotics are not profitable as they are often held in reserve until traditional antibiotic treatment fails (Power, 2006). Moreover, resistance to new antibiotics inevitably occurs, and antibiotic courses are short - unlike drugs used to treat long-term chronic health problems (Power, 2006). Pharmaceutical companies are therefore increasingly reluctant to invest in antibiotic research and development and many companies have now abandoned antibiotic research such as AstraZeneca, Sanofi, and most recently Novartis (The Business Times, 2018). GlaxoSmithKline has also placed its antibiotic development pipeline under review (The Business Times, 2018). Consequently, alternative antimicrobial therapies - both conventional and novel - have attracted greater interest and funding.

1.3.1. Vaccination

A conventional but efficient strategy to tackle pathogenic infections including AMR infections is vaccination. Vaccines act prophylactically by preventing the occurrence of disease, and consequently eliminating the need to prescribe antibiotics, leading to reduced levels of AMR (Jansen *et al.*, 2018). It is estimated that between 2001 and 2020, vaccination will have saved over 20 million lives in low- and middle-income countries (Ozawa *et al.*, 2017). Particularly successful vaccines include glycoconjugate vaccines developed against *Haemophilus influenzae* type b (Hib) and *Streptococcus pneumoniae*. A study in the year 2000 found that 16.6% of Hib strains worldwide had developed protective β-lactamases (Hoban and Felmingham, 2002) and the successful development of a glycoconjugate vaccine comprising Hib polysaccharide

capsule and carrier proteins resulted in a reduction in mortality rates and levels of AMR (Heilmann *et al.*, 2005). Vaccines therefore represent a highly effective strategy to reduce global morbidity, mortality and AMR, although there are associated challenges. One challenge is 'vaccine escape' which can occur either through the escape of strains that are not covered by the vaccine, or mutations arising within a vaccine component, preventing the elicitation of an immune response and rendering the vaccine non-protective (Barnett *et al.*, 2015). Since 2003, at least 39 *S. pneumoniae* vaccine escape mutants of have arisen due to genetic recombination that has resulted in the switching of capsule types (Brueggemann *et al.*, 2007). Further challenges include enabling access to vaccines in developing countries and remote locations, and achieving global implementation of a vaccine to achieve disease eradiation (Jansen *et al.*, 2018).

1.3.2. Anti-virulence factors

Novel antimicrobials present alternative strategies to tackle AMR. One example is the development of anti-virulence factors. Anti-virulence factors are defined as molecules that inhibit a mechanism required for bacterial pathogenesis but do not exert a bacteriostatic or bactericidal effect upon the bacterium (Rasko and Sperandio, 2010). Potential virulence targets are numerous and can encompass all stages of pathogenic infection, ranging from initial colonisation (e.g. adhesins) to establishment of disease (e.g. signalling, communication and biofilm formation) and ultimate damage to host cells (e.g. secretion of toxins) (Rasko and Sperandio, 2010). Inhibition of one or more of these pathogenic mechanisms would reduce the virulence potential of the pathogen and aid pathogen clearance by the host immune system (Totsika, 2016). The primary advantage of anti-virulence factors over conventional antibiotics is that pathogens are not destroyed and the evolutionary pressure to develop resistance is lowered (Totsika, 2016). Anti-virulence factors could be implemented as a single therapy or administered in combination with existing antibiotics to increase antibiotic lifespan (Cegelski *et al.*, 2008). Despite the therapeutic potential of anti-virulence factors, research is still in early phases, and although the selection pressure is reduced, resistance to anti-virulence factors is likely to ultimately arise.

1.3.3. Phage therapy

One of the most promising antimicrobial strategies involves the use of whole bacteriophages. Bacteriophages are viruses which infect bacteria that possess a receptor specific for that particular strain of bacteriophage (Salmond and Fineran, 2015). Bacteriophages replicate within host bacteria and then utilise holin-lysin systems to kill the host (Wang *et al.*, 2000). Holins perforate the cytoplasmic membrane, allowing peptidoglycan-destroying endolysins to access the cell wall, and ultimately cause host cell lysis which results in the extracellular release of bacteriophages (Wang *et al.*, 2000). Bacteriophages were discovered in the early 1900s (D'Herelle, 2007; Twort, 1915) and their implementation as an antimicrobial therapy shortly followed in 1920 when bacteriophages were successfully used to cure 4 patients of *Shigella dysenteriae* (Summers, 1999). This marked the first documented case of phage therapy.

Despite the early success of phage therapy, clinical trials were largely abandoned by the West in the 1940s due to the enormous success of penicillin, and Western research subsequently focused on antibiotic development instead of bacteriophages (Cisek *et al.*, 2017). In contrast, Eastern European countries and the Soviet Union continued to invest in bacteriophage research and centres for phage therapy treatment became established in locations such as Tbilisi, Georgia (Summers, 2012). As new antibiotic development entered a void in the late 1980s, worldwide interest in phage therapy was renewed, although commitment to phage therapy research was hindered by Western scepticism of previously conducted clinical trials which were often poorly documented and controlled (Cisek *et al.*, 2017). This scepticism has now largely abated and phage therapy has attracted a further surge of interest, with the first North American phage therapy centre opening in 2018 (Center for Innovative Phage Applications and Therapeutics., 2018). This establishment was significantly inspired by the successful treatment of a disseminated antibiotic-resistant *Acinetobacter baumannii* infection with a personalised cocktail of bacteriophages (Schooley *et al.*, 2017). Bacteriophages can therefore eradicate AMR infections and also have a narrow-host range which may reduce the development of resistance (Hyman and Abedon, 2010). Resistance to

bacteriophages is inevitable, however, as bacteria can mutate surface receptors to prevent bacteriophage recognition (Hyman and Abedon, 2010). There have also been reports of host immune responses to phage such as neutralising antibodies that could potentially limit the efficacy of bacteriophage treatment (Łusiak-Szelachowska *et al.*, 2014). Phage therapy is an exciting avenue of antimicrobial research but requires further research and clinical trials to improve the efficacy of treatment and reduce the probability of phage resistance arising.

1.3.4. Enzybiotics

There has also been research into the potential implementation of bacteriostatic/cidal enzymes (‘enzybiotics’) as an antimicrobial therapy. Such enzymes are usually derived from either bacteria or bacteriophages and frequently contain hydrolytic properties (Kamath and Pai, 2013). Many bacteria secrete hydrolytic enzymes directly into neighbouring bacterial cells in which the antibacterial toxicity of the enzymes results in destruction of the target cell (Cianfanelli *et al.*, 2016). Antibacterial enzymes include phospholipases which hydrolyse phospholipid bilayers, and peptidoglycan-active (PG-active) enzymes, such as peptidases and lysozymes, which break down bacterial cell walls (Russell *et al.*, 2014). Hydrolytic enzymes derived from bacteriophages include PG-active enzymes such as the *Salmonella* phage endolysin Gp110 which demonstrates lysozyme activity against bacterial cell walls (Rodríguez-Rubio *et al.*, 2016). Similarly to anti-virulence factors, enzybiotics remain in early stages of research and bacteriostatic/cidal mechanisms of action will lead to the development of resistance, although enzybiotics could increase the efficacy of treatment if administered in combination with antibiotics.

Vaccination, anti-virulence factors, bacteriophages and enzybiotics collectively represent several different strategies to target AMR, however this thesis will discuss a particularly novel approach to combatting AMR that involves the use of a bacterium as a ‘living antibiotic’. This bacterium is *Bdellovibrio bacteriovorus*.

2. Introduction to *Bdellovibrio bacteriovorus*

2.1. An overview of *B. bacteriovorus*

Bdellovibrio species are small, vibroid-shaped Gram-negative δ-proteobacteria that are found ubiquitously in terrestrial and aquatic environments (Stolp and Starr, 1963). The Type species, *Bdellovibrio bacteriovorus,* has two different lifestyles: a predatory host-dependent (HD) lifestyle in which *B. bacteriovorus* invades and kills prey bacteria in order to replicate, and a rarer, non-predatory, host-independent (HI) lifecycle (Stolp and Starr, 1963) (Figure 2).

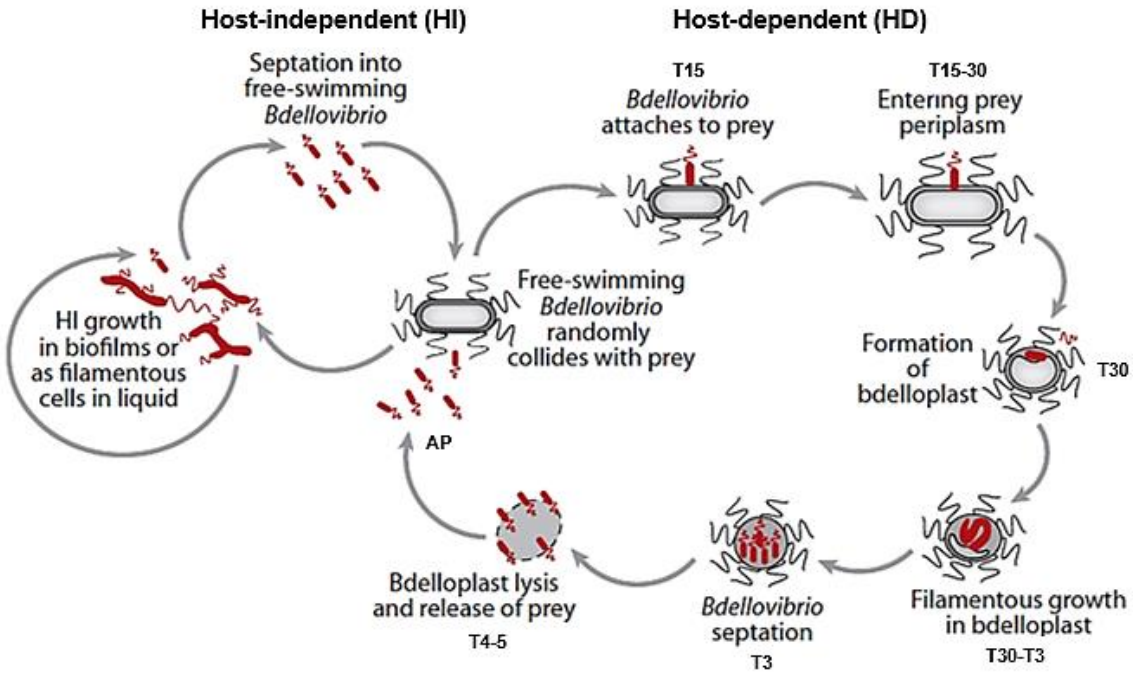

Figure 2. Life cycles of *Bdellovibrio bacteriovorus*

Host-dependent (HD) fast-swimming 'attack-phase' (AP) *B. bacteriovorus* attach to and then invade Gram-negative cells via the secretion of hydrolytic enzymes that sculpt an entry pore in the prey cell wall. T15-30 and T3-5: min and h post-invasion, respectively. *B. bacteriovorus* enzymes further remodel the prey cell wall, causing the host cell to form a spherical 'bdelloplast' which provides an osmotically-stable niche in which *B. bacteriovorus* can replicate. Filamentous predator growth and septation are followed by prey cell lysis and the release of attack-phase *B. bacteriovorus*. *B. bacteriovorus* can also enter a rare (~1 in 10^7 cells) host-independent (HI) life cycle. HI cells are slow-growing, non-predatory and usually filamentous but morphologically diverse. (Sockett, 2009).

2.2. The predatory lifecycle of *B. bacteriovorus*

Predatory 'attack-phase' *B. bacteriovorus* utilises either swimming motility, with a single polar flagellum (in aqueous environments) (Shilo, 1969), or gliding motility (on surfaces and biofilms) (Lambert *et al.*, 2011) to scout for Gram-negative prey bacteria to which it attaches using type IV pili (Chanyi and Koval, 2014; Evans *et al.*, 2007; Mahmoud and Koval, 2010). The predator squeezes through the outer membrane and creates a reinforced pore in the prey cell wall to allow passage into the inner periplasm (Kuru *et al.*, 2017). *B. bacteriovorus* then re-seals the entry pore and modifies prey peptidoglycan, both strengthening and rounding the cell wall to form a spherical 'bdelloplast' that enables *B. bacteriovorus* to inhabit an osmotically-stable intraperiplasmic niche (Kuru *et al.*, 2017; Lerner *et al.*, 2012). *B. bacteriovorus* attaches to the prey cytoplasmic membrane, secreting hydrolytic enzymes to degrade nucleic acids and proteins in the cytoplasm (Hespell *et al.*, 1975; Matin and Rittenberg, 1972), and disrupting the electron transport chain across the cytoplasmic membrane which kills the prey cell (Rittenberg and Shilo, 1970). Prey nucleotides are transported across the cytoplasmic membrane and directly incorporated into the growing *B. bacteriovorus* genome (Ruby *et al.*, 1985). *B. bacteriovorus* grows filamentously until it septates into ~4-6 progeny cells which secrete additional cell wall-modifying enzymes to lyse the host cell and then scout for new prey to invade (Shilo, 1969).

2.3. The non-predatory lifecycle of *B. bacteriovorus*

Although the default lifestyle of *B. bacteriovorus* is predatory, a small proportion of cells (~1 in 10^7) can undergo a lifestyle transition to become host-independent (HI) in which cells grow in nutrient-rich environments in the absence of prey (Seidler and Starr, 1969). The most common mechanism underlying this lifestyle switch involves a genetic mutation in the host-interaction (hit) locus which contains type IV pili-associated genes required for predator entry into prey cells (Capeness *et al.*, 2013; Cotter and Thomashow, 1992). HI cells usually grow slowly as long, morphologically diverse filaments and replicate via a range of mechanisms to produce additional filamentous cells or new attack-phase

predatory cells (Hobley *et al.,* 2012b). This ability to survive independently from a host may account for the initially surprisingly large genome size (3.8 Mb) of *B. bacteriovorus*. Until recently, HI *B. bacteriovorus* cells had only been observed in the laboratory and it was possible that this lifestyle was purely a laboratory-induced phenomenon. However, in 2012 a new environmental strain was isolated from the river Tiber and named *B. bacteriovorus* Tiberius (Hobley *et al.*, 2012b). *B. bacteriovorus* Tiberius could grow host-independently, confirming that the host-independent lifecycle also occurs naturally in the environment.

2.4. *B. bacteriovorus* predation *in vivo*

Due to a natural predatory life cycle, *B. bacteriovorus* presents itself as a potential novel therapeutic agent. AMR poses a serious threat to human health and continues to develop and rapidly spread. Pathogens comprising the 'ESKAPE' group (*Enterococcus faecium*, *Staphylococcus aureus*, *Klebsiella pneumoniae*, *Acinetobacter baumannii*, *Pseudomonas aeruginosa* and *Enterobacter spp*.) are particularly associated with AMR and all except the Gram-positive *S. aureus* are potential targets for *B. bacteriovorus* (Rice, 2008). Moreover, in contrast to an antibiotic, *B. bacteriovorus* possesses an entire suite of predatory enzymes and can employ multiple killing processes simultaneously, therefore it is unlikely that resistance to the predator could arise. As a consequence of the broad target range of *B. bacteriovorus*, it is likely that predator cells would be directly applied to wound infections as opposed to internal systemic infections due to potential disruption of the normal human gut microflora which comprises a wide range of bacteria.

B. bacteriovorus has thus far shown very promising results in animal infection model studies. One of the first successful studies was carried out by Atterbury *et al.* (2011) who showed that *B. bacteriovorus* could clear infections of *Salmonella enterica* serovar Enteritidis in chickens. *B. bacteriovorus* administered to healthy chicks had no observable negative impacts on their health or well-being. Subsequent administration of *B. bacteriovorus* to *Salmonella*-colonised chicks reduced *Salmonella* numbers in the gut and *Salmonella*-induced gut inflammation in comparison to controls. In subsequent

studies, *B. bacteriovorus* has been topically applied to both fish skin (Chu and Zhu, 2010) and cattle eye infections (Boileau *et al.*, 2016). *B. bacteriovorus* also reduced the burden of *K. pneumoniae* in rat lungs (Shatzkes *et al.*, 2016) and intravenous inoculation into mice was demonstrated to be safe (Shatzkes *et al.*, 2015). *B. bacteriovorus* has also been successfully applied to zebrafish larvae which possess a vertebrate innate immune system. This infection model also permits the visualisation of an infection course due to the transparency of zebrafish larvae. Willis *et al.* (2016) injected zebrafish with a lethal dose of antibiotic-resistant *Shigella flexneri*, followed by either injection of *B. bacteriovorus* or a buffer control. *B. bacteriovorus* application resulted in a ~35% increase in zebrafish survival and was shown to work in concert with zebrafish neutrophils and macrophages to clear the infection. Importantly, *B. bacteriovorus* persisted non-pathogenically in zebrafish and was eventually cleared by the innate immune system.

2.5. Research project objectives

To develop *B. bacteriovorus* as a successful antibacterial therapeutic, it is imperative that we acquire a greater understanding of the intricate predatory mechanisms of this bacterium. In this thesis, I describe the results from two 15 week rotation projects on *B. bacteriovorus* carried out at the University of Birmingham and the University of Nottingham. My first rotation project was based at the University of Birmingham and carried out under the supervision of Dr Andrew Lovering who studies the structural biology of predatory *B. bacteriovorus* enzymes. In this project, I used biochemical and structural techniques to investigate a mechanism of motility which is important for *B. bacteriovorus* location of prey and subsequent exit from the prey host. The second rotation project was based at the University of Nottingham (my host PhD institution) and carried out under the supervision of Professor Liz Sockett, who uses genetic and microscopic techniques to study the role of different *B. bacteriovorus* enzymes and the predatory ability of *B. bacteriovorus* within *in vivo* infection models such as zebrafish. In this project, I employed these genetic and microscopic methods to investigate the role of *B. bacteriovorus* cell wall-

modifying enzymes during predation, asking whether the enzymes act on predator or on prey. Taken together, these projects provide new insights into two fundamental processes: motility and modification of cell walls, which are critical to the predatory lifestyle of this unique bacterium. The research is relevant to the future development of whole *B. bacteriovorus* predator cells as an antibacterial therapy and also informs on the utilisation of predatory enzymes as enzybiotics.

UNIVERSITY OF BIRMINGHAM

CHAPTER 2: Structural and functional insights into the regulation of gliding motility in *Bdellovibrio bacteriovorus*

University of Birmingham rotation project

Supervised by Dr Andrew Lovering

Abstract

Bdellovibrio bacteriovorus is a small predatory bacterium that invades Gram-negative prey, replicates within the periplasm and then lyses the host cell. This predatory ability presents *B. bacteriovorus* as a potential therapeutic to treat human pathogens and tackle the growing problem of antimicrobial resistance. *B. bacteriovorus* uses gliding motility on surfaces to scout for prey cells and to ultimately facilitate exit from the dead host. The bacterial second messenger, cyclic-di-GMP, positively regulates gliding motility in *B. bacteriovorus*. Cyclic-di-GMP signals are transduced through PilZ domains of receptor proteins. Some *B. bacteriovorus* PilZ proteins also contain a domain of unknown function, DUF4339, to which we assign a putative GYF fold. Eukaryotic GYF domains bind proline-rich peptides and important binding residues are conserved in bacterial GYF domains. Moreover, *B. bacteriovorus* gliding motor proteins contain proline-rich regions, and deletion of the gene encoding the PilZ: GYF protein Bd3100 causes changes in gliding reversal frequencies. We therefore hypothesised that *B. bacteriovorus* PilZ: GYF hybrid proteins may bind cyclic-di-GMP and interact with the gliding motor to regulate gliding motility. We aimed to test this hypothesis by crystallising the PilZ: GYF hybrid, Bd1996. Bd1996 homologues from two different *B. bacteriovorus* strains were successfully expressed and purified. Bd1996 bound c-di-GMP *in vitro*, however, neither protein homologue could be crystallised during the time-frame of the project.

3. Introduction

3.1. Gliding motility in *B. bacteriovorus*

B. bacteriovorus utilises two different mechanisms of motility: flagellar-mediated swimming motility and appendage-independent gliding motility (Lambert *et al.* 2011; Stolp and Starr, 1963). Flagellar motility is powered by a single, polar, ensheathed flagellum which rapidly propels *B. bacteriovorus* cells through aqueous environments at speeds of up to 160 μm s^{-1} (Stolp and Starr, 1963). Flagellar motility is essential for the efficient location of, and exit from, prey bacteria within aqueous environments, however the physical rotary force generated by the flagellum itself is not required to penetrate prey cell walls (Lambert *et al.*, 2006).

B. bacteriovorus can alternatively move by gliding, a mechanism of motility that is used by a range of microorganisms including δ-proteobacteria and cyanobacteria, although it is most frequently studied in *Myxococcus xanthus*, a predatory bacterium that is related to *B. bacteriovorus* (McBride, 2001). Gliding motility is characterised by the appendage-independent movement of cells along surfaces, driven by a proton motive force (Nan *et al.*, 2011). The molecular mechanisms underpinning gliding are poorly understood, however, the current model involves multiprotein motor complexes (of Agl/Glt proteins) that span the outer membrane, periplasm and inner membrane (Figure 3) (Nan *et al.*, 2010). Motor complexes are proposed to interact with focal adhesins which propel the cell along an external track of deposited extracellular polysaccharide (Ducret *et al.*, 2012). The mechanism additionally requires an internal track which may be mediated by MreB or the cell wall (Nan *et al.*, 2011). *B. bacteriovorus* requires gliding motility to scout for prey on solid surfaces (Lambert *et al.*, 2011), for predation within biofilms (Medina *et al.*, 2008) and to escape the bdelloplast at the end of a predatory cycle (Hobley *et al.*, 2012a). *B. bacteriovorus* contains 4 gliding operons, each comprised of 8-10 genes including many homologues of *M. xanthus* gliding genes (Lambert *et al.*, 2010).

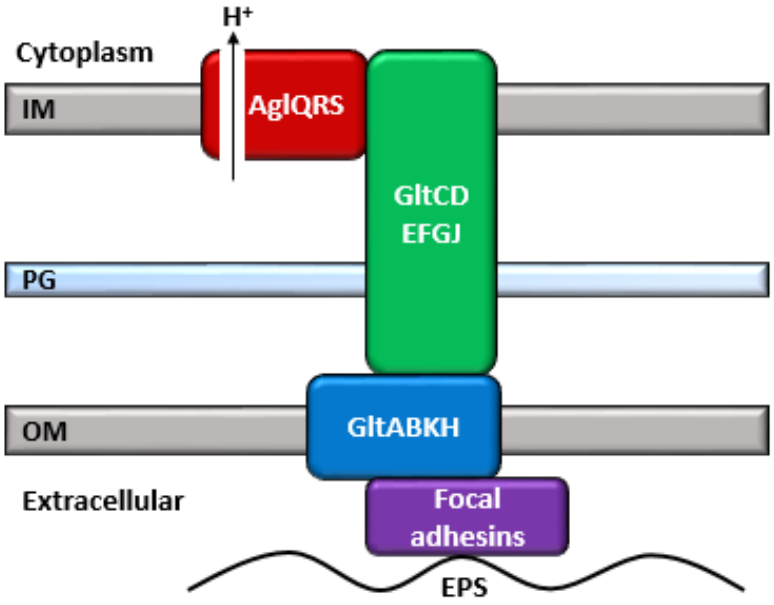

Figure 3. Gliding motility motor complex

The gliding motor consists of a multiprotein complex, comprising Agl proteins (Q, R & S) and Glt proteins (A-H & J) which span the inner membrane (IM), periplasm and outer membrane (OM). The pumping of protons from the periplasm into the cytoplasm generates the proton motive force required to power the motor. Movement is mediated by both an internal track (MreB or the peptidoglycan cell wall (PG)) and an external track (via the interaction of focal adhesins with extracellular polysaccharide (EPS)).

3.2. **Cyclic-di-GMP regulates gliding motility in *B. bacteriovorus***

B. bacteriovorus gliding motility is positively regulated by bis-(3´-5´)-cyclic dimeric guanosine monophosphate (cyclic-di-GMP or c-di-GMP), a ubiquitous bacterial signalling molecule (Hobley *et al.* 2012a). C-di-GMP is a nucleotide second messenger that regulates many diverse cellular functions including motility, biofilm formation and virulence (Römling *et al.*, 2013). C-di-GMP is particularly associated with the life stage transition from motility to sessility (Simm *et al.*, 2004), and the acute to chronic virulence switch in persistent infections (Moscoso *et al.*, 2011). C-di-GMP regulates flagellar and type IV pili-mediated motility in many bacteria (Boehm *et al.*, 2010; Skotnicka *et al.*, 2015), however, regulation of gliding motility has, thus far, solely been observed in *B. bacteriovorus*. C-di-GMP signals are transduced through effector proteins that usually contain the c-di-GMP-binding PilZ domain (Amikam and Galperin, 2006; Benach *et al.*, 2007). *B. bacteriovorus* has at least 18 proteins with C-terminal PilZ domains (Rotem *et al.*, 2016) and several of these proteins also contain an N-terminal domain of unknown function, DUF4339. Our bioinformatics analyses suggest that DUF4339 is very likely to represent a bacterial GYF domain (HHPred: 99.13% probable match). GYF domains have primarily been characterised in eukaryotes in which they bind proline-rich peptides via conserved hydrophobic residues (Figure 4), however, bacterial GYF domains are also predicted to bind proline-rich peptides (Balaji and Aravind, 2007). *B. bacteriovorus* contains proline-rich proteins at the inner membrane which include components of the gliding motor complex. Furthermore, deletion of the gene encoding the PilZ: GYF protein Bd3100 caused changes in the frequency of gliding reversals (Taylor, 2013). We therefore propose a model in which c-di-GMP binds to an effector PilZ domain, inducing a conformational change that either licenses a positive interaction or relieves an inhibitory interaction of the GYF domain with the gliding motor.

To test this hypothesis, previous work has attempted to crystallise PilZ: GYF proteins from *B. bacteriovorus* HD100 such as Bd1996. A single Bd1996 needle was grown but did not optimally diffract, therefore this project will attempt to generate a new crystal form of Bd1996. We will also clone a homologue of

Bd1996 (63% identity) from the Mexican *B. bacteriovorus* strain SKB1291214 to ascertain whether the Bd1996$_{Mex}$ homologue crystallises more readily.

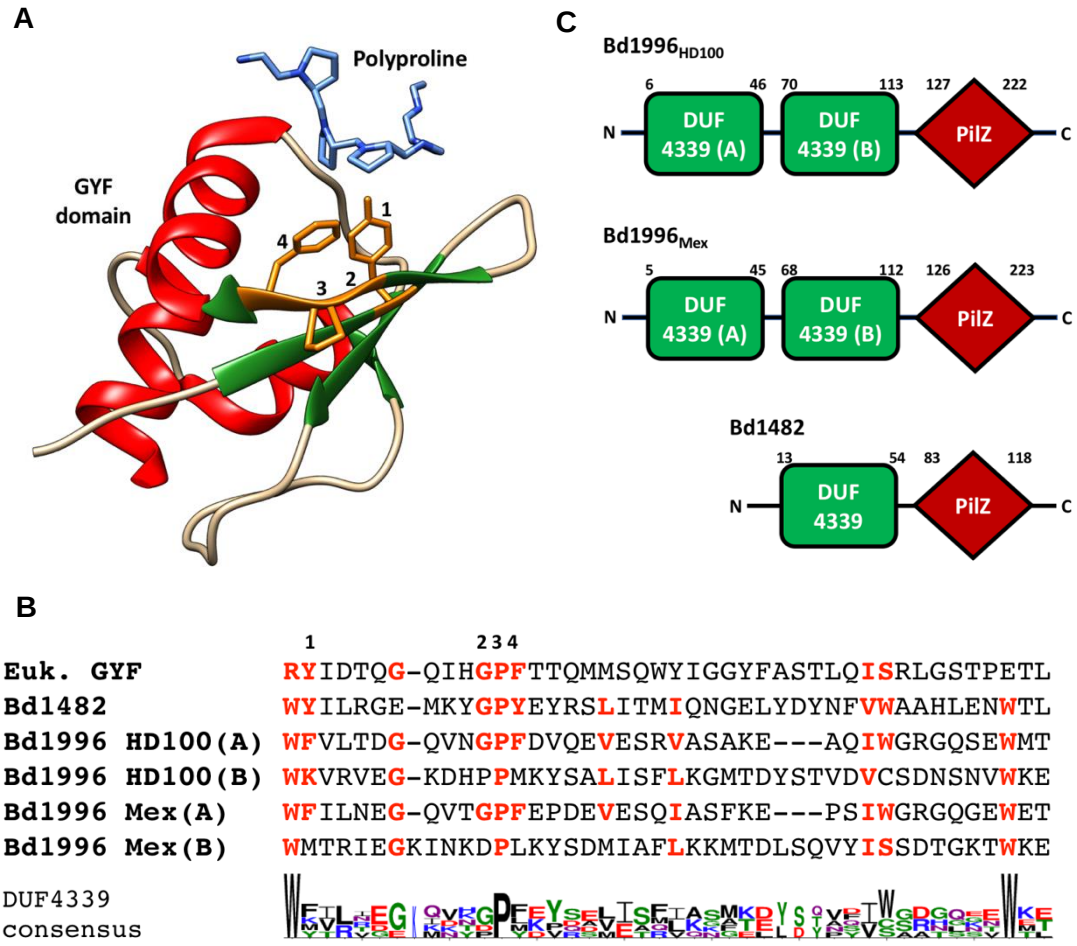

Figure 4. *B. bacteriovorus* DUF4339 has a predicted GYF fold

A. Eukaryotic GYF domain of *S. cerevisiae* Smy2 in complex with a proline-rich peptide (PDB: 3FMA). Numbers 1-4 are conserved residues important for polyproline-binding and correspond to residues indicated in B. **B.** Sequence alignment of DUF4339 domains of Bd1482 and Bd1996 from *B. bacteriovorus* HD100 and the Bd1996 homologue from Mexican *B. bacteriovorus* strain SKB1291214. Euk. GYF: Smy2 GYF domain. Conserved residues are highlighted in red. Bd1996 contains two GYF domains (A & B) and (B) appears to have diverged from the *B. bacteriovorus* DUF4339 consensus. Sequence alignments and the DUF4339 consensus were generated using T-Coffee and WebLogo 3, respectively (Crooks *et al.*, 2004; Di Tommaso *et al.*, 2011). **C.** Hybrid protein domain structures of Bd1996 (HD100 and Mex homologues) and Bd1482 (HD100).

3.3. Research project aims

In this project, we aimed to express, purify, and confirm that *B. bacteriovorus* PilZ protein, Bd1996, is a c-di-GMP receptor, and to ultimately obtain a crystal structure of the protein. Several *B. bacteriovorus* PilZ proteins also contain N-terminal DUF4339 domains which we have annotated as putative bacterial GYF domains. A crystal structure of Bd1996 would allow us to test our hypothesis that the GYF domain binds polyproline-rich sites in candidate gliding motor proteins. Consequently, this work will enable greater insight into the complexity of gliding motility signalling complexes.

4. Materials and Methods

4.1. Generation of the construct p*bd1996$_{Mex}$*

4.1.1. Restriction-free cloning

The construct p*bd1996$_{Mex}$* was generated through restriction-free cloning with a primer pair designed to anneal to both the gene target and the destination vector (Figure 5). Primers and plasmids referred to in this report are listed in Tables 1 and 2, respectively. The first PCR reaction amplified *bd1996$_{Mex}$* from *B. bacteriovorus* SKB1291214 genomic DNA (gDNA). PCR reactions (100 µl) contained 0.4 µM of each primer, 400 µM of dNTPs, 1.5 µl of 2U/µl VELOCITY polymerase (Bioline), 20 µl of Hi-Fi buffer (5X), 69.5 µl of water and 1 µl of gDNA. The following thermocycling parameters were used: initial denaturation at 98 °C for 4 min, followed by 30 cycles of denaturation at 98 °C for 30 s, an annealing gradient from 50 – 60 °C for 45 s, and extension at 72 °C for 1 min 30 s. A final extension at 72 °C for 10 min was performed. 4 µl of PCR products were loaded onto a 1% agarose gel alongside 4 µl of 1 kb DNA ladder (NEB). Gels were run at 90 V for 40 min and visualised under UV light. PCR products were then purified with a QIAquick® PCR Purification Kit (QIAGEN) and combined. A second PCR reaction using a 9:1 ratio of initial PCR product to destination vector pET-28a was performed. Thermocycling conditions were the same with the following exceptions: an annealing gradient from 55 – 65 °C and a 10 min extension step during 35 cycles of amplification.

4.1.2. Transformation of PCR product into *Escherichia coli*

Prior to transformation, 1 µl of DpnI was added to combined second-round PCR products and incubated at 37 °C for 1 h to remove methylated parental template. The product was purified with the QIAquick® PCR Purification Kit and concentrated down to 5 µl with a Hetovac VR-1 centrifugal vacuum concentrator (HETO). 5 µl were added to 50 µl of chemically-competent *E. coli* cloning strain XL10-Gold and incubated on ice for 30 min. Cells were heat-shocked at 42 °C for 45 s, then incubated on ice for 2 min. 900 µl of lysogeny broth (LB) were added to the cells and the cells were incubated at 37 °C with orbital shaking at

180 rpm for 1 h. Cells were then microfuged at 13,000 rpm for 2 min and resuspended in 200 µl of LB. 100 µl were dispensed onto LB plates supplemented with 100 µg ml^{-1} of kanamycin and incubated at 37 °C overnight.

4.1.3. Verification of p*bd1996$_{Mex}$* construction

Colonies were recovered and screened by PCR in 30 µl reactions containing: 15 µl of MyTaq^{R} Red mix (2X, Bioline), 0.3 µM of each pET-28a screening primer and 13 µl of water. The following thermocycling parameters were used: initial denaturation at 95 °C for 8 min, followed by 35 cycles of denaturation at 98 °C for 25 s, annealing at 50 °C for 25 s, and extension at 72 °C for 2 min 20 s. Plasmids were purified from PCR-positive clones with a QIAprep® Spin Miniprep Kit (QIAGEN) and sequenced to verify successful plasmid construction. The p*bd1996$_{Mex}$* construct was then transformed into *E. coli* expression strain BL21(DE3) and colonies were again screened by colony PCR.

4.2. Bacterial culture and protein expression

10 ml of LB were inoculated with a single colony of *E. coli* BL21(DE3) containing the expression construct and cultured overnight at 37 °C with orbital shaking at 180 rpm. The entire overnight culture was used to inoculate 1 l of auto-induction (AI) media (10 g l^{-1} tryptone, 5 g l^{-1} yeast extract, 3.55 g l^{-1}, Na_2HPO_4, 3.4 g l^{-1} KH_2PO_4, 2.68 g l^{-1} NH_4Cl, 20 ml of sugar mix (25 g l^{-1} glucose, 100 g l^{-1} lactose, 250 g l^{-1} glycerol), 2.5 ml of trace metals, 1 ml of 2 M $MgSO_4$ and 100 µg ml^{-1} of kanamycin). The 1 l culture was grown in baffled flasks at 37 °C for ~ 3.5 h, then protein was expressed overnight at 18 °C.

4.3. Protein purification

The overnight expression culture was centrifuged at 6,000 rpm for 10 min at 4 °C. 45 ml of Buffer A (20 mM HEPES pH 7.5, 300 mM NaCl, 20 mM imidazole, 0.05% Tween 20) and ~ 5 mg of lysozyme were added to the cell pellet and tumbled for 30 min at 4 °C. Cells were then sonicated on ice, centrifuged at 20,000 rpm for 1 h at 4 °C, and the supernatant applied to a Ni^{2+} column. Bd1996

was eluted in a 1:1 ratio of 200 mM EDTA pH 8: 100 mM sodium citrate pH 6. Eluted protein fractions were mixed with 2X SDS loading dye, heated at 90 °C for 10 min, then loaded onto a 15% Tris-HCl SDS-PAGE gel alongside 5 µl of HyperPAGE Pre-stained Protein Marker (Bioline). SDS-PAGE gels were run at 180 V for 1 h, stained with Coomassie Brilliant Blue (0.2% Coomassie Brilliant Blue R-250, 50% methanol, 10% glacial acetic acid) for at least 1 h, then de-stained in 20% methanol: 10% glacial acetic acid for at least 1 h. Protein fractions were pooled and dialysed in a ~ 1:100 ratio of protein: desired dialysis buffer at 4 °C overnight. Following dialysis, protein was concentrated to ~ 1 ml by centrifugation in a 10 kDa molecular weight cutoff Vivaspin® centrifugal concentrator (Generon) at 4,000 rpm and 4 °C. Protein concentration was determined with Pierce™ Coomassie Plus (Bradford) Assay Reagent (Thermo Scientific) and either directly used in crystallography trays or further purified by size-exclusion chromatography on an AKTA Prime (Amersham Biosciences) if required.

4.4. Protein crystallisation trials

Protein crystallisation trials were set up with a wide range of commercially available sparse-matrix screens (Molecular Dimensions). JCSG-*plus*™ was routinely selected as an initial screen against classic polyethylene glycol (PEG) precipitant and salt conditions over a pH range of 4-10. Additional screens included BCS (PEG smears), MIDAS*plus*™ (non-PEG precipitants); Morpheus® (additional ligands); and Clear Strategy™ (user-controlled pH). Screens were performed by sitting drop vapour diffusion in 96-well plates, with a 1:1 drop ratio of protein: screen condition. Plates were incubated at 18 °C and periodically checked for crystals under a Nikon SMZ800 stereomicroscope.

4.5. Cyclic-di-GMP binding

20 µM of $Bd1996_{Mex}$ was mixed in a 1:1 ratio with 40 µM of Monolith NT™ Protein Labelling Kit BLUE-NHS (Nanotemper Technologies) and incubated in the dark at room temperature for 30 min. Unreacted dye was removed via a gravity flow column and the labelled protein eluted in buffer containing 20 mM

HEPES and 200 mM NaCl at pH 7. Labelled protein was microfuged at 13,000 rpm for 10 min at 4 °C to remove aggregates. C-di-GMP was titrated against $Bd1996_{Mex}$ on a Monolith NT.115 MST machine. C-di-GMP binding induced a change in fluorescence intensity, and as fluorescence changes due to material loss were excluded through an SDS-denaturation test, initial fluorescence could directly be used to determine the binding affinity.

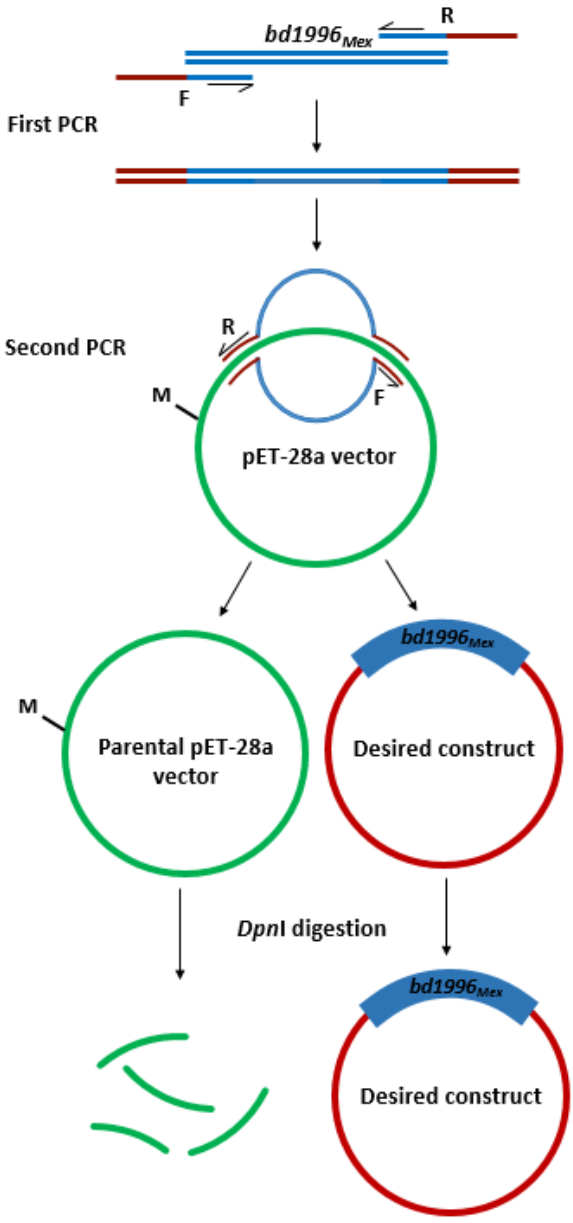

Figure 5. Schematic describing the construction of p*bd1996*$_{Mex}$
Restriction-free cloning was used to generate the construct p*bd1996*$_{Mex}$ and requires long hybrid primers that anneal to both the target gene (blue) and the destination vector (green). In the first PCR reaction, the gene target is amplified from gDNA, generating a PCR product that contains the gene flanked by primer ends that will anneal to the destination vector. In the second PCR reaction, the original PCR product is used as a 'mega-primer', annealing to the plasmid and allowing synthesis of the construct. Finally, any remaining parental template is separated from the synthesised construct via DpnI digestion which breaks down the methylated (indicated by M) parental template but not the new construct which is non-methylated.

Table 1. Primers used in this study		
Primer name	**Description**	**Primer sequence (5'-3')**
bd1996$_{Mex}$ FWD	Hybrid primers for cloning the *bd1996*$_{Mex}$ gene of *B. bacteriovorus* SKB1291214 into the vector pET-28a. Bases that anneal to the gene are indicated in bold. The remaining bases anneal to the vector.	ATGGGCAGCAGCCATCATCATCATCATCACA GCAGC**ATGTCGAAAATTTGGTTTATCTTGAAT GAAGG**
bd1996$_{Mex}$ REV		TCAGTGGTGGTGGTGGTGGTGCTCGAGT **CTAGGAGATCGTCGCAAATTTGCG**
pET-28a FWD	pET-28a vector sequencing primers	TAATACGACTCACTATAGGG
pET-28a REV		GCTAGTTATTGCTCAGCGG

Table 2. Plasmids used in this study		
Plasmids	**Description**	**Source**
pET-28a	Destination vector for *bd1996*$_{Mex}$, N-terminal His-tag, Kan^R	Lab stock
p*bd1996*$_{HD100}$	*bd1996*$_{HD100}$ in pET-28a, N-terminal His-tag, Kan^R	Lab stock
p*bd1996*$_{Mex}$	*bd1996*$_{Mex}$ in pET-28a, N-terminal His-tag, Kan^R	This study

5. Results

5.1. Expression and purification of Bd1996$_{HD100}$

Bd1996$_{HD100}$ was expressed in *E. coli* BL21(DE3) and purified by Ni-NTA affinity chromatography. Figure 6 shows that Bd1996$_{HD100}$ (25 kDa) was successfully overexpressed and purified to a high degree, indicated by the presence of few contaminating bands in the eluted fractions. The protein was dialysed into 20 mM sodium citrate pH 6, concentrated down to ~ 30 mg ml^{-1} and aliquots were snap-frozen and stored at – 80 °C.

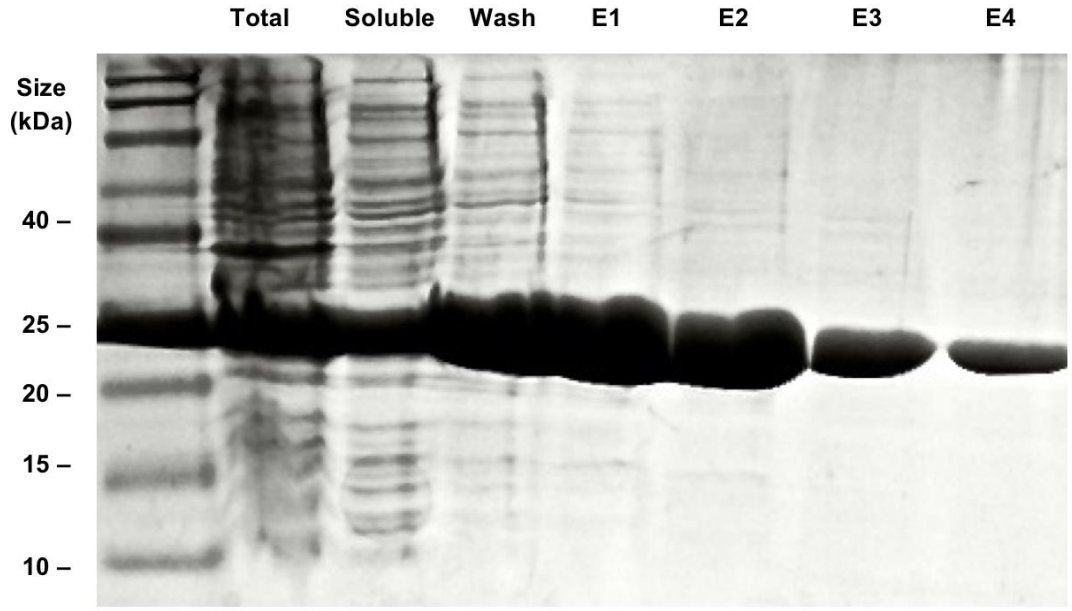

Figure 6. Purification of Bd1996$_{HD100}$ by Ni-NTA affinity chromatography

Bd1996$_{HD100}$ was purified by Ni-NTA affinity chromatography. Total: total protein extracted from cells. Soluble: soluble protein fraction. Wash: unbound protein. E1-4: eluted fractions. 5 µl (total, soluble) or 20 µl (wash, E1-4) of sample were loaded onto a 15% Tris-HCl SDS-PAGE gel alongside 5 µl of HyperPAGE Pre-stained Protein Marker. Gels were run at 180 V for 1 h and stained with Coomassie Brilliant Blue.

5.2. Construction of p*bd1996$_{Mex}$*

5.2.1. Amplification of *bd1996$_{Mex}$*

bd1996$_{Mex}$ was amplified from *B. bacteriovorus* SKB1291214 gDNA (Figure 7). Bands of the correct size (690 bp) were generated and PCR products were subsequently purified and combined.

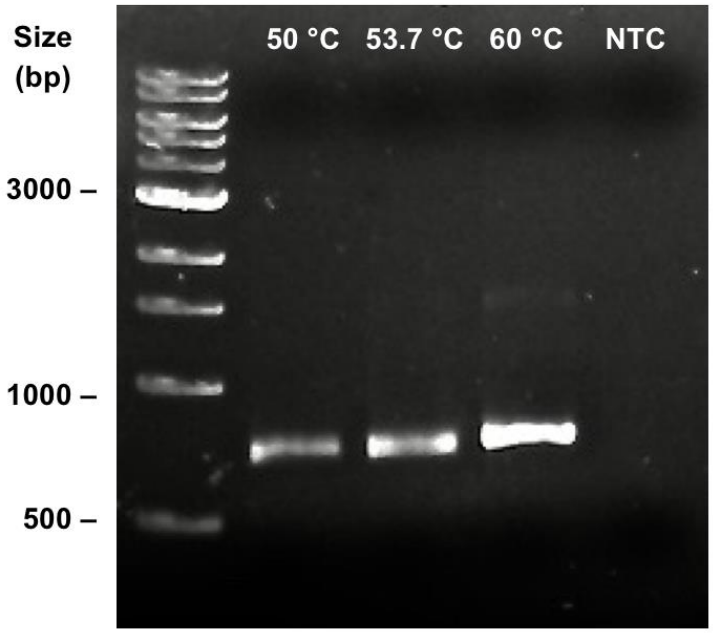

Figure 7. Amplification of *bd1996$_{Mex}$* by PCR

bd1996$_{Mex}$ was amplified from *B. bacteriovorus* SKB1291214 gDNA using an annealing temperature gradient from 50 – 60 °C. NTC: no template negative control. Each well contains 4 µl of PCR product run on a 1% agarose gel at 90 V for 40 min and compared against 4 µl of 1 kb DNA ladder.

5.2.2. Verification of p*bd1996$_{Mex}$* construction

Purified PCR product from Figure 7 was then included as a 'mega-primer' in a second PCR reaction with the vector pET-28a to generate the construct p*bd1996$_{Mex}$* (Figure 8). Methylated parental template was then removed via DpnI digestion and the PCR product was purified, concentrated and transformed into *E. coli* XL10-Gold. Successful plasmid construction was confirmed by Sanger sequencing of plasmids purified from transformants. p*bd1996$_{Mex}$* was then transformed into *E. coli* BL21(DE3) and clones were screened by colony PCR using primers specific for *bd1996$_{Mex}$* (Figure 9). Bands of the expected size (690 bp) were observed for both clones but not for the pET-28a empty vector control, confirming the successful transformation of p*bd1996$_{Mex}$* into *E. coli* BL21(DE3).

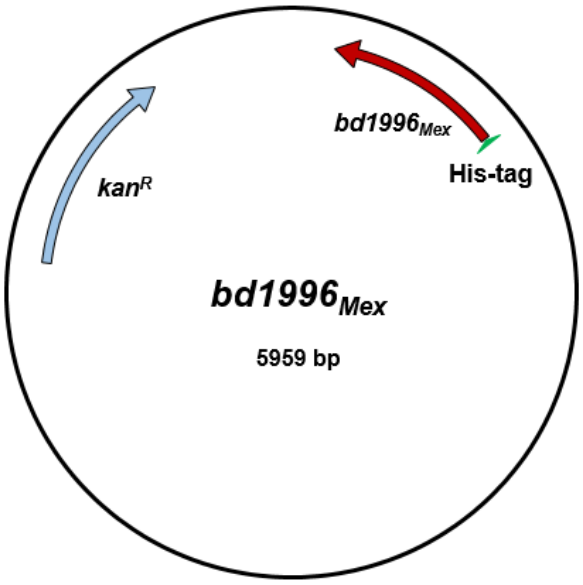

Figure 8. Plasmid map of the construct p*bd1996$_{Mex}$*

Sequence data confirmed the successful construction of p*bd1996$_{Mex}$*, a pET-28a vector that contains *bd1996$_{Mex}$* with an N-terminal His-tag (6xHis). kanR: kanamycin resistance marker.

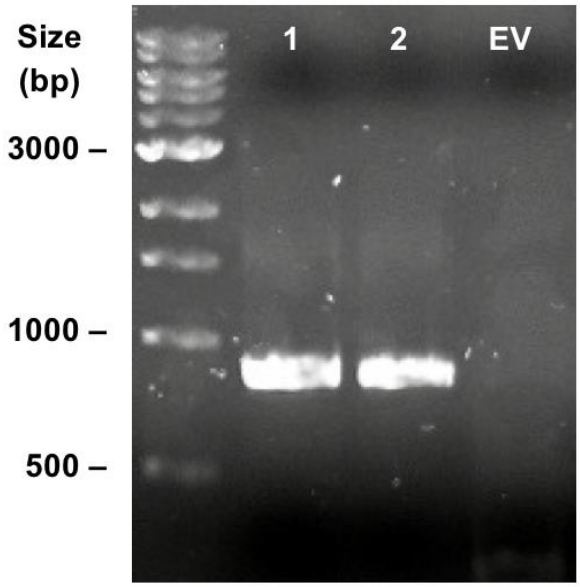

Figure 9. Confirmation of the presence of p*bd1996$_{Mex}$* in *E. coli* BL21(DE3)

E. coli BL21(DE3) clones (1 & 2) were screened by colony PCR using *bd1996$_{Mex}$* primers to confirm the presence of p*bd1996$_{Mex.}$* EV: pET-28a empty vector negative control. Each well contains 4 µl of PCR product run on a 1% agarose gel at 90 V for 40 min and compared against 4 µl of 1 kb DNA ladder.

5.3. Expression and purification of Bd1996$_{Mex}$

Bd1996$_{Mex}$ was expressed in *E. coli* BL21(DE3) and purified by Ni-NTA affinity chromatography, followed by size-exclusion chromatography to obtain a purer sample. The protein was dialysed into either 20 mM sodium citrate pH 6, or 20 mM HEPES, 200 mM NaCl, 1 mM dithiothreitol (DTT), pH 7. Figure 10 only shows the purification of Bd1996$_{Mex}$ in sodium citrate buffer for simplicity, however both purification profiles were very similar. Bd1996$_{Mex}$ (25 kDa) was successfully overexpressed and purified to a higher degree following size-exclusion, indicated by the presence of fewer contaminating bands in the size-exclusion peak fractions compared to the initial Ni-NTA purification sample. The peak fractions were combined and concentrated down to ~ 18 mg ml^{-1} (sodium citrate buffer) or ~ 25 mg ml^{-1} (HEPES buffer) and aliquots were snap-frozen and stored at – 80 °C.

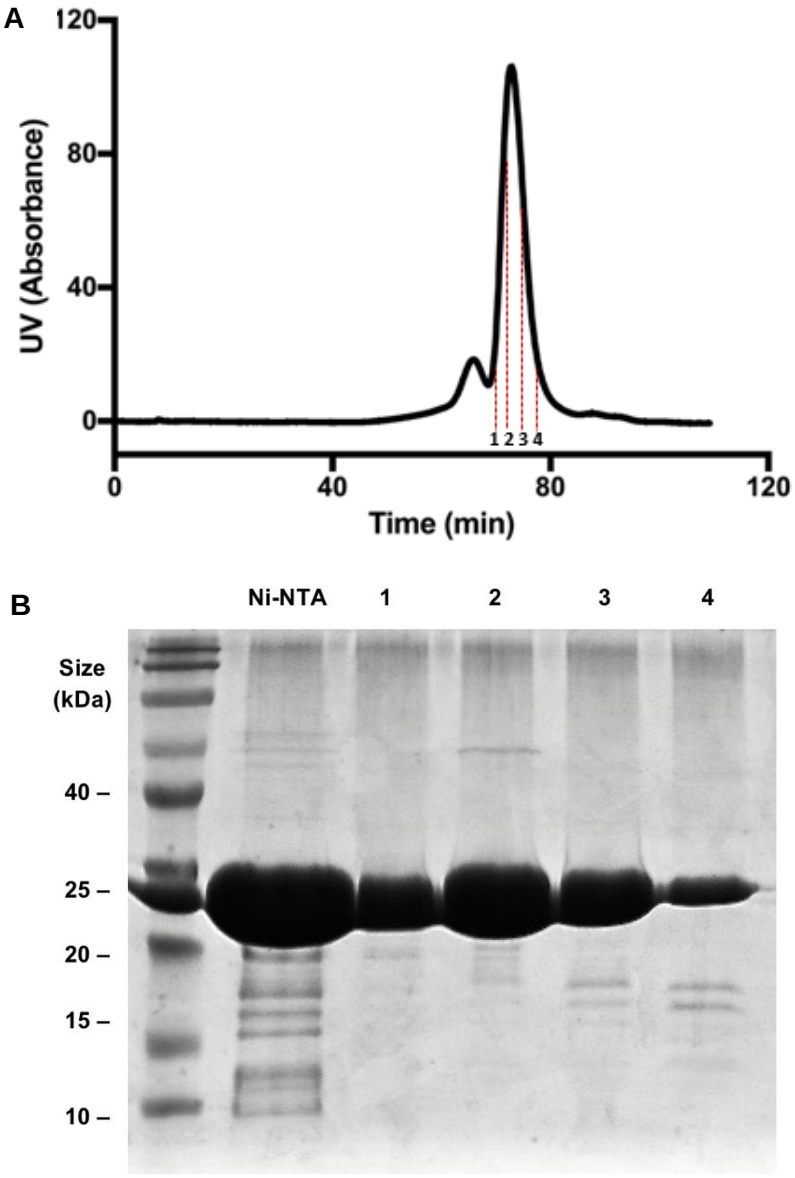

Figure 10. Purification of Bd1996$_{Mex}$ by size-exclusion chromatography

Bd1996$_{Mex}$ was firstly purified by Ni-NTA affinity and then by size-exclusion chromatography. **(A)** Size-exclusion trace showing a sharp peak for Bd1996$_{Mex}$ at ~ 70-80 min. **(B)** A selection (1-4) of eluted fractions from this peak were run on an SDS-PAGE gel alongside a sample from the Ni-NTA affinity purification (Ni-NTA) to allow comparison of purity. Each well contains 20 µl of sample loaded onto a 15% Tris-HCl SDS-PAGE gel alongside 5 µl of HyperPAGE Pre-stained Protein Marker. Gels were run at 180 V for 1 h and stained with Coomassie Brilliant Blue.

5.4. Bd1996$_{Mex}$ binds cyclic-di-GMP

Bd1996 is a PilZ domain protein and therefore a candidate c-di-GMP receptor, however the protein has not previously been shown to bind c-di-GMP. Bd1996$_{Mex}$ was labelled with a primary amine-reactive dye and c-di-GMP was titrated against the protein. Ligand-binding induced a change in fluorescence intensity, with higher concentrations of c-di-GMP causing an increase in protein fluorescence. Initial fluorescence was directly used to generate a dose-response curve (Figure 11) and determine a binding affinity of 2.5 µM.

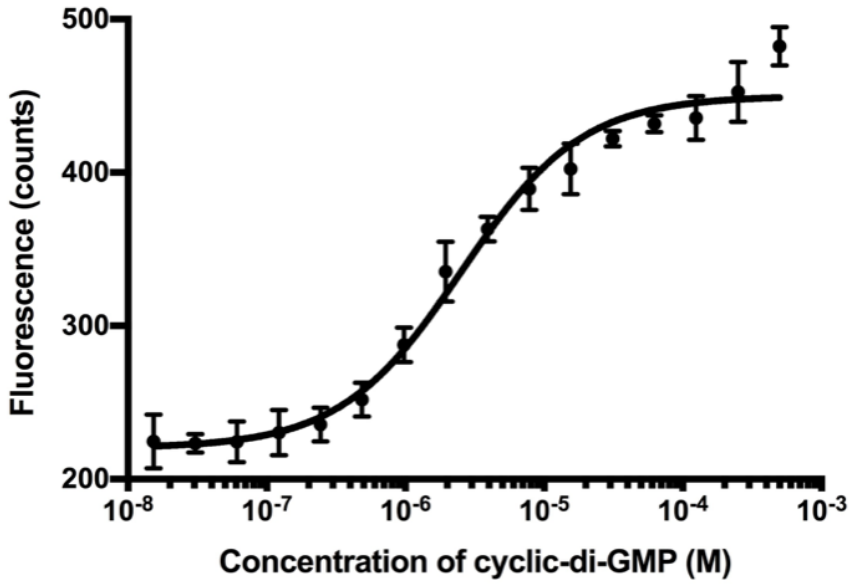

Figure 11. Bd1996$_{Mex}$ binds cyclic-di-GMP

Cyclic-di-GMP was titrated against fluorescently-labelled Bd1996$_{Mex}$ from a concentration of 500 µM to 0.0153 µM. A K_d of 2.5 µM was determined from the dose-response curve. The experiment was carried out in triplicate and error bars represent standard deviation from the mean.

5.5. Protein crystallisation trials

$Bd1996_{HD100}$ (20 mM sodium citrate pH 6 buffer) was trialed in the screens JCSG-*plus*™, BCS and Clear Strategy™. $Bd1996_{HD100}$ was also dialysed into two alternative buffers: HEPES (20 mM HEPES, 200 mM NaCl, pH 7) and Tris (20 mM Tris, 200 mM NaCl, pH 8) and trialed in a Mini Screen. Protein concentrations ranged from 15 – 30 mg ml^{-1}. Most drops were either clear or gelatinous, precipitating in few conditions, and no significant difference was observed in HEPES or Tris buffers. $Bd1996_{Mex}$ (20 mM sodium citrate pH 6 buffer) was trialed in JCSG-*plus*™, BCS, Clear Strategy™, Mini Screen, MIDAS*plus*™, Morpheus®, and JBScreen Classic 7 at 25 mg ml^{-1}. $Bd1996_{Mex}$ was further dialysed into HEPES buffer containing 1 mM DTT as the protein contains two cysteine residues that may form a disulfide bond non-conducive to optimal crystallisation. The protein was trialed in JCSG-*plus*™ and BCS screens at a concentration of 18 mg ml^{-1} with the addition of c-di-GMP in a molar excess of ~ 2.5. Unfortunately, no protein crystals were grown in the time-frame of 3 months.

6. Discussion

Cellular concentrations of c-di-GMP are controlled by the reciprocal activity of GGDEF diguanylate cyclases (Paul *et al.*, 2004) and EAL/HD-GYP phosphodiesterases which synthesise and hydrolyse c-di-GMP, respectively (Bobrov *et al.*, 2005; Dow *et al.*, 2006). *B. bacteriovorus* contains 5 GGDEFs and 7 phosphodiesterases (6 HD-GYPs and 1 EAL), in addition to a c-di-GMP-I riboswitch predicted to act as a c-di-GMP sink during attack phase (Karunker *et al.*, 2013; Rendulic *et al.*, 2004). Hobley *et al.* (2012a) showed that 4 of the 5 GGDEFs were responsible for a distinct phenotype: DgcA controls gliding motility-facilitated exit from prey, DgcB and CdgA are important for predatory invasion, and DgcC regulates the conversion of predatory cells to host-independently (HI) growing cells. GGDEFs contain I-sites which typically function in feedback inhibition (Chan *et al.*, 2004; Christen *et al.*, 2006) but can bind c-di-GMP in enzymatically inactive GGDEFs (Duerig *et al.*, 2009). CdgA is an inactive GGDEF and localises to the biting pole, suggesting that CdgA may receive signals from DgcB and subsequently interact with predatory invasion proteins at the pole (Hobley *et al.*, 2012a). Different GGDEF mutant phenotypes also suggest that *B. bacteriovorus* exhibits specificity between GGDEFs and cognate c-di-GMP receptors, which may be mediated by timed, localised bursts of c-di-GMP (Hobley *et al.*, 2012a). C-di-GMP receptors include the PilZ protein family (Benach *et al.*, 2007). Here, we showed that PilZ protein, Bd1996, bound c-di-GMP at a K_d of 2.5 µM. K_d values for PilZ proteins usually range from ~ 50 nM – 2 µM (Hengge, 2009), although lower c-di-GMP binding affinities have been reported (Rotem *et al.*, 2016). The K_d of 2.5 µM is within the estimated range of intracellular c-di-GMP concentrations (Römling *et al.*, 2013), suggesting that c-di-GMP binding by the PilZ domain is probably the first event in our proposed gliding motility signalling pathway.

Until recently, most c-di-GMP receptors were known to solely bind c-di-GMP through PilZ domains or I-sites. Rotem *et al.* (2016) used a c-di-GMP capture-compound mass-spectrometry methodology to identify novel c-di-GMP receptors in *B. bacteriovorus*. There are 18 predicted PilZ proteins in *B. bacteriovorus*, however this study revealed 65 putative novel effectors that

specifically bound c-di-GMP in either attack-phase or HI cultures. The c-di-GMP binding of 2 novel effectors, Bd2402 and Bd2924, was further examined using microscale thermophoresis. Bd2402 bound c-di-GMP at a high affinity (K_d = 0.399 µM), probably through a novel PilZ variant domain, whereas Bd2924 bound c-di-GMP at a low affinity (K_d = 7.57 µM) through an unorthodox novel domain. These results suggest that *B. bacteriovorus* contains an extensive c-di-GMP signalling network comprising receptors that bind c-di-GMP through PilZ domains and alternative novel domains.

As *M. xanthus* and *B. bacteriovorus* are closely related, it is likely that these bacteria share similar features of gliding motility regulation. Pogue *et al.* (2017) showed that PilZ-like protein, PlpA, regulates gliding motility in *M. xanthus* by inhibiting the reversal of gliding motors. PlpA directly binds to the motor complex component, AglS, although the mechanism of this interaction was not investigated. PlpA contains the c-di-GMP binding motif, RxxxR- N20-30-D/NxSxgG, however, c-di-GMP is not required for the regulatory function of PlpA on gliding motility. PlpA did not bind c-di-GMP *in vitro* but may bind c-di-GMP *in vivo* or bind to alternative nucleotides such as cyclic-di-AMP or cyclic-AMP-GMP. In *M. xanthus*, it is possible that an unidentified protein is stimulated by a nucleotide signalling molecule and then activates PlpA which binds to AglS in the motor complex. *B. bacteriovorus*, in comparison, may regulate gliding motility through a signalling complex comprising a single multi-domain protein, the PilZ: GYF hybrid, which functions to both receive signals (PilZ) and bind the motor complex (GYF).

We hypothesised that PilZ: GYF hybrid proteins bind to proline-rich gliding motor proteins and this should be experimentally investigated in future work. A crystal structure of Bd1996 bound to c-di-GMP would inform the locking of the protein in an activated GYF domain conformation. Subsequent pull-down assays with *B. bacteriovorus* cell lysate would reveal proteins with which Bd1996 interacts. In the absence of a crystal structure, future work could involve the purification of Bd1996 GYF domains in isolation (and therefore free of PilZ-regulation) and

their utilisation in pull-down assays to identify binding partners. Alternatively, motor complex components such as AglR and AglS could be cloned and protein-protein interaction studies performed with the Bd1996 GYF domains. It would also be informative to construct fluorescent fusion proteins for both Bd1996 and the gliding motor to observe whether Bd1996 co-localises with the gliding motor complex. Unfortunately, neither $Bd1996_{HD100}$ nor the homologue $Bd1996_{Mex}$ crystallised during this project, despite testing a range of protein concentrations, buffers, additives and crystallisation screens. Future work could also include a thermal shift assay to assess the stability of Bd1996 in different buffers and the crystallisation of alternative PilZ: GYF hybrid proteins.

5. Conclusions

B. bacteriovorus is a predatory bacterium that could be exploited as a potential novel therapeutic to treat antimicrobial-resistant infections. *B. bacteriovorus* uses gliding motility to both scout for prey to invade and to facilitate exit from dead host cells. Gliding motility has been linked to the bacterial second messenger c-di-GMP which binds to PilZ domain proteins. Here, I successfully expressed and purified the PilZ protein, Bd1996, from the *B. bacteriovorus* strains HD100 and SKB1291214. Bd1996 bound c-di-GMP *in vitro* with a K_d of 2.5 μM, however, neither protein homologue crystallised during the time-frame of this project. Future work could involve further optimisation of Bd1996 crystal trials, and the construction of isolated Bd1996 GYF domains to identify interacting partners which may include components of the gliding motor complex.

CHAPTER 3: Molecular characterisation of L,D-transpeptidases in the predatory bacterium *Bdellovibrio bacteriovorus*

University of Nottingham rotation project

Supervised by Professor Liz Sockett

Abstract

Bdellovibrio bacteriovorus is a predatory, vibroid-shaped δ-proteobacterium which invades and then replicates within the periplasm of Gram-negative prey bacteria. Modification of peptidoglycan cell walls is an important predatory process that involves a repertoire of cell wall-modifying enzymes. These include enzymes that cut (endo- or carboxypeptidation) and link (transpeptidation) peptide chains within peptidoglycan. L,D-transpeptidases (LDTPs) catalyse the formation of 3-3 cross-links between *meso*-diaminopimelic acid residues in adjacent peptide chains, thereby linking layers of peptidoglycan. LDTP domains can, however, be repurposed evolutionarily to catalyse additional or alternative enzymatic reactions such as endo- or carboxypeptidation. *Escherichia coli* contains 6 LDTPs, however, the genome of *B. bacteriovorus* HD100 encodes 19 LDTP-family proteins, a number of which may catalyse these alternative hydrolytic reactions. Previous work has shown that 2 *B. bacteriovorus* LDTPs reinforce the prey cell wall during predation, maintaining an osmotically-stable niche in which the predator can replicate. However, additional roles of *B. bacteriovorus* LDTPs have yet to be elucidated. In this project, molecular genetics and microscopy were used to investigate the function of the two LDTP-family proteins: Bd1402, a predicted L,D-endopeptidase, and Bd1075, a predicted L,D-carboxypeptidase. Fluorescent fusion proteins showed that Bd1402 is secreted into the periplasm of the prey in which it may modify the prey cell wall. In contrast, Bd1075 localised to the *B. bacteriovorus* predator itself and an unmarked deletion of *bd1075* resulted in the formation of predator cells that were straight, in comparison to vibroid wild-type cells. These data suggest that Bd1075 is the curvature-determinant of *B. bacteriovorus* HD100. Future work will aim to elucidate the mechanism by which Bd1075 confers a vibroid shape and assess the importance of *B. bacteriovorus* vibroid morphology within the context of predatory interaction and invasion.

8. Introduction

8.1. The bacterial cell wall

8.1.1. Peptidoglycan

The peptidoglycan cell wall is a complex macromolecular structure that surrounds the cytoplasmic membrane of nearly all bacteria. The cell wall primarily acts as a protective barrier against both internal osmotic pressures and extracellular threats to bacterial survival such as toxins and antimicrobials (Silhavy *et al.*, 2010). However, the cell wall also defines bacterial shape through interaction with cytoskeletal proteins such as the actin-like MreB, which maintains the morphology of rod-shaped bacteria by guiding the action of cell wall synthesis machinery (Jones *et al.*, 2001).

Different bacterial groups can possess cell wall structures with diverse compositions (Silhavy *et al.*, 2010). Gram-positive bacteria have a thick cell wall (~ 20-80 nm) that forms 90% of bacterial dry weight. Gram-negative bacteria, in contrast, have thinner cell walls (~7-8 nm) that account for only 10% of cell dry weight. However, the Gram-negative cell wall is surrounded by a lipopolysaccharide layer of outer membrane that is absent from Gram-positives.

Peptidoglycan is the core component of the cell wall and comprises polysaccharide glycan chains joined by short stem peptide linkages to form a recalcitrant, mesh-like network (Figure 12). Glycan chains contain alternating residues of N-acetylglucosamine (NAG) and N-acetylmuramic acid (NAM) which are linked by β-(1,4)-glycosidic bonds (Vollmer *et al.*, 2008). In Gram-negative bacteria, the stem peptide is initially comprised of the 5 amino acids L-alanine, D-glutamic acid, *meso*-diaminopimelic acid (*m*-DAP), D-alanine and D-alanine at positions 1-5, respectively. Structural integrity of the cell wall is maintained via cross-links between stem peptides of parallel glycan chains (Figure 12). Cross-linking can be catalysed by either D,D- or L,D-transpeptidase enzymes. The Gram-negative cell envelope is further stabilised by the L,D-transpeptidase-mediated covalent attachment of Braun's lipoprotein in the outer membrane to the peptidoglycan cell wall (Braun, 1975; Magnet *et al.*, 2007).

Peptidoglycan biosynthesis is initiated in the cytoplasm with the Mur pathway-mediated synthesis of the pentapeptide unit UDP-N-acetylmuramic acid (Barreteau *et al.*, 2008). The phosphotransferase MraY then attaches this unit to the inner membrane C_{55} lipid carrier via a pyrophosphate linkage (Ikeda *et al.*, 1991). Glycosyltransferase MurG subsequently attaches NAG via a second pyrophosphate linkage to form a complete C_{55}-PP lipid II precursor unit (Mohammadi *et al.*, 2007). MurJ then flips the lipid II precursor across the inner membrane into the periplasm, allowing subsequent cell wall assembly by penicillin-binding proteins (PBPs) (Sham *et al.*, 2014). High molecular weight PBPs are partially redundant, bifunctional enzymes that possess both glycosyltransferase (GTase) and transpeptidase (TPase) activities (Bertsche *et al.*, 2005). Initial action involves the GTase-mediated attachment of lipid II glycans to the nascent peptidoglycan chain via a β-(1,4)-glycosidic bond. TPase activity then cross-links stem peptides of parallel glycan chains. This cross-linkage is usually catalysed by D,D-transpeptidases which form 4-3 cross-links between D-alanine^4 and *m*-DAP^3 in adjacent stem peptides.

8.1.2. L,D-transpeptidases

D,D-transpeptidase activity is ubiquitous, however, a less common group of enzymes, L,D-transpeptidases (LDTPs), can catalyse the alternative formation of 3-3 cross-links between *m*-DAP^3 and *m*-DAP^3 in adjacent stem peptides (Mainardi *et al.*, 2000). *Escherichia coli* possesses at least 5 LDTPs: ErfK, YcfS and YbiS, which anchor outer membrane protein Braun's lipoprotein to peptidoglycan, and YcbB and YnhG which catalyse 3-3 *m*-DAP cross-linking (Magnet *et al.*, 2007; Magnet *et al.*, 2008). A sixth LDTP, YafK, has been identified but has not yet been characterised (Kuru *et al.*, 2017).

LDTP domains can be repurposed evolutionarily, however, therefore a protein annotated as an LDTP may catalyse additional or alternative enzymatic reactions; *Helicobacter pylori* Csd6 was originally classified as an LDTP but actually functions as a hydrolase, showing L,D-carboxypeptidase activity (Kim *et al.*, 2015). Peptidoglycan hydrolases can be categorised into two main groups: glycosidases and peptidases. Glycosidases cleave the glycan

backbone and include N-acetylglucosamidases, and N-acetylmuramidases (lysozymes and lytic transglycosylases) (Lee and Huang, 2013). Peptidases hydrolyse peptide bonds and include endopeptidases which cleave stem peptide cross-links (D,D- for 4-3 cross-links, and L,D- for 3-3 cross-links) and carboxypeptidases which cleave the terminal stem peptide amino acid (D,D- for D-alanine^{5}, L,D- for D-alanine^{4}, and D,L- for *m*-DAP^{3}) (Lee and Huang, 2013).

The *B. bacteriovorus* genome encodes an unusually large number of LDTPs (19), which is suggestive of their importance, and due to their activity on peptidoglycan, these LDTPs may play critical roles in predation. *B. bacteriovorus* LDTPs could modify the predator's own peptidoglycan to resist osmotic changes during predation, or to provide flexibility to squeeze through the narrow entry pore, or to maintain the low immunogenicity of *B. bacteriovorus* (Schwudke *et al.*, 2003). LDTPs could additionally modify prey cell peptidoglycan at various points in the predatory cycle, aiding entry, exit or stabilising the bdelloplast structure.

B. bacteriovorus LDTPs have been categorised into 6 phylogenetic groups based on protein homology (personal communication from Dr Andrew Lovering & Mr Christopher Graham) (Figure 13). Group 1, 2 and 4 LDTP domains share homology with *E. coli* YafK, ErfK/Ybis or YcbB LDTP domains, respectively, however group 3, 5 and 6 LDTPs of *B. bacteriovorus* do not share homologues with *E. coli* and are thus termed unique or divergent. Group 3 *bd1176* and *bd0886* represent the most extensively characterised LDTPs in *B. bacteriovorus*. Bdelloplasts formed by a *B. bacteriovorus Δbd1176*/*Δbd0886* mutant were significantly less stable under osmotic challenge than bdelloplasts formed by the wild-type (Kuru *et al.*, 2017). This suggests that the group 3 *bd1176* and *bd0886* strengthen the bdelloplast peptidoglycan to provide a stable replicative niche for the *B. bacteriovorus* predator. Subsequent work on group 4 has suggested that this group of LDTPs may also act to stabilise the bdelloplast during predation (unpublished data), however, the roles of many *B. bacteriovorus* LDTPs remain to be elucidated.

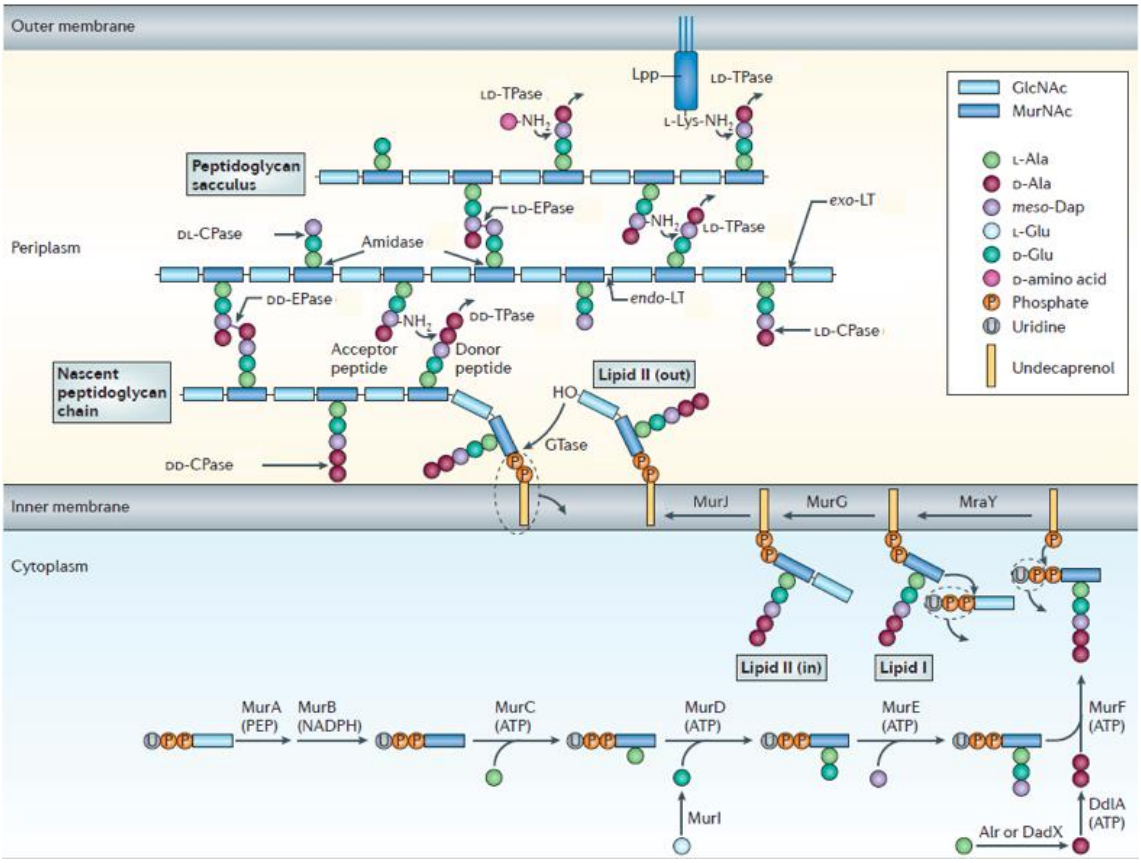

Figure 12. Bacterial peptidoglycan cell wall synthesis

The cytoplasmic Mur pathway (MurA-F) synthesises the pentapeptide unit UDP-N-acetylmuramic acid which is then attached to the inner membrane C_{55} lipid carrier (undecaprenol) by MraY. MurG attaches NAG and the resulting lipid II precursor is flipped into the periplasm by MurJ. Glycosyltransferases (GTase) add lipid II to the nascent peptidoglycan chain and D,D-transpeptidases (DD-TPase) catalyse 4-3 cross-links between stem peptides. L,D-transpeptidases can catalyse either the alternative formation of the 3-3 cross-links between stem peptides or the attachment of Braun's lipoprotein (Lpp) to peptidoglycan. Depicted hydrolytic peptidases include D,D- and L,D-endopeptidases (EPases) which cleave 4-3 and 3-3 cross-links, respectively, and D,D-, L,D-, or D,L-carboxypeptidases (CPases) which cleave 5th, 4th, and 3rd position stem peptide residues, respectively. Amidases cleave stem peptides from glycan chains and exo- or endolytic transglycosylases (LTs) cleave bonds within the glycan chain. GlcNac: N-acetylglucosamine (NAG); MurNAc: N-acetylmuramic acid (NAM). (Typas *et al.*, 2012).

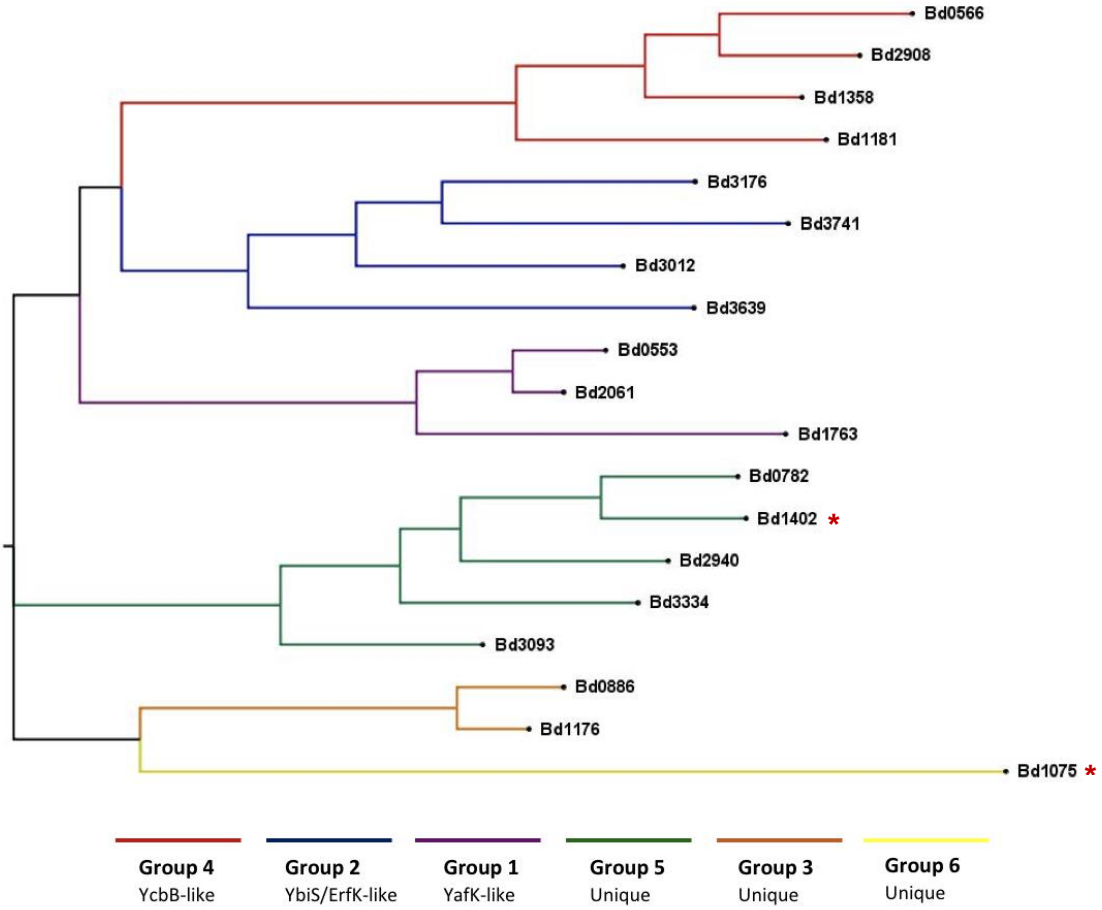

Figure 13. Phylogenetic tree of *B. bacteriovorus* L,D-transpeptidases

A maximum likelihood phylogenetic tree was generated from 19 *B. bacteriovorus* complete LDTP protein sequences. Red asterisks indicate Bd1402 (group 5) and Bd1075 (group 6) which are investigated in this project. The figure was constructed by the author using raw tree data gratefully obtained from Mr Christopher Graham, an MSci student in our lab, who performed the analysis. Phylogenetic analyses were performed using MEGA7 (Kumar *et al.*, 2016) in which 1000 replicates of the bootstrap test were conducted.

8.2. Research project aims

In this research project, the roles of two divergent LDTPs will be investigated. Group 5 comprises a selection of divergent LDTPs from which *bd1402* was chosen for investigation as a high resolution crystal structure of this protein has been obtained by collaborator and former Wellcome Trust DTP rotation project supervisor, Dr Andrew Lovering. Structural and biochemical analysis revealed that Bd1402 shows L,D-endopeptidase activity through hydrolysis of 3-3 cross-linkages - an activity that is rare in nature, and therefore of interest for further investigation. Bd1075 is the only LDTP that comprises its own group (group 6) and the predicted structure of Bd1075 reveals similarity to the crystallised protein Csd6 of *H. pylori*. Csd6 is classified as an L,D-carboxypeptidase which hydrolyses the bond between D-alanine^{4} and *m*-DAP^{3} in the stem peptide, and recent data have shown that Bd1075 also demonstrates L,D-carboxypeptidase activity *in vitro* (personal communication from Dr Lovering). In *H. pylori*, Csd6 fulfills roles in the deglycosylation of flagellar protein FlaA and contributes to the helical cell shape. We therefore hypothesised that Bd1075 may affect the cell shape and/or flagellum of *B. bacteriovorus*.

Firstly, the timing of *bd1402* and *bd1075* expression during a predatory cycle will be measured by reverse-transcriptase PCR. Gene expression analysis will be complemented by visualisation of protein production and localisation during predation. To achieve this, both new host-dependent (HD) and host-independent (HI) strains will be constructed in which a fluorescent mCherry tag is fused to the C-terminus of each LDTP. In addition, new HD and HI strains containing in-frame unmarked deletions of each LDTP will be constructed to allow phenotypic comparison between LDTP mutants and the wild-type. Together, these approaches will provide insight into the function of these two divergent LDTP-family proteins.

9. Materials and Methods

Primers, plasmids and strains referred to in this report are listed in Appendix tables 3, 4 and 5, respectively.

9.1. Bacterial culture

E. coli DH5α and S17-1 were routinely cultured in YT broth (5 g l^{-1} Difco yeast extract, 8 g l^{-1} Difco tryptone, 5 g l^{-1} NaCl, pH 7.5), shaking at 37 °C overnight, or on YT plates (media supplemented with 10 g l^{-1} Sigma select agar) incubated at 37 °C overnight. Media were supplemented with 50 µg ml^{-1} kanamycin where appropriate.

Host-dependent (HD) *B. bacteriovorus* HD100 was cultured in Ca/HEPES buffer (0.295 g l^{-1} $CaCl_2 \cdot 2H_2O$, 5.94 g l^{-1} HEPES free acid, pH 7.6) containing *E. coli* S17-1 prey shaking at 29 °C for 24-48 h. For growth on solid media, *B. bacteriovorus* HD100 was cultured with *E. coli* S17-1 prey on YPSC overlay plates (0.25 g l^{-1} MgSO4, 0.5 g l^{-1} NaOAc, 1 g l^{-1} broadbean peptone, 1 g l^{-1} yeast extract, 0.25 g l^{-1} $CaCl_2 \cdot 2H_2O$, pH 7.6, containing 10 g l^{-1} (bottom) or 6 g l^{-1} (top) Sigma select agar) at 29 °C until plaques were observed. Media were supplemented with 50 µg ml^{-1} kanamycin where appropriate.

Host-independent (HI) *B. bacteriovorus* was cultured in rich PY broth (10 g l^{-1} broadbean peptone, 3 g l^{-1} Difco yeast extract, pH 6.8), shaking at 29 °C overnight, or on PY plates (media supplemented with 10 g l^{-1} Sigma select agar) at 29 °C until colonies were observed.

9.2. Reverse-transcriptase PCR

To determine the gene expression profiles of *bd1402* and *bd1075* during predation, reverse-transcriptase PCR (RT-PCR) was performed using the QIAGEN OneStep RT-PCR kit. RT-PCR primers were designed to generate an 80-120 bp product and RNA template had previously been isolated from 8 different time points during *B. bacteriovorus* HD100 predation on *E. coli* S17-1. PCR reactions (25 µl) contained: 0.6 µM of each primer, 400 µM of dNTPs, 1X RT-PCR Buffer, 1X Q Solution, 1 µl of RT-PCR Enzyme Mix, 0.5 µl of template

RNA, and 12.2 µl of RNase-free water. The following thermocycling parameters were used: 50 °C for 30 min, 94 °C for 15 min, followed by 30 cycles of 94 °C for 1 min, 50 °C for 1 min, and 72 °C for 1 min, and a final step of 72 °C for 10 min. 15 µl of PCR reactions were run on a 2% agarose gel alongside 10 µl of 100 bp ladder (NEB). Gels were run at 100 V for 45 min and visualised under UV light.

9.3. Construction of knockout and mCherry fusion strains

Plasmid constructs were generated by Gibson Assembly cloning in which multiple overlapping DNA fragments are amplified and ligated into a non-replicative suicide vector (Gibson *et al.*, 2009). The plasmid then integrates into the genome by homologous recombination in a first cross-over event. Counter-selection in sucrose results in a second cross-over event because the genome-integrated suicide vector contains *sacB* which encodes the enzyme levansucrase that converts sucrose into a toxic product (Gay *et al.*, 1983; Reyrat *et al.*, 1998; Steinmetz *et al.*, 1983). This selection pressure therefore forces a second cross-over event in which the plasmid is excised from the genome and the final exconjugant strain containing either a gene deletion or mCherry-tagged gene is generated (Figure 14).

9.3.1. Amplification of DNA fragments for Gibson Assembly

To generate unmarked in-frame deletions of *bd1402* and *bd1075*, upstream and downstream flanking regions of each gene were individually amplified by PCR. For generation of mCherry-tagged genes, 3 fragments were amplified: the upstream region and gene, *mCherry* gene, and the downstream region. PCR reactions (100 µl) contained: 0.5 µM of each primer, 200 µM of dNTPs, 1X Q Solution, 1 µl of Phusion polymerase, 1X Phusion HF buffer, 1 µl of template DNA, and 55 µl of Analar water. The following thermocycling parameters were used: initial denaturation at 98 °C for 3 min, followed by 30 cycles of denaturation at 98 °C for 30 s, annealing at 60 °C for 30 s, and extension at 72 °C for 90 s. A final extension at 72 °C for 5 min was performed. 4 µl of PCR reactions were run on a 0.8% agarose gel alongside 10 µl of 1 kb ladder (NEB). Gels were run at 100 V for 45 min and visualised under UV light.

9.3.2. Gibson Assembly

To prepare DNA fragments for Gibson Assembly, PCR products were purified by gel extraction with the GenElute™ Gel Extraction Kit (Sigma). DNA fragments were cloned into the suicide vector pK18*mobsacB* (cut with EcoRI and HindIII), using the NEBuilder® HiFi DNA Assembly Kit (NEB). Fragments were either inserted into the vector in a ratio of 3:1 (deletion constructs) or 5:1 (mCherry constructs), respectively, and assemblies were performed at 50 °C for 60 min.

9.3.3. Suicide construct verification

To verify suicide plasmid construction, 2 µl of Gibson Assembly products were transformed into 50 µl of chemically-competent *E. coli* DH5α cells (NEB) according to the manufacturer's instructions. White colonies were isolated from YT plates containing 50 µg ml^{-1} kanamycin and 40 µg ml^{-1} of X-Gal and IPTG. Following an initial diagnostic restriction digest, purified plasmids were transformed into 200 µl of the chemically-competent donor strain *E. coli* S17-1, screened by further restriction digests, and finally verified by Sanger sequencing (Source Bioscience).

9.3.4. Conjugation of constructs into *B. bacteriovorus* HD100

To conjugate plasmid constructs into *B. bacteriovorus*, *E. coli* S17-1 donor strains containing each construct were incubated with recipient wild-type *B. bacteriovorus*. Although *B. bacteriovorus* is predatory upon the *E. coli*, prey numbers exceed *B. bacteriovorus* numbers and conjugation can still occur. To prepare conjugations, 10 ml of each *E. coli* S17-1 donor strain and 10 ml lysates of wild-type *B. bacteriovorus* HD100 (10 ml Ca/HEPES, 600 µl of *E. coli* S17-1 prey, and 200 µl of a previous *B. bacteriovorus* HD100 lysate) were cultured overnight. Cells were then centrifuged at 5,100 rpm for 20 min (*B. bacteriovorus* HD100) or 5 min (*E. coli* S17-1). *B. bacteriovorus* HD100 pellets were resuspended in residual supernatant and applied to a nylon membrane on the surface of a PY plate. *E. coli* pellets were resuspended in 100 µl of YT and applied to the nylon membrane. PY plates were incubated at 29 °C overnight.

Cells were removed from the membrane by resuspension in 1 ml Ca/HEPES, then spread onto YPSC overlay plates. Following incubation at 29 °C for 4 days, host-dependent merodiploid plaques were picked into 2 ml lysates and cultured for 48 h.

9.3.5. Generation and verification of exconjugant strains

To generate and then verify the construction of exconjugant mutant strains, 50 µl of *B. bacteriovorus* HD100 2 ml lysates were aliquoted into a lysate containing 2 ml Ca/HEPES (5% sucrose) and 150 µl of heat-killed *E. coli* S17-1. Following at least 5 rounds of successful prey lysis in sucrose, serial dilutions of *B. bacteriovorus* HD100 were cultured on YPSC overlay plates containing *E. coli* S17-1 prey for 7 days. Resulting plaques were then picked into 96 well plates containing Ca/HEPES and *E. coli* S17-1 and cultured overnight at 29 °C. 20 µl from these wells were aliquoted into two 96 well plates containing either Ca/HEPES and *E. coli* S17-1, or Ca/HEPES, S17-1 pZMR100 (kan^R) and kanamycin. Kanamycin-sensitive clones were initially screened by PCR, followed by genomic DNA (gDNA) extraction from 10 ml lysates of PCR-positive clones using a GenElute™ Bacterial Genomic DNA Kit (Sigma). PCR verification was performed using gDNA template, Phusion polymerase and primers designed to anneal at least 100 bp away from the site of homologous recombination into the genome. PCR products were purified by gel extraction and sequenced for final confirmation of the construction of 4 *B. bacteriovorus* HD100 mutant strains. To derive HI mutant strains, 50 ml lysates of each *B. bacteriovorus* HD100 mutant strain were cultured overnight, filtered through a 0.45 µm membrane, then centrifuged at 5,100 rpm for 20 min. Cell pellets were resuspended in 100 µl of PY then spread onto PY plates. Small colonies were recovered after incubation at 29 °C for 7 days. HI strain construction was confirmed by PCR and mCherry fluorescence.

9.4. Microscopy

Microscopy was used to observe and determine the timing of mCherry-tagged LDTP production and any potential defect caused by LDTP gene deletion during the predatory cycle. For time course microscopy, synchronous predations

involving *B. bacteriovorus* HD100 predator and *E. coli* S17-1 prey were prepared in a ratio of 5:4:3 of 10X *B. bacteriovorus* HD100, *E. coli* S17-1 (OD_{600} = 1), and Ca/HEPES, respectively. At each time point, 10 µl of cells were removed and immobilised on a microscope slide comprising a thin layer of 1% agarose Ca/HEPES. Samples were imaged on a Nikon Eclipse Ti-E inverted fluorescence microscope with a Plan Apo 100x/1.45 Ph3 objective lens and Andor Neo sCMOS camera. An exposure time of 2 s was used to detect mCherry fluorescence. Images were acquired with Nikon NIS software and subsequently analysed using the Fiji distribution of ImageJ software (Schindelin *et al.*, 2012). For measurements of cell curvature, images were analysed using the MicrobeJ plug-in for ImageJ (Ducret *et al.*, 2016).

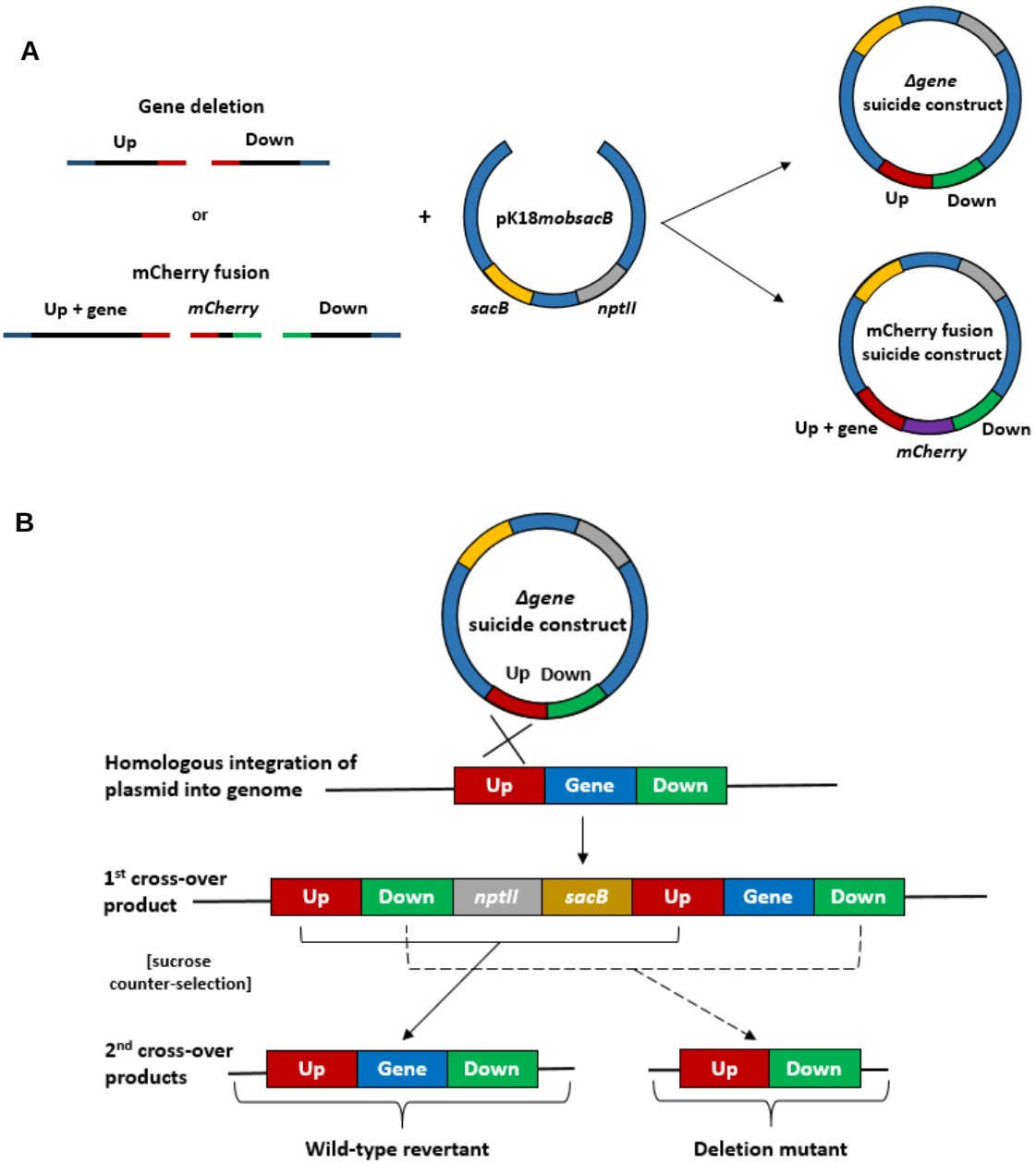

Figure 14. Cloning strategy to construct gene deletion and mCherry fusion strains

A. DNA fragments are amplified by PCR using primers which generate fragments with overlapping ends. 'Up' and 'Down' refer to the 1 kb regions up- and downstream of the gene, respectively. Fragments are then combined with the cut vector pK18*mobsacB* in a Gibson Assembly reaction to produce suicide constructs containing a kanamycin-resistance marker (*nptII*). **B**. Suicide constructs (only gene deletion construct shown for simplicity but the mechanism also applies to mCherry fusions) are then conjugated into the *B. bacteriovorus* genome, causing a first cross-over event in which the plasmid integrates into the genome. Counter-selection in sucrose triggers a second cross-over event as *sacB* converts sucrose to a toxic product, resulting in genomic-excision of the plasmid, and generation of either a wild-type revertant or the desired mutant. Revertants and mutants can subsequently be distinguished by PCR.

10. Results

10.1. Bioinformatics analyses

Bd1402 is a 265 amino acid protein with a predicted molecular weight of 28 kDa and Bd1075 is a 332 amino acid protein with a molecular weight of 38 kDa. Both proteins have been annotated as L,D-transpeptidases due to the prediction of an LDTP catalytic domain within each protein (Figure 15A). To predict protein localisation within the cell, protein sequences were entered into the online signal peptide prediction server SignalP 4.1. Both Bd1402 and Bd1075 contained an N-terminal signal peptide sequence (Appendix Figure 27). The presence of a signal peptide suggests that a protein is capable of Sec-dependent translocation across the cytoplasmic membrane and into the periplasmic space. Therefore it is possible that Bd1402 and Bd1075 are translocated into the periplasm, however, subsequent secretion across the outer membrane into the extracellular environment of the bdelloplast cannot be determined by bioinformatics analyses. Neither Bd1402 nor Bd1075 share an LDTP homologue in *E. coli* at the genome level of homology, however, a sequence alignment of Bd1402 and Bd1075 with the 6 known *E. coli* LDTPs reveals regions of amino acid conservation, including conservation of the catalytic cysteine residue (Appendix Figure 28).

Although the crystal structure of Bd1402 has been solved by Dr Lovering, the structure of Bd1075 remains unknown, however a predicted model structure aligns very well (Tm score = 0.889, where 1 = perfect match) with the crystallised L,D-carboxypeptidase, Csd6, of *H. pylori* (Figure 15B). Kim *et al.* (2015) suggest that the L,D-carboxypeptidase activity of Csd6 (which, like Bd1075, was originally classified as an LDTP) is due to differently-shaped active site pocket dictated by longer catalytic domain loops I and III. A sequence alignment of Bd1075 against Csd6 revealed that loops I and III of Bd1075 are of the same length as Csd6 (Figure 16). Predicted similarity between Bd1075 and Csd6 is supported by the recent evidence that Bd1075 shows L,D-carboxypeptidase activity *in vitro.* The homology between Bd1075 and Csd6 led to the hypothesis that Bd1075 may fulfill similar roles in *B. bacteriovorus* to Csd6 in *H. pylori* (cell shape-determination and flagellar regulation).

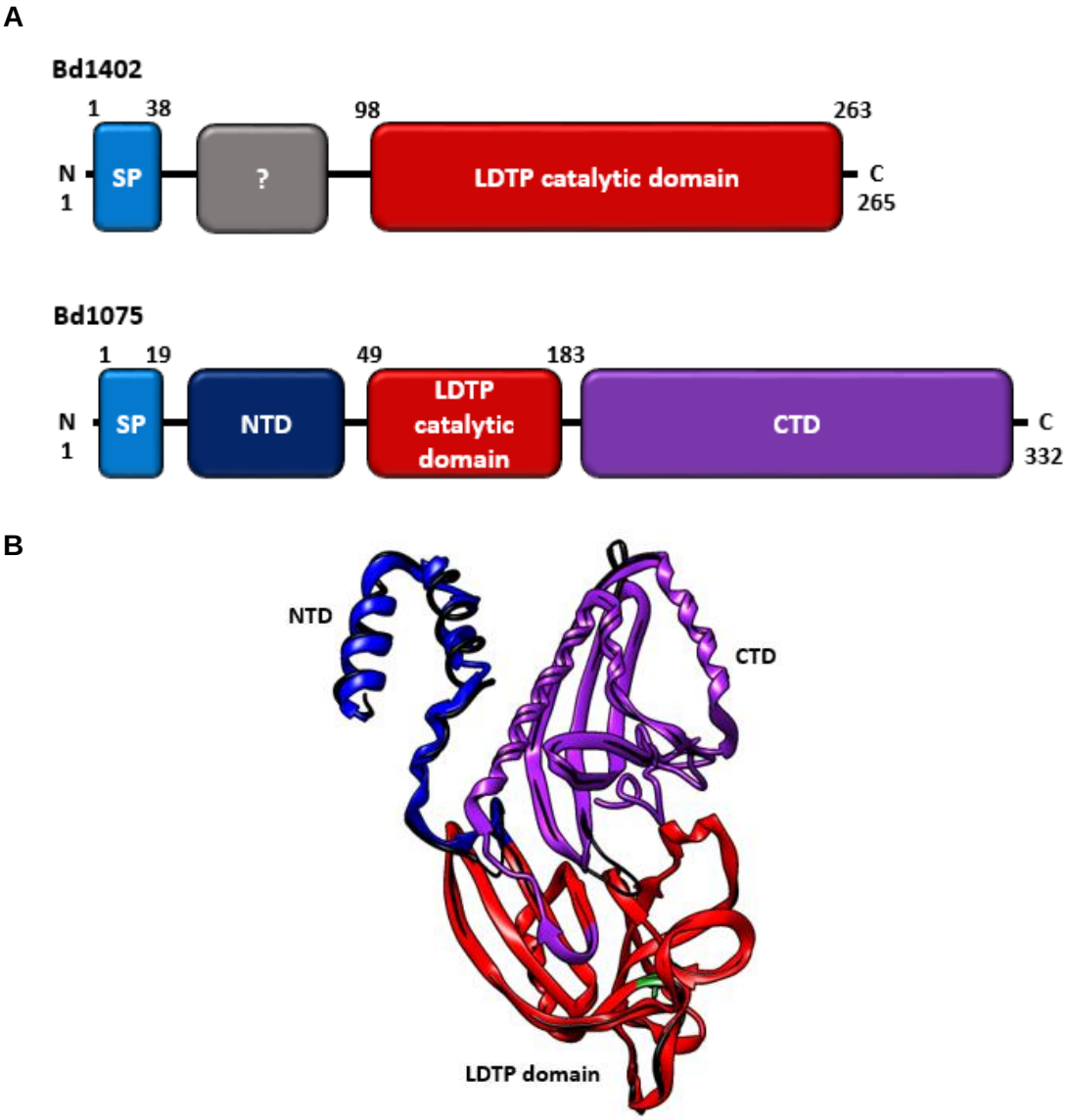

Figure 15. Predicted structures of Bd1402 and Bd1075

A. The predicted domain structures of Bd1402 and Bd1075 are depicted using data collected from the Pfam database (Sonnhammer *et al.*, 1997). Numbers indicate amino acid position. N & C: N- and C-termini. SP: signal peptide, the presence of which was predicted by the online server SignalP 4.1 (Petersen *et al.*, 2011). ?: potential unknown domain, NTD: N-terminal domain, CTD: C-terminal domain. LDTP catalytic domains are shown in red. **B.** Structure alignment between a 3D model prediction of Bd1075 (chain coloured by domain structure, catalytic cysteine residue depicted in green) and the most similar template in the PDB (4xzzA: *H. pylori* Csd6, black chain). Tm score = 0.889 where 1 = perfect match between two structures. The Bd1075 model prediction and alignment were generated using the I-TASSER server (Zhang, 2008).

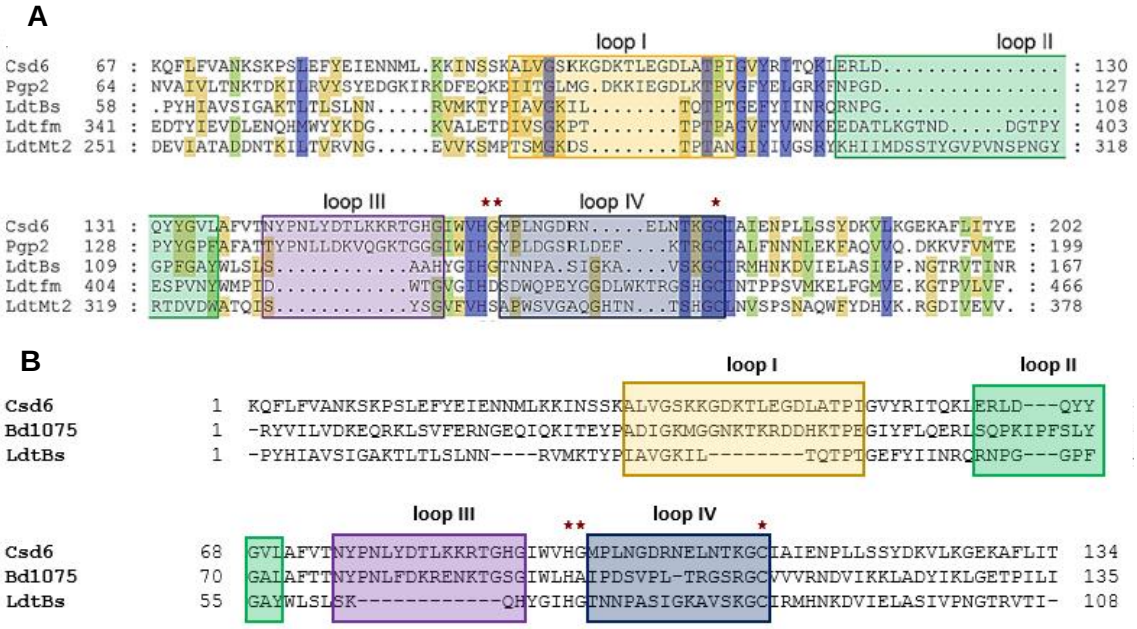

Figure 16. Sequence alignment of L,D-carboxypeptidase and L,D-transpeptidase domains

A. Sequence alignment of the L,D-carboxypeptidase domains of Csd6 (*H. pylori*) and Pgp2 (*Campylobacter jejuni*) against the L,D-transpeptidase domains of LdtBs (*Bacillus subtilis*), Ldtfm (*Enterococcus faecium*), and LdtMt2 (*Mycobacterium tuberculosis*). Red asterisks indicate the catalytic triad (His-160, Gly-161, and Cys-176 in Csd6). Loops I-IV are shown in coloured boxes. Loops I and III are longer in the L,D-carboxypeptidases Csd6 and Pgp2. (Kim *et al.*, 2015). **B**. Sequence alignment of the catalytic domains of Csd6, Bd1075 and LdtBs, showing that the extension of loops I and III is also present in Bd1075. Sequence alignments were generated using PROMALS3D (Pei and Grishin, 2014).

10.2. Gene expression of *bd1402* and *bd1075* during predation

RT-PCR was performed to determine the timing of expression of each LDTP during a predatory cycle as this may provide an indication as to the role of the enzyme (Figure 17). mRNA was isolated from *B. bacteriovorus* HD100 predation on *E. coli* S17-1 prey at different time points across the predatory cycle. *bd1402* demonstrated low constitutive gene expression during predation with a slight expression peak between ~15-45 min, a time period during which *B. bacteriovorus* attaches to and invades the *E. coli* prey cell. *bd1075*, in contrast, demonstrated high constitutive and unvarying gene expression throughout the predatory cycle.

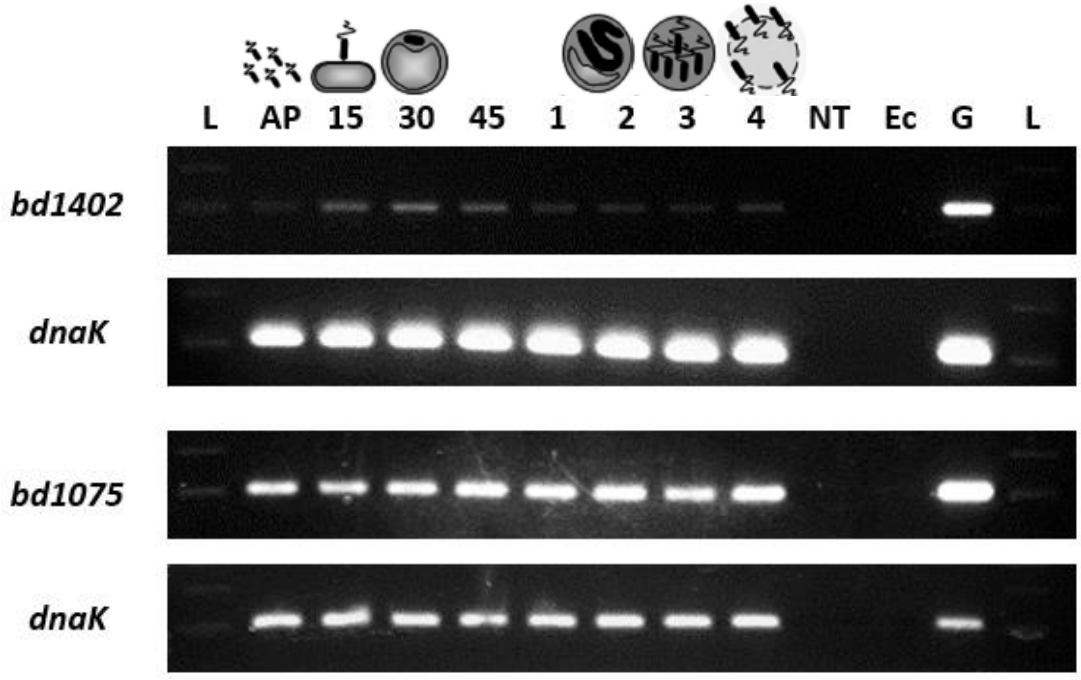

Figure 17. RT-PCR showing gene expression of *bd1402* and *bd1075* during predation

RNA template was previously isolated from a synchronous predation of *B. bacteriovorus* HD100 on *E. coli* S17-1 prey at time points stated in the figure above. Gene specific primers listed in Appendix Table 1 were used to amplify ~100 bp fragments internal to each gene. L: 100 bp ladder, AP: attack-phase, 15-45 and 1-4: min and h post-infection, respectively, NT: no template H_2O control, Ec: *E. coli* S17-1 control RNA, G: wild-type *B. bacteriovorus* HD100 genomic DNA positive control. Control gene *dnaK* was constitutively expressed throughout predation in all reactions and two independent biological repeats were performed for each gene.

10.3. Construction of knockout and mCherry fusion strains

Multiple overlapping DNA fragments were amplified by PCR using wild-type *B. bacteriovorus* HD100 gDNA and pAKF56 (plasmid containing *mCherry* gene) templates. PCR products were then gel purified and ligated into the suicide vector pK18*mobsacB* in a Gibson Assembly reaction. For gene deletions, the desired insert comprised 1 kb of upstream and 1 kb of downstream gene flanking regions (Figure 18 A & B). For mCherry fusions, the desired insert contained the gene of interest from which the stop codon had been removed, *mCherry*, and 1 kb of each flanking region (Figure 18 C & D).

Plasmid constructs were transformed into *E. coli* DH5α for initial diagnostic restriction digests, followed by *E. coli* S17-1 for further diagnostic digests, and were finally verified by Sanger sequencing. Sequencing also revealed that a point mutation of A to C (resulting in an amino acid change of histidine to proline) had been introduced into the *Δbd1402* construct but that this was 5 bases upstream of the *bd1402* gene start codon. However, an amino acid change would have no consequence in a deletion construct and the neighbouring gene, *bd1403*, is both transcribed divergently and is 488 bp upstream from *bd1402*, therefore the transcription of *bd1403* should not be affected (Figure 19A). Similarly, a possible point deletion of one A from a string of 9 As ~16 bp downstream from the *mCherry* gene in the *bd1075-mCherry* construct was detected, however this is very unlikely to have an effect on the transcription of the *bd1075-mCherry* fusion, and the neighbouring gene, *futA*, is both transcribed divergently and is 67 bp downstream from *bd1075* (Figure 19B). Consequently, all 4 constructs were carried forward and conjugated in *B. bacteriovorus* HD100, resulting in single cross-over kanamycin-resistant merodiploid strains.

Merodiploid strains then entered successive rounds of predatory growth on *E. coli* prey in the presence of sucrose. Sucrose imposes a selective pressure upon *B. bacteriovorus* to excise the genome-integrated plasmid which contains the gene *sacB*, encoding the enzyme levansucrase which converts sucrose to a product toxic to the cell. Plasmid excision results in a second cross-over event in which either the desired mutant or wild-type revertant is generated. Following

at least 5 rounds of growth in sucrose, successful double cross-over strains of *B. bacteriovorus* were identified by sensitivity to kanamycin.

Eight kanamycin-sensitive clones were screened from predatory cultures by PCR for *Δbd1402, bd1402-mCherry and bd1075-mCherry*, and 7/8, 4/8 and 4/8 were putative mutants, respectively. For *Δbd1075*, however, 50 kanamycin-sensitive clones had to be screened until a putative mutant could be identified, suggesting that this gene may be difficult to delete in host-dependent predatory cultures. Following this initial PCR screen with low-quality template, PCR-positive clones were cultured in 10 ml lysates, from which gDNA was extracted. Final confirmatory PCRs were then performed using gDNA template and primers designed to anneal to gDNA at least 100 bp upstream and downstream of the region of homologous recombination. Putative *Δbd1402* and *Δbd1075* strain PCR products were ~ 1 kb smaller than the wild-type, suggesting that both genes were successfully deleted (Figure 20). Similarly, putative *bd1402-mCherry* and *bd1075-mCherry* strain products were ~ 711 bp larger than the wild-type, suggesting that both strains were successfully constructed. PCR products were subsequently gel purified and sent for Sanger sequencing which provided final verification of the successful construction of the 4 new *B. bacteriovorus* HD100 strains.

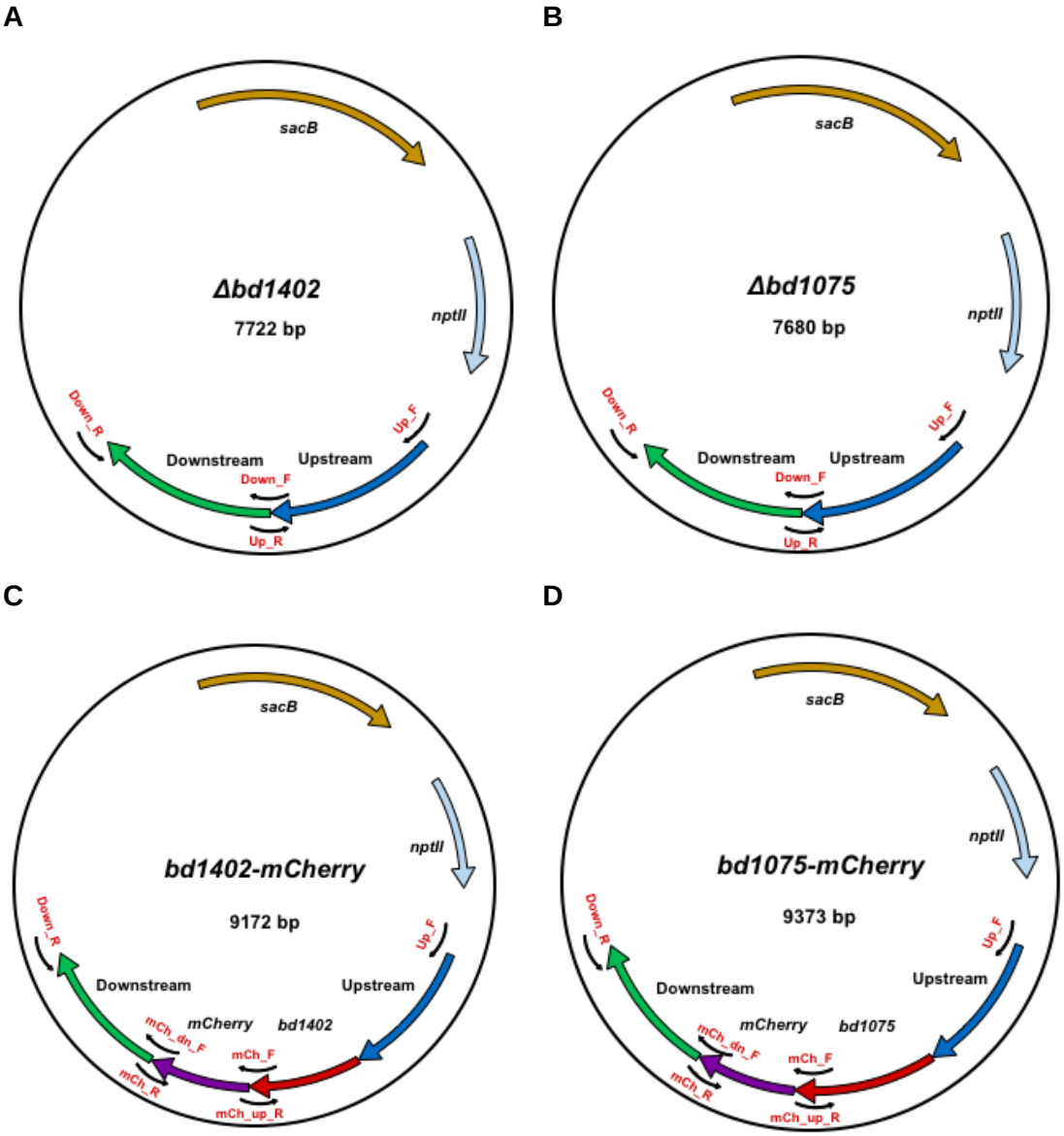

Figure 18. Suicide construct plasmid maps and primer positions

1 kb of upstream and downstream gene regions were cloned into the suicide vector pK18*mobsacB* to generate the plasmids *Δbd1402* **(A)** and *Δbd1075* **(B)** which contain a deletion allele of each gene. Two further plasmids containing a C-terminal mCherry tag of each gene were constructed: *bd1402-mCherry* **(C)** and *bd1075-mCherry* **(D)**. *sacB*: gene encoding the enzyme levansucrase which converts sucrose to a toxic product. *nptII*: antibiotic resistance marker that confers resistance to kanamycin. Primers used to generate overlapping fragments for Gibson Assembly are indicated by black arrows with red names and are listed in Appendix Table 3.

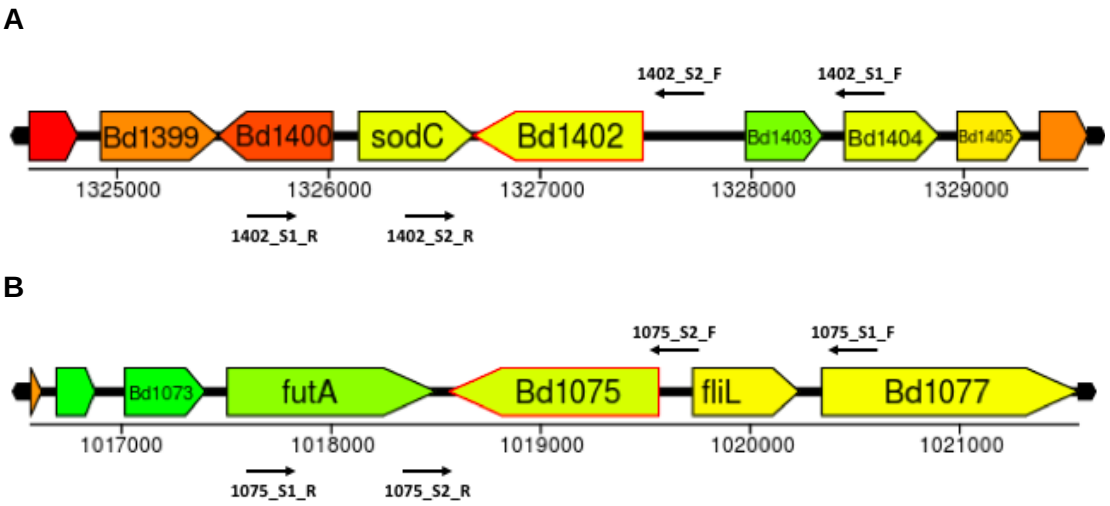

Figure 19. Regions around *bd1402* and *bd1075* on the *B. bacteriovorus* HD100 genome

5 kb genomic regions showing the genetic loci of *bd1402* **(A)** and *bd1075* **(B)**. *bd1403* is both 488 bp upstream and transcribed divergently from *bd1402* and should therefore be unaffected by the point mutation introduced 5 bp upstream from the *bd1402* deletion allele. Similarly, *futA*, 67 bp downstream from *bd1075* should be unaffected by a possible point deletion ~ 16 bp downstream from the *bd1075-mCherry* construct. Arrows indicate genomic flanking primers used to screen and subsequently sequence potential successful mutants. Primers are listed in Appendix Table 3. Numbers refer to bp from the origin of replication. Data were retrieved from the *x*BASE genomic database (Chaudhuri and Pallen, 2006).

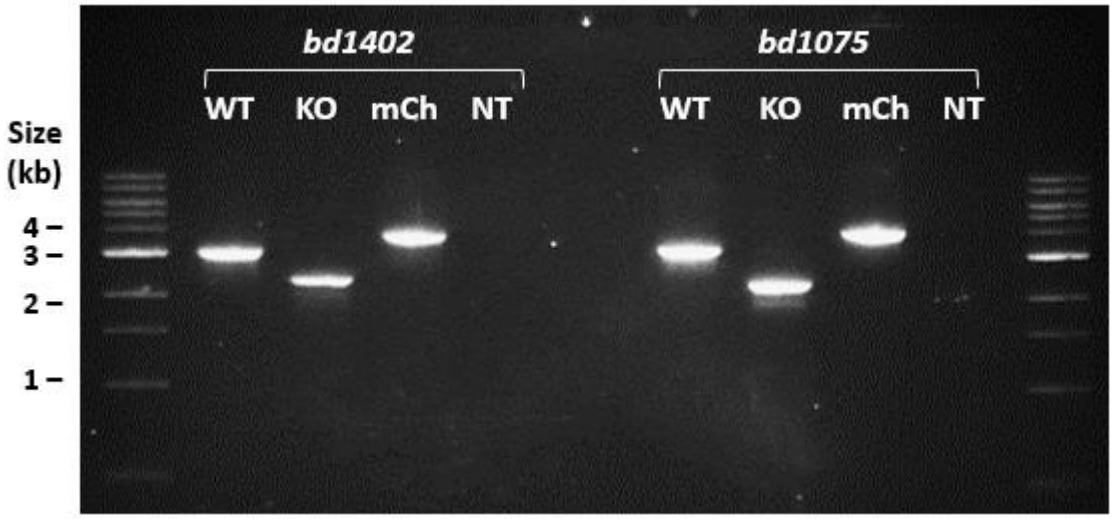

Figure 20. *bd1402* and *bd1075* knockouts and mCherry fusions were verified by PCR using primers shown in Figure 19.

gDNA isolated from *B. bacteriovorus* HD100 lysates served as template in PCR reactions containing primers 1402_S1_F/R or 1075_S1_F/R designed to anneal >100 bp away from the site of homologous recombination into the genome (Figure 19). WT: wild-type gDNA. NT: No template H_2O negative control. *bd1402* bands were all of the expected sizes: wild-type (WT) = 3,097 bp, knockout (KO) = 2,355 bp, and mCherry fusion (mCh) = 3,805 bp. *bd1075* bands were also of the correct sizes: WT = 3,319 bp, KO = 2,334 bp, and mCh = 4,027 bp. These KO and mCh clones were then sequenced to confirm the successful construction of *bd1402* and *bd1075* knockout and mCherry fusion strains.

10.4. Predation time course assays

The timing of protein production and the cellular address to which a protein localises can provide clues as to its function, therefore the fluorescence of mCherry-tagged Bd1402 and Bd1075 was monitored at key time points during predation (Figures 21 & 22). Bd1402 appears to be produced from ~ 45 min, with fluorescence slightly increasing until prey cell lysis at 4-5 h. Localisation of Bd1402 fluorescence in the bdelloplast further suggests Bd1402 is secreted into the prey periplasm in which it may modify the prey cell wall. Bd1075-mCherry, in contrast, is highly fluorescent throughout all stages of predation within the *B. bacteriovorus* predator cells themselves, suggesting that Bd1075 is a predator self-modifying enzyme. Images acquired from attack-phase and 3 h time points that support these hypotheses are highlighted in Figure 23. Predation time courses were also performed for *Δbd1402* and *Δbd1075* (Figure 24), however, no significant phenotypic differences in the predatory process were observed for these deletion strains. These predation experiments could only be performed once due to the time constraints of this project and should therefore be repeated. The *Δbd1402* and *Δbd1075* time courses would benefit from repetition using lower starting concentrations of *B. bacteriovorus* predator cells as a high number of attack-phase *B. bacteriovorus* cells were present throughout the experiment. As a consequence, the difference in the number of invaded prey (bdelloplasts) vs non-invaded prey could not be observed nor quantified.

Figure 21. Predation time course of *B. bacteriovorus* HD100 *bd1402-mCherry*

A synchronous predation of *B. bacteriovorus* HD100 *bd1402-mCherry* on *E. coli* S17-1 prey was prepared and images captured at the time points 0-45 min and 1-5 h post-infection. An exposure time of 2 s was used for acquisition of mCherry fluorescence. One experiment was performed. Scale bar: 2 µm.

Figure 22. Predation time course of *B. bacteriovorus* HD100 *bd1075-mCherry*

A synchronous predation of *B. bacteriovorus* HD100 *bd1075-mCherry* on *E. coli* S17-1 prey was prepared and images captured at the time points 0-45 min and 1-5 h post-infection. An exposure time of 2 s was used for acquisition of mCherry fluorescence. One experiment was performed. Scale bar: 2 µm.

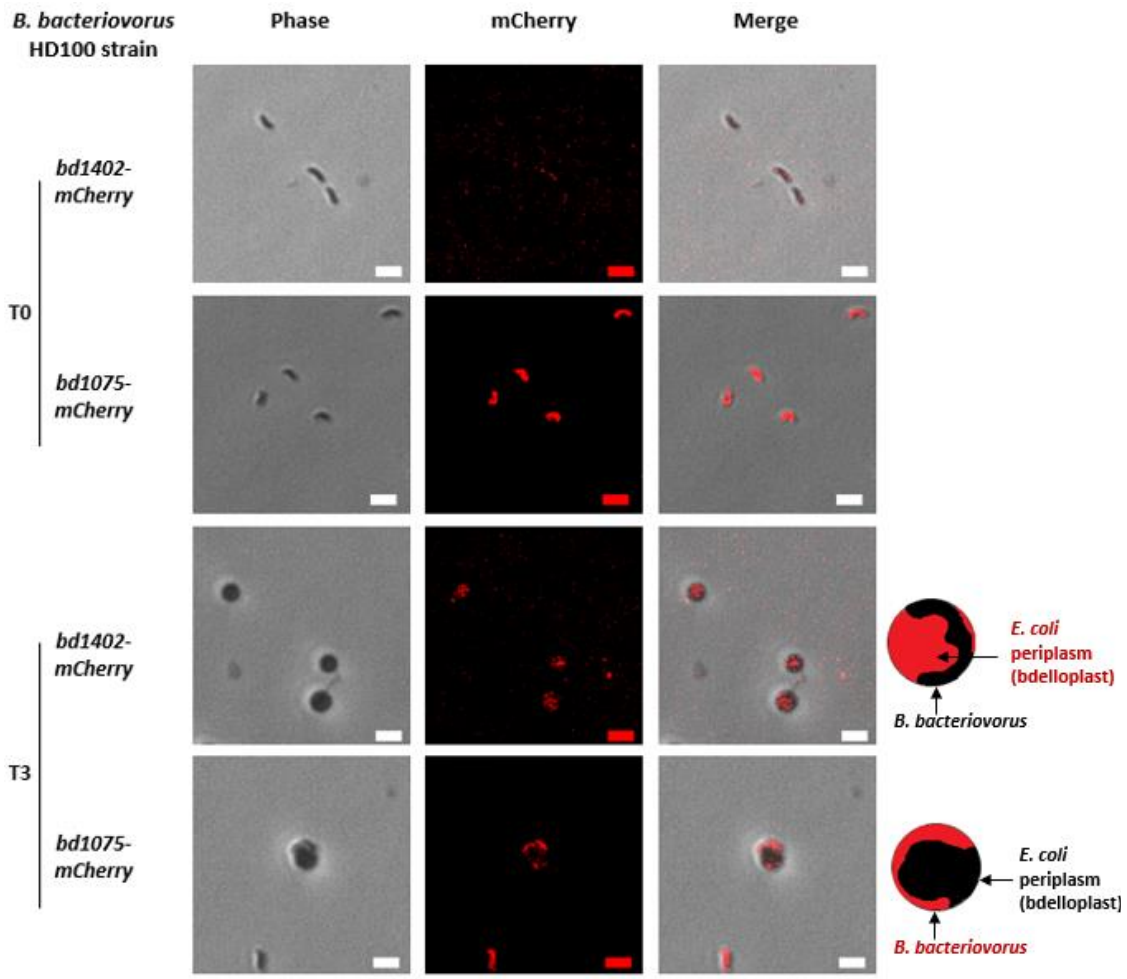

Figure 23. Magnified fluorescence time course images from Figures 21 & 22

Magnified images acquired at two particular time points during the fluorescent time courses shown in Figures 21 & 22 are depicted. T0: Attack-phase *B. bacteriovorus* HD100 cells scouting for *E. coli* prey to invade. Fluorescence of Bd1075-mCherry within the vibroid-shaped *B. bacteriovorus* cells can clearly be observed in contrast to Bd1402-mCherry attack-phase cells which do not appear fluorescent. At T3 (3 hours into the predatory cycle), the *B. bacteriovorus* filament begins to septate into new progeny cells. Fluorescence of Bd1075-mCherry at T3 appears to represent this dividing filament, suggesting that Bd1075 remains within the predator. Bd1402-mCherry fluorescence, however, appears more rounded instead of filamentous, supporting the idea that Bd1402 is secreted into the bdelloplast. Cartoon drawings adjacent to T3 'merge' images illustrate these observations. Scale bar: 2 µm.

Figure 24. Preliminary predation time course analyses *of B. bacteriovorus* HD100 *Δbd1402* and *Δbd1075* strains

Synchronous predations of *B. bacteriovorus* HD100 *Δbd1402* and *Δbd1075* on *E. coli* S17-1 prey were prepared and images captured at the time points 0-45 min and 1-5 h post-infection. One experiment was performed per strain. Scale bar: 2 µm.

10.5 Characterisation of host-independent mutant strains

Host-independent (HI) *bd1402*-mCherry, *bd1075*-mCherry, *Δbd1402* and *Δbd1075* strains were derived from HD strains. To derive HI strains, 50 ml of each HD strain were cultured overnight, filtered to remove *E. coli*, and then incubated on plates until small HI colonies appeared. Host-independent *B. bacteriovorus* cells grow as a mixed population of mainly sessile cells with diverse morphologies and mechanisms of replication. Replication can occur by the very slow process of sequential budding of new attack-phase cells from an HI filament. Alternatively, HI filamentous cells can form an unusual replicative structure in which the end cell of the filament is sacrificed to form a rounded bdelloplast-like structure called an 'autobdelloplast' (Hobley *et al.*, 2012b). The adjacent cell then elongates into the autobdelloplast and divides to produce 2 or 3 small, motile attack-phase cells which are then released. This cannibalistic mechanism of replication may function to provide a developmental chamber for rapid, motile attack-phase cell release. Localisation of peptidoglycan-modifying enzymes within HI cells undergoing autobdelloplast-mediated replication may be suggestive of protein function, therefore HI strains containing mCherry-tagged *bd1402* and *bd1075* were examined by microscopy (Figure 25). Bd1075-mCherry localised to the entire filament length, however Bd1402-mCherry was solely fluorescent in the rounded autobdelloplast structures which could support the hypothesis that Bd1402 is secreted into the periplasm of the prey cell in which it could modify the prey cell wall during predation.

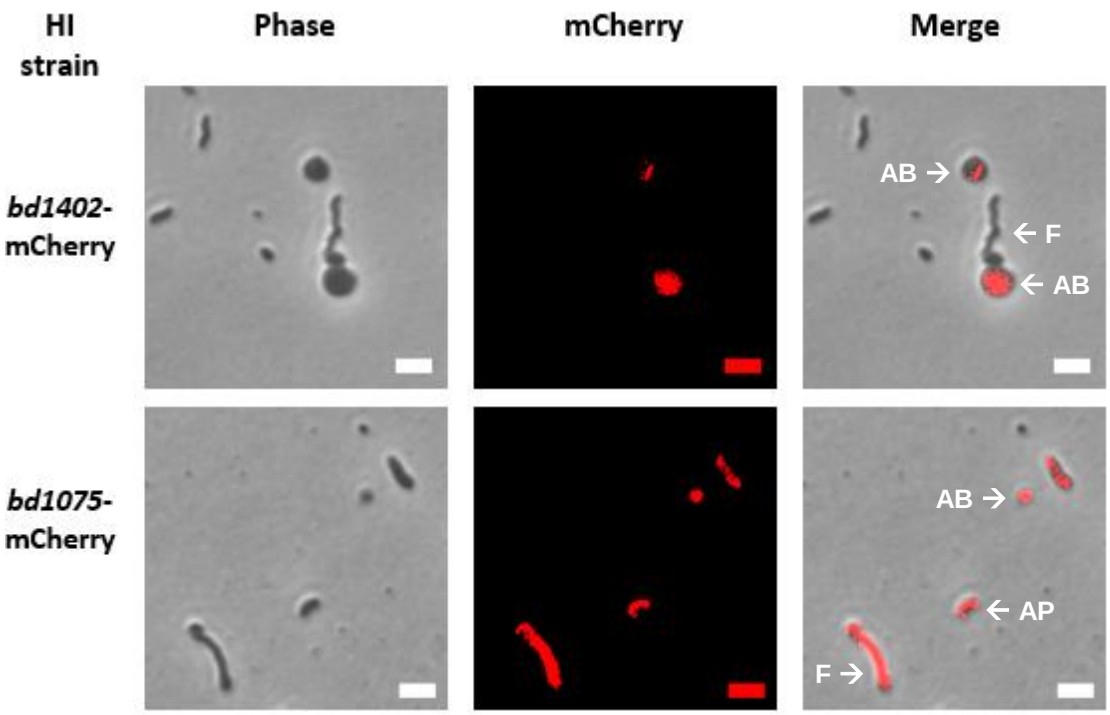

Figure 25. Preliminary microscopy of host-independent *bd1402* and *bd1075* strains

Host-independent (HI) strains were cultured overnight and images taken on a fluorescence microscope. An exposure time of 2 s was used for acquisition of mCherry fluorescence. One experiment was performed for each strain. Autobdelloplasts (AB), filamentous cells (F) and attack-phase cells (AP) are indicated by arrows in the merge channel. Scale bar: 2 µm.

10.6. Predatory *B. bacteriovorus* HD100 *Δbd1075* is non-vibroid shaped

B. bacteriovorus HD100 WT and *Δbd1075* strains were revived from frozen stocks, cultured on *E. coli* S17-1 prey for 24 h and then examined microscopically. *B. bacteriovorus* HD100 wild-type cells are vibroid in shape, however cells of the HD100 *Δbd1075* mutant were straight rods instead of curved (Figure 26A). Curvature of 450 cells was subsequently quantified using the MicrobeJ plug-in for Fiji and this revealed a statistically significant difference in curvature between the wild-type and *Δbd1075* mutant (Figure 26B). These data suggest that Bd1075 is a cell shape-determinant of *B. bacteriovorus* predatory cells.

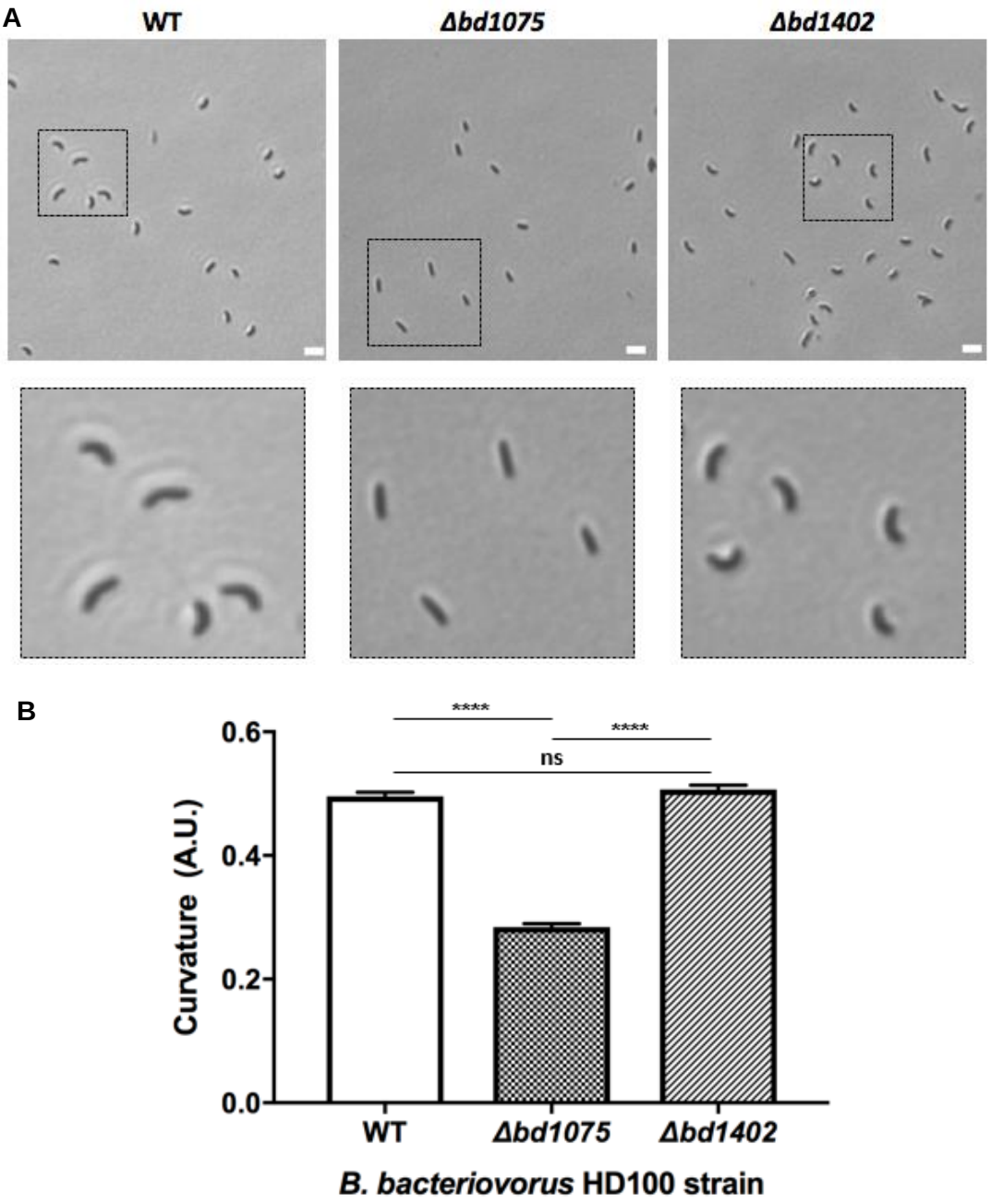

Figure 26. *B. bacteriovorus* HD100 *Δbd1075* cells are non-vibroid shaped

B. bacteriovorus HD100 strains were cultured on *E. coli* S17-1 prey and images were acquired after 24 h **(A)**. Scale bar: 2 µm. Boxed regions are magnified in the second row of images displayed. Wild-type (WT) and *Δbd1402* cells were vibroid-shaped, however *Δbd1075* cells were straight and non-vibroid. Cell curvature was then quantified by the MicrobeJ plug-in for Fiji software **(B)**. A.U.: arbitrary units. ns: not significant. Data represent 6 biological replicates from one experiment. n = 450 cells per replicate. Error bars represent standard error of the mean. There was a statistically significant difference between the curvature of WT and *Δbd1075* cells (**** = $p<0.0001$), as determined by the Mann-Whitney test.

11. Discussion

L,D-transpeptidases are closely linked to antibiotic resistance and were originally discovered in an ampicillin-resistant strain of the Gram-positive bacterium *Enterococcus faecium* (Mainardi *et al.*, 2000). LDTPs have since been identified in a wide range of Gram-positive and Gram-negative bacteria, including *Mycobacterium tuberculosis* and *Helicobacter pylori*, for which LDTP crystal structures have been obtained (Brammer Basta *et al.*, 2015; Kim *et al.*, 2015). Critically, unlike the common D,D-transpeptidases that catalyse 4-3 bonds, LDTPs are penicillin-insensitive, and therefore the formation of 3-3 bonds may represent a mechanism of resistance to some β-lactam antibiotics (Mainardi *et al.*, 2005). In *E. coli,* 3-3 *m*-DAP cross-links account for 3% and 10% of total cross-links in log phase and stationary phase, respectively, suggesting that 3-3 bond formation increases in response to cellular stress (Schwarz *et al.*, 1969). Deletion of the 3 *E. coli* LDTPs which covalently bond Braun's lipoprotein to peptidoglycan resulted in loss of outer membrane stability, whereas deletion of the 2 LDTPs that form 3-3 *m*-DAP cross-links between stem peptides did not cause an notable phenotype (Sanders and Pavelka, 2013). However, deletion of all 5 LDTPs disrupted cell growth when cells were starved of *m*-DAP (Sanders and Pavelka, 2013).

In comparison to *E. coli*, *B. bacteriovorus* has an unusually large number of LDTPs (19) that are predicted to carry out diverse roles during its predatory lifecycle. *bd1402* was most highly expressed 15-45 min into the predatory cycle. For *B. bacteriovorus* LDTPs, a delay between transcriptional expression peak and microscopic observation of fluorescent fusion proteins has previously been noted (unpublished observations from our lab). This could be due to either a delay in protein production or a requirement for sufficient protein accumulation prior to detection by microscopy. The *bd1402* RT-PCR therefore suggested that Bd1402 is produced from at least ~45 min into predation and this was then corroborated by visualisation of Bd1402-mCherry from 45 min until the end of the predatory cycle.

Classification of a protein as an LDTP is dependent upon the presence of an L,D-transpeptidase catalytic domain containing a conserved cysteine residue in

the active site (in contrast to serine in D,D-transpeptidases) (Mainardi *et al.*, 2005). The LDTP catalytic domain can, however, be repurposed to catalyse alternative biochemical reactions such as carboxypeptidation or endopeptidation. The crystal structure of Bd1402 suggests that the protein actually uses L,D-endopeptidase activity to hydrolyse 3-3 *m*-DAP cross-links (personal communication from Dr Lovering). Data from this study further revealed that Bd1402 is secreted across the outer membrane of *B. bacteriovorus* into the *E. coli* periplasm of the bdelloplast. Future experiments should therefore aim to validate the putative L,D-endopeptidase activity of Bd1402 upon the *E. coli* cell wall. Validation of enzyme activity requires purification of the bdelloplast peptidoglycan sacculus following predation, however the bdelloplast sacculus is lysed upon *B. bacteriovorus* exit. Lambert *et al.* (2016) discovered that deacetylation of the prey cell wall by *B. bacteriovorus* marks the wall for destruction at the end of predation and that deletion of 2 deacetylases (*Δbd0468/Δbd3279*) from *B. bacteriovorus* results in the persistence of bdelloplast sacculi following predator exit. The *Δbd1402* suicide plasmid could therefore be conjugated into the double deacetylase mutant to give the triple mutant *Δbd1402*/*Δbd0468/Δbd3279* which would allow purification of *E. coli* peptidoglycan sacculi at the end of predation. Comparison of muropeptide profiles between sacculi resulting from *B. bacteriovorus* wild-type and *Δbd1402* mutant predations would reveal the presence/absence of different peptidoglycan subunits, from which earlier enzymatic activities can deduced (Desmarais *et al.*, 2013).

This project revealed that Bd1075, which comprises its own LDTP group in *B. bacteriovorus* (group 6) was produced constitutively within the predator cell itself throughout the predatory lifecycle. Furthermore, in contrast to vibroid wild-type cells, a host-dependent *Δbd1075* deletion strain of *B. bacteriovorus* resulted in straight, non-vibroid cells that were still predatory. Together, these data identify Bd1075 as the first self-modifying LDTP of *B. bacteriovorus* and suggest that Bd1075 is a determinant of *B. bacteriovorus* cell shape.

Bacterial cell shape is defined by the cell wall, however, the cytoskeleton can indirectly but critically influence cell shape by guiding the action of cell wall

biosynthetic enzymes. MreB is a bacterial actin-like cytoskeletal element, the action of which defines rod-shaped bacteria (Jones *et al.*, 2001). MreB is tethered to the inner membrane protein RodZ, and interacts with MreC and MreD to form a scaffold that can position periplasmic peptidoglycan enzymes like PBPs (Divakaruni *et al.*, 2007; Kruse *et al.*, 2005; van den Ent *et al.*, 2010). Peptidoglycan synthesis is thought to drive the movement of MreB filaments around the circumference of the cell wherein MreB localises to and straightens regions of negative curvature (van Teeffelen *et al.*, 2011). *B. bacteriovorus* contains 2 essential rod-shape-determining MreBs: MreB1 and MreB2. MreB1 perturbation resulted in inability of the predator to elongate within the bdelloplast, and MreB2 perturbation resulted in release of attack-phase cells with elongated, branched and spherical morphologies (Fenton *et al.*, 2010a).

Bacterial intermediate filament-like (IF-like) cytoskeletal elements can also define cell shape of which the best-described example is crescentin (CreS) from the crescent-shaped α-proteobacterium *Caulobacter crescentus* (Ausmees *et al.*, 2003). CreS localises to the inner membrane where it exerts a compressive force on the cell wall, reducing peptidoglycan synthesis upon one side of the cell, and ultimately inducing cell curvature (Cabeen *et al.*, 2009). IF-like proteins such as CreS frequently contain coiled-coil repeat domains. A systematic search for proteins containing coiled-coil repeat domains in *B. bacteriovorus* yielded one hit: *bd2697* (also called Ccrp), which shares limited homology to *C. crescentus* CreS (21%) (Fenton *et al.*, 2010c). Deletion of *ccrp* caused minor cellular deformations but did not alter the vibroid cell shape. Data collected in this project instead present the peptidoglycan-active enzyme, Bd1075, as the determinant of vibroid cell shape.

There are many examples of peptidoglycan-active enzymes (particularly hydrolases) influencing bacterial morphogenesis. In *Campylobacter jejuni*, D,L-carboxypeptidase Pgp1 and L,D-carboxypeptidase Pgp2 contribute to helical cell shape (Frirdich *et al.*, 2012, 2014). Similarly, in *H. pylori* 5 endo/carboxypeptidases, Csd1-4 and Csd6 collectively define helical morphology (Sycuro *et al.*, 2010, 2012, 2013). The predicted structure of Bd1075 aligns well with *H. pylori* Csd6 which contains an LDTP domain but acts

as an L,D-carboxypeptidase to cleave tetrapeptides to tripeptides. Csd6 also deglycosylates the flagellin FlaA to regulate motility, suggesting a possible additional role for Bd1075 associated with flagellar motility, although *Δbd1075* cells appeared to swim normally (data not shown) (Asakura *et al.*, 2010).

Future experimental work will involve complementation of the *B. bacteriovorus* HD100 *Δbd1075* deletion by expression of Bd1075 *in trans*, which should cause reversion to the vibroid wild-type phenotype. We will also use biochemical and microscopic techniques to investigate the mechanism by which Bd1075 generates cell curvature in *B. bacteriovorus*. Initial experiments should further examine the enzymatic activities of Bd1075. This would involve the comparison of muropeptide profiles between the *B. bacteriovorus* peptidoglycan sacculi of wild-type and *Δbd1075* strains. These results would be complemented by muropeptide analysis of *B. bacteriovorus* sacculi that have been treated *in vitro* with purified Bd1075. Together these data would experimentally validate the enzymatic activities of Bd1075. In this project, fluorescently-tagged Bd1075 appeared to localise to the entire attack-phase predator cell, suggesting that *B. bacteriovorus* continues to produce Bd1075 following curve formation during intra-periplasmic growth and division. Retaining Bd1075 in fully-formed attack-phase cells may be a strategy to resist sudden osmotic changes within the environment. Curve formation would presumably occur at the point at which the long *B. bacteriovorus* filament septates into multiple progeny cells (~3-4 h into predation). Bd1075-mCherry localisation at this time point was difficult to resolve, therefore this investigation would benefit from utilising super-resolution microscopy such as 3D-structured illumination microscopy (3D-SIM) to more accurately visualise the localisation of Bd1075.

Investigations into Bd1075 localisation and function will hopefully provide an understanding of *how B. bacteriovorus* generates self-curvature, however they do not tackle the fundamental question of *why* this bacterium is curved. The helical morphology of *H. pylori* is believed to facilitate efficient motility through the gastric mucosa which is necessary for gastrointestinal tract colonisation (Sycuro *et al.*, 2010). The periplasmic polymer CrvA was recently identified as the cell curvature-determinant of *Vibrio cholerae* (Bartlett *et al.*, 2017). CrvA-

mediated curvature increased *V. cholerae* motility through dense soft-agar matrices and promoted colonisation in animal models, suggesting that vibroid morphology is important for *V. cholerae* motility in viscous environments, and consequently, pathogenesis. We hypothesise that, while not essential for predation, the curved shape of *B. bacteriovorus* may contribute towards motility through dense aqueous environments, or help overcome repulsive physical forces in close proximity to prey cells, ultimately aiding attachment to prey. Curvature could additionally facilitate entry to and/or exit from prey cells. Future experiments will be designed to test these hypotheses. Although the question of why bacteria have certain morphologies may be difficult to answer, shape is evolutionarily conserved within different groups, and therefore must confer a selective advantage which benefits bacterial survival (Young, 2006, 2007).

12. Conclusions

This project aimed to investigate the function of two unique L,D-transpeptidases of *B. bacteriovorus* HD100: *bd1402* and *bd1075*. Initial gene expression analysis revealed that *bd1402* is constitutively expressed at low levels throughout the predatory cycle, with a small but observable expression peak between ~ 15 and 45 min. *bd1075* was constitutively and highly expressed during predation, including within attack-phase cells. LDTP-tagging with the fluorescent protein mCherry showed that Bd1402 is secreted into the periplasm of the prey in which it may modify the bdelloplast cell wall. This observation was supported by fluorescence microscopy showing that, in host-independent cells, Bd1402 localised solely to bdelloplast-like replicative structures. Bd1075, in contrast, localised to *B. bacteriovorus* predator cells throughout predation, suggesting that the enzyme modifies the predator cell wall. Unmarked gene deletions revealed that *B. bacteriovorus* HD100 *Δbd1075* cells were straight and non-vibroid in shape, compared to curved, vibroid wild-type cells. These data suggest that Bd1075 is a cell-shape determinant of *B. bacteriovorus* HD100. Future experiments will aim to elucidate the mechanism underpinning the determination of *B. bacteriovorus* vibroid cell shape and address the question of whether vibroid morphology is important to the predatory lifestyle.

13. Appendix

Table 3. Primers used in this study

Primer name	Description	Primer sequence (5'-3')
1402_RTPCR_F	*bd1402* RT-PCR primers	ATGTCCACTCGGGAAGTGAC
1402_RTPCR_R		AACCGGAGTTGTTGCTGAAC
1075_RTPCR_F	*bd1075* RT-PCR primers	ACAACGATCAGTTGCTGGTG
1075_RTPCR_R		AAGTGTCACCGGACTTGAGG
dnaK_RTPCR_F	*dnaK* RT-PCR primers	TGAGGACGAGATCAAACGTG
dnaK_RTPCR_R		AAACCAGGTTGTCGAGGTTG
1402_up_F	*bd1402* Gibson Assembly primers	CGTTGTAAAACGACGGCCAGTGCCATTCAGGGACAAGAAAAGG
1402_up_R		AGCATGCCGATGATGACACGAGGTGTTCGTC
1402_down_F		ACACCTCGTGTCATCATCGGCATGCTTAAGG
1402_down_R		GGAAACAGCTATGACCATGATTACGGGTGTTACGTCCGATTCC
1402_mCh_up_R		CCTTGCTCACCATCTTGGCAAAGGCGTAAATC
1402_mCh_F		CGCCTTTGCCAAGATGGTGAGCAAGGGCGAG
1402_mCh_R		TGTGATCAAGTAATTACTTGTACAGCTCGTCCATG
1402_mCh_dn_F		GCTGTACAAGTAATTACTTGATCACAGGCTTTG
1075_up_F	*bd1075* Gibson Assembly primers	CGTTGTAAAACGACGGCCAGTGCCAGACCATCGGAACCGCGTG
1075_up_R		CTAGTTTATTGCGTCTCATAAATACTATTATGCCCGAATAGGAC
1075_down_F		AGTATTTATGAGACGCAATAAACTAGGCTGTAAAG
1075_down_R		GGAAACAGCTATGACCATGATTACGAGCCAAGTTGGTTTTGTATTC
1075_mCh_up_R		CCTTGCTCACCATTTGCGTTTTCTGGGAAGAGG
1075_mCh_F		CCAGAAAACGCAAATGGTGAGCAAGGGCGAG
1075_mCh_R		TTTACAGCCTAGTTTACTTGTACAGCTCGTCCATG
1075_mCh_dn_F		GCTGTACAAGTAAACTAGGCTGTAAAGGCAAAAAAAAAG
pK18_F		AACTGTTGGGAAGGGCGAT

pK18_R	pK18*mobsacB* suicide construct sequencing primers	GACTGGAAAGCGGGCAGT
1402_S1_F	*bd1402* screening/sequencing primers	CCGCACCAAGGTTGTAACTG
1402_S1_R		TCGTTGGCTCGCATGTAAAG
1402_S2_F		AAACCAGTTGACCCGTTCA
1402_S2_R		AGGCCACTTTAATCCGGACA
1075_S1_F	*bd1075* screening/sequencing primers	GGTGATGCCGTTTTCATGGA
1075_S1_R		AGTGAAAACGCAATGAAAGGGA
1075_S2_F		GCAGATGTCTCTTGTGCTTCA
1075_S2_R		CGGTGGTTTTGCTGAAGACA

Table 4. Plasmids used in this study		
Plasmid	**Description**	**Source**
pK18*mobsacB*	Suicide vector into which all four inserts were cloned (kan^R, *lacZα*, *sacB*)	Schäfer *et al.*, (1994)
pAKF56	Plasmid template containing *mCherry* gene	Fenton *et al.*, (2010b)
p*Δbd1402*	Derivative of pK18*mobsacB* containing *bd1402* upstream and downstream regions to generate an in-frame deletion of *bd1402*	This study
p*bd1402-mCherry*	Derivative of pK18*mobsacB* containing *bd1402* upstream region, *bd1402* gene, *mCherry* gene and *bd1402* downstream region to generate a *bd1402-mCherry* fusion	This study
p*Δbd1075*	Derivative of pK18*mobsacB* containing *bd1075* upstream and downstream regions to generate an in-frame deletion of *bd1075*	This study
p*bd1075-mCherry*	Derivative of pK18*mobsacB* containing *bd1075* upstream region, *bd1075* gene, *mCherry* gene and *bd1075* downstream region to generate a *bd1075-mCherry* fusion	This study

Table 5. Strains used in this study

Strain	Description	Source
E. coli DH5α	*E. coli* cloning strain (F- endA1 hsdR17 (rk –mk –) supE44 thi-1 recA1 gyrA (Nalr) relA1 Δ(laclZYA-argF) U169 deoR (80dlacΔ(lacZ)M15))	Simon *et al.*, (1983)
E. coli S17-1	*E. coli* strain for conjugation of plasmids into *B. bacteriovorus* HD100 (thi, pro, hsdR– , hsdM+ , recA; integrated plasmid RP4- Tc::Mu-Kn::Tn7)	Hanahan, (1983)
E. coli S17-1:pZMR100	S17-1 strain containing the plasmid pZMR100 (kan^R) to confer kanamycin resistance to prey	Rogers *et al.*, (1986)
B. bacteriovorus HD100	*B. bacteriovorus* Type strain, genome sequenced, wild-type	Rendulic *et al.*, (2004)
B. bacteriovorus HD100 Δ*bd1402*	*B. bacteriovorus* HD100 containing an in-frame deletion of *bd1402*	This study
B. bacteriovorus HI Δ*bd1402*	*B. bacteriovorus* HI strain containing an in-frame deletion of *bd1402* derived from the HD100 Δ*bd1402* strain	This study
B. bacteriovorus HD100 *bd1402-mCherry*	*B. bacteriovorus* HD100 containing a *bd1402-mCherry* fusion	This study
B. bacteriovorus HI *bd1402-mCherry*	*B. bacteriovorus* HI strain containing a *bd1402-mCherry* fusion derived from the HD100 *bd1402-mCherry* strain	This study
B. bacteriovorus HD100 Δ*bd1075*	*B. bacteriovorus* HD100 containing an in-frame deletion of *bd1075*	This study
B. bacteriovorus HI Δ*bd1075*	*B. bacteriovorus* HI strain containing an in-frame deletion of *bd1075* derived from the HD100 Δ*bd1075* strain	This study
B. bacteriovorus HD100 *bd1075-mCherry*	*B. bacteriovorus* HD100 containing a *bd1075-mCherry* fusion	This study
B. bacteriovorus HI *bd1075-mCherry*	*B. bacteriovorus* HI strain containing a *bd1075-mCherry* fusion derived from the HD100 *bd1075-mCherry* strain	This study

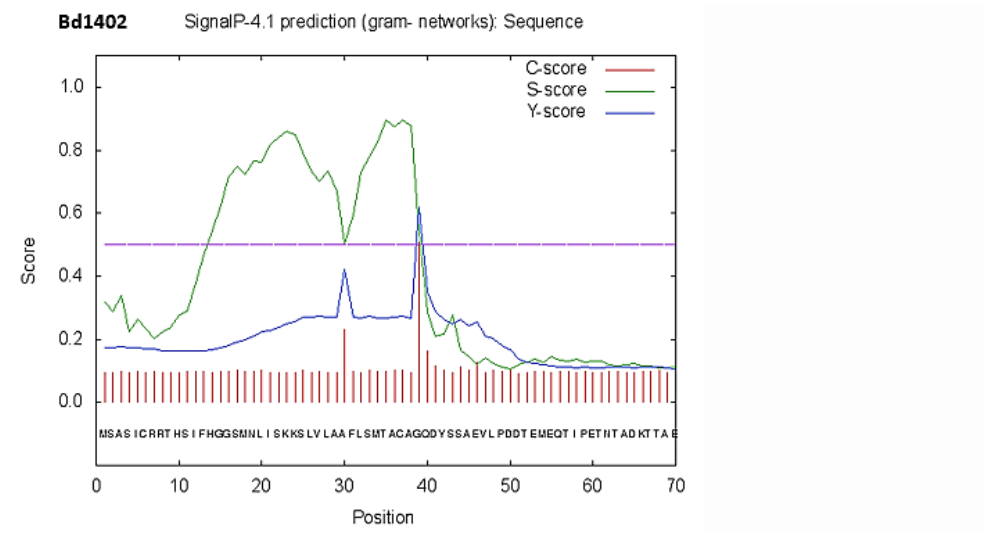


```
# Measure  Position  Value    Cutoff   signal peptide?
  max. C    39        0.506
  max. Y    39        0.619
  max. S    37        0.897
  mean S     1-38     0.594
       D     1-38     0.607   0.570    YES
Name=Sequence   SP='YES' Cleavage site between pos. 38 and 39: ACA-GQ D=0.607 D-cutoff=0.570 Networks=SignalP-noTM
```

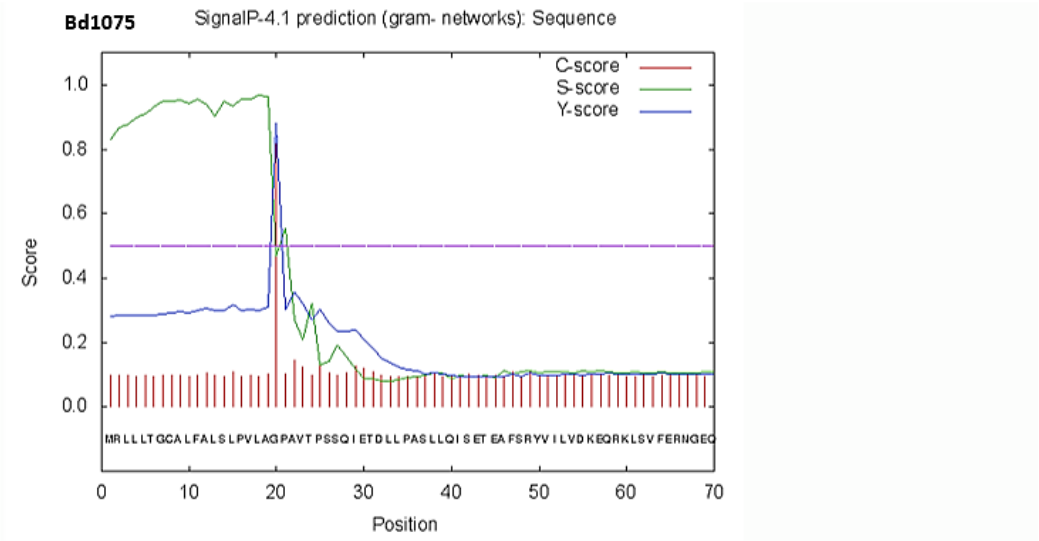


```
# Measure  Position  Value    Cutoff   signal peptide?
  max. C    20        0.817
  max. Y    20        0.880
  max. S    18        0.967
  mean S     1-19     0.928
       D     1-19     0.902   0.570    YES
Name=Sequence   SP='YES' Cleavage site between pos. 19 and 20: VLA-GP D=0.902 D-cutoff=0.570 Networks=SignalP-noTM
```

Figure 27. Signal peptide predictions for Bd1402 and Bd1075

Bd1402 and Bd1075 protein sequences were entered into the SignalP 4.1 online server (Petersen *et al.*, 2011) to predict the presence or absence of an N-terminal signal peptide. The outputs in the figure above show that both proteins contain signal peptides, suggesting that they are translocated across the cytoplasmic membrane.

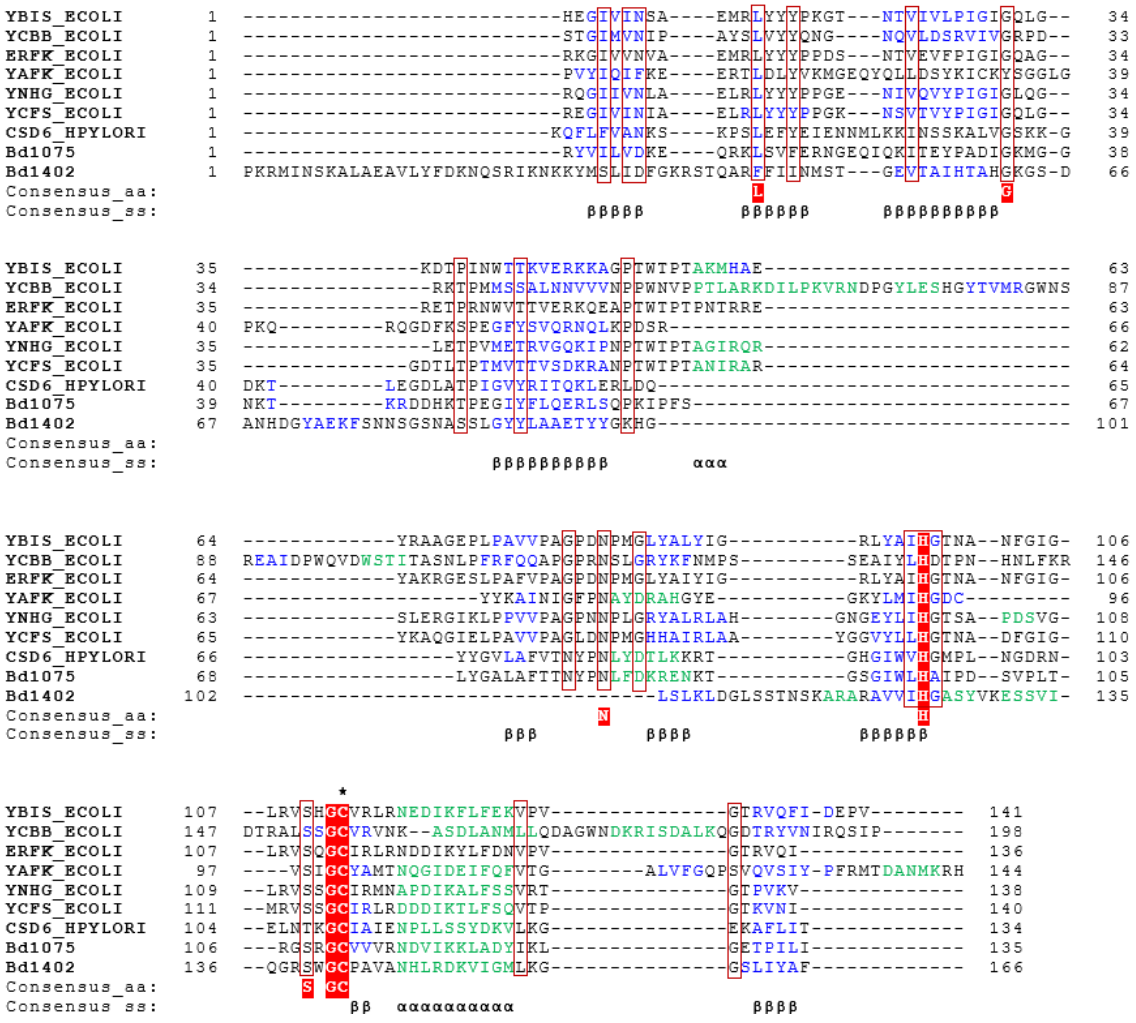

Figure 28. Sequence alignment of different L,D-transpeptidase domains

Sequence alignment of LDTP catalytic domains from the LDTP proteins of *E. coli* (YbiS, YcbB, ErfK, YafK, YnhG and YcfS), *H. pylori* (Csd6), and *B. bacteriovorus* (Bd1075 and Bd1402). Residues predicted to comprise β-strands and α-helices are depicted in blue or green, respectively. Consensus secondary structure (α: α-helix, β: β-strand) and consensus amino acid predictions are shown beneath the alignment. Strongly conserved residues are boxed in red and completely conserved residues are shown in white text on a red background. *: conserved catalytic cysteine residue. The sequence alignment was generated using PROMALS3D (Pei and Grishin, 2014).

CHAPTER 4: Discussion and conclusions

14. Discussion and future perspectives

This MRes thesis has concerned the possible exploitation of a predatory bacterium called *Bdellovibrio bacteriovorus* as a novel antimicrobial therapeutic. *B. bacteriovorus* can destroy a wide-range of Gram-negative bacteria including priority AMR pathogens such as carbapenemase-resistant *Klebsiella pneumoniae* both *in vitro* and *in vivo*. In contrast to most antimicrobials, simple genetic resistance to the *B. bacteriovorus* predator has not been observed in prey bacteria. Moreover, *B. bacteriovorus* is non-pathogenic in humans. Together, this evidence indicates that this bacterial predator has promising potential as a novel therapeutic to treat AMR infections. If *B. bacteriovorus* is to be implemented as a therapeutic in humans, then it is essential that we first improve our understanding of the mechanisms that underpin a predatory lifestyle. In this thesis, I have presented the results from two short rotation projects which focussed on envelope processes associated with bacterial predation.

14.1. First rotation project

The first rotation project at the University of Birmingham investigated the regulation of gliding motility which is important for *B. bacteriovorus* predation that occurs on surfaces, allowing scouting for prey and exit from the prey cell at the end of a predatory cycle. We hypothesised that regulation occurs via a c-di-GMP signalling mechanism that involves PilZ: GYF hybrid proteins and attempted to crystallise one of these hybrid proteins, Bd1996. Bd1996 from two different strains of *B. bacteriovorus* was successfully expressed and purified from *E. coli*. Bd1996 bound c-di-GMP *in vitro*, however a crystal structure could not be achieved within the time-frame of the project. Due to the difficulty of crystallising Bd1996, future approaches could consider the crystallisation of alternative PilZ: GYF proteins, although two of these (Bd3100 and Bd1482) have also shown resistance to crystallisation attempts. The project could also benefit from using protein-protein interaction techniques to identify Bd1996

binding partners and confirm whether the GYF domain interacts with components of the gliding motor. Construction of a *B. bacteriovorus* strain in which Bd1996 is fluorescently-tagged would allow the visualisation of Bd1996 cellular localisation at different time points during the predatory lifecycle. The additional incorporation of fluorescently-tagged gliding motor components (of a different colour) would facilitate the identification of any co-localisation between Bd1996 and the gliding motor complex.

14.2. Second rotation project

The second rotation project at the University of Nottingham focussed on the role of cell wall-modifying enzymes. Modification of predator and prey cell walls is important in predation and involves a plethora of different peptidoglycan-active (PG-active) enzymes. Proteins that modify the prey cell wall have been characterised previously (e.g. Bd3459, a DD-endo(carboxy)peptidase which causes rounding of prey peptidoglycan - and therefore the prey cell - into a spherical bdelloplast that contains the predator). Enzymes that modify the predator cell wall, however, had not previously been specifically identified, despite the strong likelihood that *B. bacteriovorus* modifies its own cell wall to aid physical entry into host cells and tolerate the osmotic differences that are encountered upon entry to and exit from prey.

In this project, I investigated the cellular locations and functions of two proteins: Bd1402, a predicted L,D-endopeptidase which breaks 3-3 cross-links between peptide chains, and Bd1075, a predicted L,D-carboxypeptidase which cleaves tetrapeptides to tripeptides, shortening peptide chains. Bd1402 appeared to be secreted into the periplasm of the prey, suggesting that it may modify the prey cell wall. No immediate predation phenotype was observed upon deletion of *bd1402* and the strain was still predatory upon *E. coli*, however, only limited phenotypic analysis could be achieved within the short time-frame of the project. Moreover, Bd1402 is phylogenetically grouped with 4 additional proteins within group 5 of L,D-transpeptidase family proteins (personal communications from Dr Lovering & Mr Graham) (Figure 13), therefore it is possible that these proteins act synergistically and that deleting a single member of the group is insufficient to generate a notable phenotype. Consequently, future work could consider the

construction of additional group 5 gene deletions within the genetic background of the *Δbd1402* mutant strain, which may result in a distinctive knockout phenotype.

In contrast to Bd1402, Bd1075 localised to the *B. bacteriovorus* predator itself and deletion of *bd1075* resulted in the formation of straight rod-shaped predator cells in comparison to vibroid wild-type cells. These observations mark Bd1075 as the first self-modifying PG-active enzyme and vibroid cell shape-determinant to be identified in *B. bacteriovorus.* Moreover, Bd1075 has demonstrated L,D-carboxypeptidase activity on peptidoglycan (personal communication from Dr Lovering) and therefore represents a hydrolytic PG-active enzyme which are of particular interest due to their antibacterial properties and potential as enzybiotics. We intend to conduct additional experiments to further characterise Bd1075 which will include (but not be limited to) complementation of the *bd1075* gene deletion, biochemical analysis of peptidoglycan sacculi to confirm the enzymatic activity of Bd1075, identification of Bd1075 interacting partners (which may include cytoskeletal elements), and the utilisation of super-resolution microscopy to improve the resolution of Bd1075 localisation. Cumulatively these experiments will allow this work to be completed for publication. This publication would be of interest to researchers working on antibacterial hydrolytic enzymes or bacterial cell wall architecture and morphology.

As a result of these MRes research projects, I have acquired new skills including protein bioinformatics, purification, and crystallography, molecular cloning, microscopy and the manipulation of a non-model predatory microorganism. I have also developed an awareness of the diversity of PG-active proteins which include bacterial damaging enzymes that could be explored as enzybiotic antibacterial agents.

14.3. Future perspectives for the PhD

The initial stages of the PhD will involve the completion and publishing of the Bd1075 project and we will then proceed to characterise the roles of additional *B. bacteriovorus* PG-active enzymes (which may act on predator or prey) within the predation process. If *B. bacteriovorus* is to be used as a therapeutic, then it is important to be able to aid the immunological clearance of the predator following treatment. An underexplored DNA bacteriophage specific for *B. bacteriovorus* could be used for this purpose. Phage replicate within bacteria and then use their encoded PG-active enzymes to lyse and escape from bacterial cells.

• Our laboratory has studied one DNA phage of *B. bacteriovorus* thus far (Mr Maximilian Harris, MRes student), however there is much more work to be completed in this area.

• We will also attempt to isolate ssRNA phage of *B. bacteriovorus*. In other bacteria, RNA phage bind to pili and retraction of the pilus facilities the uptake of the phage nucleic acid into the cell. Each ssRNA phage of other bacteria contains a single and specific PG-active enzyme that enables lysis of the host cell.

• It would therefore be interesting to identify PG-active enzymes from ssRNA phage of *B. bacteriovorus* as the lytic enzyme alone could facilitate the termination of *B. bacteriovorus* following treatment of infection. We will also use molecular and microscopic tools to study predators (phage) inside a predator (*B. bacteriovorus*) inside bacterial prey, as the characterisation of this intricate tripartite system has not yet been attempted.

• Bacterial infections have been successfully treated with either *B. bacteriovorus* or bacteriophages, however these have only been administered as individual therapeutics. We will therefore examine the efficacy of administering *B. bacteriovorus* and phages specific to the targeted pathogen as a combinatorial therapy, both *in vitro* and potentially *in vivo* using a zebrafish infection model.

15. Concluding remarks

Antimicrobial resistance is a large and complex global issue, the tackling of which will require the implementation of multiple combative strategies such as the improvement of antibiotic stewardship to prevent the overuse and misuse of antibiotics and the development of new antimicrobials. One promising novel antimicrobial is *Bdellovibrio bacteriovorus*, a predatory bacterium that destroys Gram-negative bacteria yet is reported to exist non-pathogenically within humans. The two research projects contained within this thesis have described investigations into the predatory envelope processes of gliding motility and cell wall-modification. In the first project, I investigated the c-di-GMP-mediated regulation of gliding motility in *B. bacteriovorus* via the biochemical characterisation of the c-di-GMP receptor protein Bd1996. In the second project, I characterised the roles of the *B. bacteriovorus* peptidoglycan-active enzymes Bd1402 and Bd1075. This study revealed Bd1075 as the first cell shape-determinant to be identified in *B. bacteriovorus* HD100, in which Bd1075 generates cell curvature. Future work will aim to elucidate the mechanism by which Bd1075 confers a vibroid shape and assess the importance of *B. bacteriovorus* vibroid morphology within the context of predatory interaction and invasion. *B. bacteriovorus* holds great potential as a novel antimicrobial, however, the development of *B. bacteriovorus* as a successful therapeutic requires a deeper understanding of the complex mechanisms that underpin the predation process. Together, these MRes research projects have provided new insights into the unique predatory lifestyle of this fascinating bacterium.

16. References

Abraham, E. P. and Chain, E. (1940) An enzyme from bacteria able to destroy penicillin., *Nature*, 146 (3713), pp. 837–837.

Achaeogen. (2018). *Achaogen launches ZEMDRI™ (plazomicin), a once-daily aminoglycoside for use in complicated urinary tract infections (cUTI).* [online] Available at: http://investors.achaogen.com/node/10231/pdf [Accessed: 2/7/18].

Aldred, K. J., Kerns, R. J. and Osheroff, N. (2014) Mechanism of quinolone action and resistance., *Biochemistry*, 53 (10), pp. 1565–1574.

Amikam, D. and Galperin, M. Y. (2006) PilZ domain is part of the bacterial c-di-GMP binding protein., *Bioinformatics*, 22 (1), pp. 3–6.

Arzanlou, M., Chai, W. C. and Venter, H. (2017) Intrinsic, adaptive and acquired antimicrobial resistance in Gram-negative bacteria., *Essays in Biochemistry*, 61 (1), pp. 49–59.

Asakura, H., Churin, Y., Bauer, B., Boettcher, J. P., Bartfeld, S., Hashii, N., *et al.* (2010) *Helicobacter pylori* HP0518 affects flagellin glycosylation to alter bacterial motility., *Molecular Microbiology*, 78 (5), pp. 1130–1144.

Atterbury, R. J., Hobley, L., Till, R., Lambert, C., Capeness, M. J., Lerner, T. R., *et al.* (2011) Effects of orally administered *Bdellovibrio bacteriovorus* on the well-being and *Salmonella* colonization of young chicks., *Applied and Environmental Microbiology*, 77 (16), pp. 5794–5803. DOI:10.1128/AEM.00426-11.

Ausmees, N., Kuhn, J. R. and Jacobs-Wagner, C. (2003) The bacterial cytoskeleton: an intermediate filament-like function in cell shape., *Cell*, 115 (6), pp. 705–713.

Balaji, S. and Aravind, L. (2007) The RAGNYA fold: a novel fold with multiple topological variants found in functionally diverse nucleic acid, nucleotide and peptide-binding proteins., *Nucleic Acids Research*, 35 (17), pp. 5658–5671.

Barlow, M. (2009) What antimicrobial resistance has taught us about horizontal gene transfer., *Methods in Molecular Biology*, 532, pp. 397–411. DOI:10.1007/978-1-60327-853-9_23.

Barnett, T. C., Lim, J. Y., Soderholm, A. T., Rivera-Hernandez, T., West, N. P. and Walker, M. J. (2015) Host-pathogen interaction during bacterial vaccination., *Current Opinion in Immunology*, 36, pp. 1–7.

Barreteau, H., Kovac, A., Boniface, A., Sova, M., Gobec, S. and Blanot, D. (2008) Cytoplasmic steps of peptidoglycan biosynthesis., *FEMS Microbiology Reviews*, 32 (2), pp. 168–207. DOI:10.1111/j.1574-6976.2008.00104.x.

Bartlett, T. M., Bratton, B. P., Duvshani, A., Miguel, A., Sheng, Y., Martin, N. R., *et al.* (2017) A periplasmic polymer curves *Vibrio cholerae* and promotes pathogenesis., *Cell*, 168 (1-2), pp. 172–185.

Benach, J., Swaminathan, S. S., Tamayo, R., Handelman, S. K., Folta-Stogniew, E., Ramos, J. E., *et al.* (2007) The structural basis of cyclic diguanylate signal transduction by PilZ domains., *The EMBO Journal*, 26 (24), pp. 5153–5166.

Bertsche, U., Breukink, E., Kast, T. and Vollmer, W. (2005) *In vitro* murein peptidoglycan synthesis by dimers of the bifunctional transglycosylase-transpeptidase PBP1B from *Escherichia coli*., *The Journal of Biological Chemistry*, 280 (45), pp. 38096–38101.

Blair, J. M. A., Webber, M. A., Baylay, A. J., Ogbolu, D. O. and Piddock, L. J. V. (2015) Molecular mechanisms of antibiotic resistance., *Nature Reviews Microbiology*, 13 (1), pp. 42–51.

Bobrov, A. G., Kirillina, O. and Perry, R. D. (2005) The phosphodiesterase activity of the HmsP EAL domain is required for negative regulation of biofilm formation in *Yersinia pestis*., *FEMS Microbiology Letters*, 247 (2), pp. 123–130. DOI:10.1016/j.femsle.2005.04.036.

Boehm, A., Kaiser, M., Li, H., Spangler, C., Kasper, C. A., Ackermann, M., *et al.* (2010) Second messenger-mediated adjustment of bacterial swimming velocity., *Cell*, 141 (1), pp. 107–116.

Boileau, M. J., Mani, R., Breshears, M. A., Gilmour, M., Taylor, J. D. and Clinkenbeard, K. D. (2016) Efficacy of *Bdellovibrio bacteriovorus* 109J for the treatment of dairy calves with experimentally induced infectious bovine keratoconjunctivitis., *American Journal of Veterinary Research*, 77 (9), pp. 1017–1028.

Borges-Walmsley, M. I., McKeegan, K. S. and Walmsley, A. R. (2003) Structure and function of efflux pumps that confer resistance to drugs., *The Biochemical Journal*, 376 (2), pp. 313–338.

Bourne, C. R. (2014) Utility of the biosynthetic folate pathway for targets in antimicrobial discovery., *Antibiotics*, 3 (1), pp. 1–28. DOI:10.3390/antibiotics3010001.

Brammer Basta, L. A., Ghosh, A., Pan, Y., Jakoncic, J., Lloyd, E. P., Townsend, C. A., *et al.* (2015) Loss of a functionally and structurally distinct

L,D-transpeptidase, LdtMt5, compromises cell wall integrity in *Mycobacterium tuberculosis*., *The Journal of Biological Chemistry*, 290 (42), pp. 25670–25685.

Braun, V. (1975) Covalent lipoprotein from the outer membrane of *Escherichia coli.*, *Biochimica et Biophysica Acta*, 415 (3), pp. 335–377.

Brueggemann, A. B., Pai, R., Crook, D. W. and Beall, B. (2007) Vaccine escape recombinants emerge after pneumococcal vaccination in the United States., *PLoS Pathogens*, 3 (11), pp. e168. DOI:10.1371/journal.ppat.0030168.

Bush, K (2012) Antimicrobial agents targeting bacterial cell walls and cell membranes., *Revue Scientifique et Technique (International Office of Epizootics)*, 31 (1), pp. 43–56. DOI:10.20506/rst.31.1.2096.

Bush, K and Bradford, P. A. (2016) β-lactams and β-lactamase inhibitors: an overview., *Cold Spring Harbor Perspectives in Medicine*, 6 (8), pp. a025247 DOI:10.1101/cshperspect.a025247.

Cabeen, M. T., Charbon, G., Vollmer, W., Born, P., Ausmees, N., Weibel, D. B., *et al.* (2009) Bacterial cell curvature through mechanical control of cell growth., *The EMBO Journal*, 28 (9), pp. 1208–1219.

Campbell, T. (2018). *A mixed-bag decision causes Achaogen's 24% tumble.* [online] Available at: https://www.fool.com/investing/2018/06/26/a-mixed-bag-decision-causes-achaogens-24-tumble.aspx [Accessed 2/7/18].

Capeness, M. J., Lambert, C., Lovering, A. L., Till, R., Uchida, K., Chaudhuri, R., *et al.* (2013) Activity of *Bdellovibrio* hit locus proteins, Bd0108 and Bd0109, links type IVa pilus extrusion/retraction status to prey-independent growth signalling., *Plos One*, 8 (11), pp. e79759. DOI:10.1371/journal.pone.0079759.

Cegelski, L., Marshall, G. R., Eldridge, G. R. and Hultgren, S. J. (2008) The biology and future prospects of antivirulence therapies., *Nature Reviews Microbiology*, 6 (1), pp. 17–27.

Center for Innovative Phage Applications and Therapeutics. (2018). *Who we are* [online] Available at: https://medschool.ucsd.edu/som/medicine/divisions/idgph/research/center-innovative-phage-applications-and-therapeutics/about/Pages/default.aspx [Accessed 3/7/18].

Centers for Disease Control and Prevention. (2013). *Antibiotic resistance threats in the United States, 2013* [online] Available at: https://www.cdc.gov/drugresistance/pdf/ar-threats-2013-508.pdf [Accessed 3/7/18].

Chan, C., Paul, R., Samoray, D., Amiot, N. C., Giese, B., Jenal, U., *et al.* (2004) Structural basis of activity and allosteric control of diguanylate cyclase., *Proceedings of the National Academy of Sciences of the United States of America*, 101 (49), pp. 17084–17089.

Chanyi, R. M. and Koval, S. F. (2014) Role of type IV pili in predation by *Bdellovibrio bacteriovorus*., *Plos One*, 9 (11), pp. e113404. DOI:10.1371/journal.pone.0113404.

Chaudhuri, R. R. and Pallen, M. J. (2006) xBASE, a collection of online databases for bacterial comparative genomics., *Nucleic Acids Research*, 34 (Suppl 1), pp. D335–7.

Christen, B., Christen, M., Paul, R., Schmid, F., Folcher, M., Jenoe, P., *et al.* (2006) Allosteric control of cyclic di-GMP signaling., *The Journal of Biological Chemistry*, 281 (42), pp. 32015–32024.

Chu, W. H. and Zhu, W. (2010) Isolation of *Bdellovibrio* as biological therapeutic agents used for the treatment of *Aeromonas hydrophila* infection in fish., *Zoonoses and Public Health*, 57 (4), pp. 258–264.

Cianfanelli, F. R., Monlezun, L. and Coulthurst, S. J. (2016) Aim, load, fire: the type VI secretion system, a bacterial nanoweapon., *Trends in Microbiology*, 24 (1), pp. 51–62.

Cisek, A. A., Dąbrowska, I., Gregorczyk, K. P. and Wyżewski, Z. (2017) Phage therapy in bacterial infections treatment: one hundred years after the discovery of bacteriophages., *Current Microbiology*, 74 (2), pp. 277–283.

Collin, F., Karkare, S. and Maxwell, A. (2011) Exploiting bacterial DNA gyrase as a drug target: current state and perspectives., *Applied Microbiology and Biotechnology*, 92 (3), pp. 479–497.

Connell, S. R., Tracz, D. M., Nierhaus, K. H. and Taylor, D. E. (2003) Ribosomal protection proteins and their mechanism of tetracycline resistance., *Antimicrobial Agents and Chemotherapy*, 47 (12), pp. 3675–3681. DOI: 10.1128/AAC.47.12.3675-3681.2003.

Cotter, T. W. and Thomashow, M. F. (1992) Identification of a *Bdellovibrio* bacteriovorus genetic locus, hit, associated with the host-independent phenotype., *Journal of Bacteriology*, 174 (19), pp. 6018–6024. DOI: 10.1128/jb.174.19.6018-6024.1992.

Crooks, G. E., Hon, G., Chandonia, J. M. and Brenner, S. E. (2004) WebLogo: a sequence logo generator, *Genome Research*, 14 (6), pp. 1188–1190.

Cui, L., Mharakurwa, S., Ndiaye, D., Rathod, P. K. and Rosenthal, P. J. (2015) Antimalarial drug resistance: literature review and activities and findings of the

ICEMR network., *The American Journal of Tropical Medicine and Hygiene*, 93 (Suppl 3), pp. 57–68.

D'Herelle, F. (2007) On an invisible microbe antagonistic toward dysenteric bacilli: brief note by Mr. F. D'Herelle, presented by Mr. Roux. 1917., *Research in Microbiology*, 158 (7), pp. 553–554.

Desmarais, S. M., De Pedro, M. A., Cava, F. and Huang, K. C. (2013) Peptidoglycan at its peaks: how chromatographic analyses can reveal bacterial cell wall structure and assembly., *Molecular Microbiology*, 89 (1), pp. 1–13.

Di Tommaso, P., Moretti, S., Xenarios, I., Orobitg, M., Montanyola, A., Chang, J.-M., *et al.* (2011) T-Coffee: a web server for the multiple sequence alignment of protein and RNA sequences using structural information and homology extension., *Nucleic Acids Research*, 39 (Suppl 2), pp. W13–7.

Divakaruni, A. V., Baida, C., White, C. L. and Gober, J. W. (2007) The cell shape proteins MreB and MreC control cell morphogenesis by positioning cell wall synthetic complexes., *Molecular Microbiology*, 66 (1), pp. 174–188.

Dönhöfer, A., Franckenberg, S., Wickles, S., Berninghausen, O., Beckmann, R. and Wilson, D. N. (2012) Structural basis for TetM-mediated tetracycline resistance., *Proceedings of the National Academy of Sciences of the United States of America*, 109 (42), pp. 16900–16905.

Dow, J. M., Fouhy, Y., Lucey, J. F. and Ryan, R. P. (2006) The HD-GYP domain, cyclic di-GMP signaling, and bacterial virulence to plants., *Molecular Plant-Microbe Interactions*, 19 (12), pp. 1378–1384.

Ducret, A., Valignat, M.-P., Mouhamar, F., Mignot, T. and Theodoly, O. (2012) Wet-surface-enhanced ellipsometric contrast microscopy identifies slime as a major adhesion factor during bacterial surface motility., *Proceedings of the National Academy of Sciences of the United States of America*, 109 (25), pp. 10036–10041.

Ducret, A., Quardokus, E. M. and Brun, Y. V. (2016) MicrobeJ, a tool for high throughput bacterial cell detection and quantitative analysis., *Nature Microbiology*, 1 (7), pp. 16077. DOI:10.1038/nmicrobiol.2016.77.

Duerig, A., Abel, S., Folcher, M., Nicollier, M., Schwede, T., Amiot, N., *et al.* (2009) Second messenger-mediated spatiotemporal control of protein degradation regulates bacterial cell cycle progression., *Genes & Development*, 23 (1), pp. 93–104.

European Commission. (2005). *Ban on antibiotics as growth promoters in animal feed enters into effect* [online] Available at: http://europa.eu/rapid/press-release_IP-05-1687_en.htm [Accessed 5/7/18].

Evans, K. J., Lambert, C. and Sockett, R. E. (2007) Predation by *Bdellovibrio bacteriovorus* HD100 requires type IV pili., *Journal of Bacteriology*, 189 (13), pp. 4850–4859. DOI:10.1128/JB.01942-06.

Fenton, A. K., Lambert, C., Wagstaff, P. C. and Sockett, R. E. (2010a) Manipulating each MreB of *Bdellovibrio bacteriovorus* gives diverse morphological and predatory phenotypes., *Journal of Bacteriology*, 192 (5), pp. 1299–1311. DOI:10.1128/JB.01157-09.

Fenton, A. K., Kanna, M., Woods, R. D., Aizawa, S. I. and Sockett, R. E. (2010b) Shadowing the actions of a predator: backlit fluorescent microscopy reveals synchronous nonbinary septation of predatory *Bdellovibrio* inside prey and exit through discrete bdelloplast pores., *Journal of Bacteriology*, 192 (24), pp. 6329–6335. DOI:10.1128/JB.00914-10.

Fenton, A. K., Hobley, L., Butan, C., Subramaniam, S. and Sockett, R. E. (2010c) A coiled-coil-repeat protein “Ccrp” in *Bdellovibrio bacteriovorus* prevents cellular indentation, but is not essential for vibroid cell morphology., *FEMS Microbiology Letters*, 313 (2), pp. 89–95. DOI:10.1111/j.1574-6968.2010.02125.x.

Food and Drug Administration. (2013). *New animal drugs and new animal drug combination products administered in or on medicated feed or drinking water of food producing animals: recommendations for drug sponsors for voluntarily aligning product use conditions with GFI #209* [online] Available at: https://www.fda.gov/downloads/AnimalVeterinary/GuidanceComplianceEnforcement/GuidanceforIndustry/UCM299624.pdf [Accessed: 4/7/18].

Food and Drug Administration. (2015). *Summary report on antimicrobials sold or distributed for use in food-producing animals* [online] Available at: https://www.fda.gov/downloads/forindustry/userfees/animaldruguserfeeactadufa/ucm534243.pdf [Accessed 4/7/18].

Frirdich, E., Biboy, J., Adams, C., Lee, J., Ellermeier, J., Gielda, L. D., *et al.* (2012) Peptidoglycan-modifying enzyme Pgp1 is required for helical cell shape and pathogenicity traits in *Campylobacter jejuni.*, *PLoS Pathogens*, 8 (3), pp. e1002602. DOI:10.1371/journal.ppat.1002602.

Frirdich, E., Vermeulen, J., Biboy, J., Soares, F., Taveirne, M. E., Johnson, J. G., *et al.* (2014) Peptidoglycan LD-carboxypeptidase Pgp2 influences *Campylobacter jejuni* helical cell shape and pathogenic properties and provides the substrate for the DL-carboxypeptidase Pgp1., *The Journal of Biological Chemistry*, 289 (12), pp. 8007–8018.

Gay, P., Le Coq, D., Steinmetz, M., Ferrari, E. and Hoch, J. A. (1983) Cloning structural gene *sacB*, which codes for exoenzyme levansucrase of *Bacillus subtilis*: expression of the gene in *Escherichia coli.*, *Journal of Bacteriology*, 153 (3), pp. 1424–1431. Available at: https://www.ncbi.nlm.nih.gov/pmc/articles/PMC221793/pdf/jbacter00250-0310.pdf.

Gibson, D. G., Young, L., Chuang, R.-Y., Venter, J. C., Hutchison, C. A. and Smith, H. O. (2009) Enzymatic assembly of DNA molecules up to several hundred kilobases., *Nature Methods*, 6 (5), pp. 343–345.

Gullberg, E. (2014) *Resistance mechanisms* [online] Available at: https://www.reactgroup.org/toolbox/understand/antibiotic-resistance/resistance-mechanisms-in-bacteria/ [Accessed: 2/7/18].

Hall, B. G. and Barlow, M. (2004) Evolution of the serine beta-lactamases: past, present and future., *Drug Resistance Updates*, 7 (2), pp. 111–123.

Hanahan, D. (1983) Studies on transformation of *Escherichia coli* with plasmids., *Journal of Molecular Biology*, 166 (4), pp. 557–580.

Heilmann, K. P., Rice, C. L., Miller, A. L., Miller, N. J., Beekmann, S. E., Pfaller, M. A., *et al.* (2005) Decreasing prevalence of beta-lactamase production among respiratory tract isolates of *Haemophilus influenzae* in the United States., *Antimicrobial Agents and Chemotherapy*, 49 (6), pp. 2561–2564. DOI:10.1128/AAC.49.6.2561-2564.2005.

Hengge, R. (2009) Principles of c-di-GMP signalling in bacteria., *Nature Reviews Microbiology*, 7 (4), pp. 263–273.

Hespell, R. B., Miozzari, G. F. and Rittenberg, S. C. (1975) Ribonucleic acid destruction and synthesis during intraperiplasmic growth of *Bdellovibrio bacteriovorus*., *Journal of Bacteriology*, 123 (2), pp. 481–491. Available at: https://jb.asm.org/content/jb/123/2/481.full.pdf.

Hoban, D. and Felmingham, D. (2002) The PROTEKT surveillance study: antimicrobial susceptibility of *Haemophilus influenzae* and *Moraxella catarrhalis* from community-acquired respiratory tract infections., *The Journal of Antimicrobial Chemotherapy*, 50 (Suppl 2), pp. 49–59.

Hobley, L., Fung, R. K. Y., Lambert, C., Harris, M. A. T. S., Dabhi, J. M., King, S. S., *et al.* (2012a) Discrete cyclic di-GMP-dependent control of bacterial predation versus axenic growth in *Bdellovibrio bacteriovorus*., *PLoS Pathogens*, 8 (2), pp. e1002493. DOI:10.1371/journal.ppat.1002493.

Hobley, L., Lerner, T. R., Williams, L. E., Lambert, C., Till, R., Milner, D. S., *et al.* (2012b) Genome analysis of a simultaneously predatory and prey-

independent, novel *Bdellovibrio bacteriovorus* from the River Tiber, supports *in silico* predictions of both ancient and recent lateral gene transfer from diverse bacteria., *BMC Genomics*, 13, pp. 670. DOI:10.1186/1471-2164-13-670.

Hyman, P. and Abedon, S. T. (2010) Bacteriophage host range and bacterial resistance., *Advances in Applied Microbiology*, 70, pp. 217–248. DOI:10.1016/S0065-2164(10)70007-1.

Ikeda, M., Wachi, M., Jung, H. K., Ishino, F. and Matsuhashi, M. (1991) The *Escherichia coli mraY* gene encoding UDP-N-acetylmuramoyl-pentapeptide: undecaprenyl-phosphate phospho-N-acetylmuramoyl-pentapeptide transferase., *Journal of Bacteriology*, 173 (3), pp. 1021–1026. DOI: 10.1128/jb.173.3.1021-1026.1991

Jansen, K. U., Knirsch, C. and Anderson, A. S. (2018) The role of vaccines in preventing bacterial antimicrobial resistance., *Nature Medicine*, 24 (1), pp. 10–19.

Jones, L. J. F., Carballido-López, R. and Errington, J. (2001) Control of cell shape in bacteria, *Cell*, 104 (6), pp. 913–922.

Kamath, V. and Pai, A. (2013) Enzybiotics- a review, *International Journal of Pharmacological Research*, 3 (4), pp.69-71. DOI:10.7439/ijpr.v3i4.56

Karunker, I., Rotem, O., Dori-Bachash, M., Jurkevitch, E. and Sorek, R. (2013) A global transcriptional switch between the attack and growth forms of *Bdellovibrio bacteriovorus*., *Plos One*, 8 (4), pp. e61850. DOI:10.1371/journal.pone.0061850.

Kim, H. S., Im, H. N., An, D. R., Yoon, J. Y., Jang, J. Y., Mobashery, S., *et al.* (2015) The cell shape-determining Csd6 protein from *Helicobacter pylori* constitutes a new family of L,D-carboxypeptidase., *The Journal of Biological Chemistry*, 290 (41), pp. 25103–25117.

Kruse, T., Bork-Jensen, J. and Gerdes, K. (2005) The morphogenetic MreBCD proteins of *Escherichia coli* form an essential membrane-bound complex., *Molecular Microbiology*, 55 (1), pp. 78–89.

Kumar, A. and Schweizer, H. P. (2005) Bacterial resistance to antibiotics: active efflux and reduced uptake., *Advanced Drug Delivery Reviews*, 57 (10), pp. 1486–1513.

Kumar, S., Stecher, G. and Tamura, K. (2016) MEGA7: molecular evolutionary genetics analysis version 7.0 for bigger datasets., *Molecular Biology and Evolution*, 33 (7), pp. 1870–1874.

Kuru, E., Lambert, C., Rittichier, J., Till, R., Ducret, A., Derouaux, A., *et al.* (2017) Fluorescent D-amino-acids reveal bi-cellular cell wall modifications

important for *Bdellovibrio bacteriovorus* predation., *Nature Microbiology*, 2 (12), pp. 1648–1657. DOI:10.1038/s41564-017-0029-y.

Lambert, C., Evans, K. J., Till, R., Hobley, L., Capeness, M., Rendulic, S., *et al.* (2006) Characterizing the flagellar filament and the role of motility in bacterial prey-penetration by *Bdellovibrio bacteriovorus*., *Molecular Microbiology*, 60 (2), pp. 274–286.

Lambert, C., Chang, C.Y., Capeness, M. J. and Sockett, R. E. (2010) The first bite-profiling the predatosome in the bacterial pathogen *Bdellovibrio*., *Plos One*, 5 (1), pp. e8599. DOI:10.1371/journal.pone.0008599.

Lambert, C., Fenton, A. K., Hobley, L. and Sockett, R. E. (2011) Predatory *Bdellovibrio* bacteria use gliding motility to scout for prey on surfaces., *Journal of Bacteriology*, 193 (12), pp. 3139–3141. DOI:10.1128/JB.00224-11.

Lambert, C., Lerner, T. R., Bui, N. K., Somers, H., Aizawa, S.-I., Liddell, S., *et al.* (2016) Interrupting peptidoglycan deacetylation during *Bdellovibrio* predator-prey interaction prevents ultimate destruction of prey wall, liberating bacterial-ghosts., *Scientific Reports*, 6, pp. 26010. DOI:10.1038/srep26010.

Lee, T. K. and Huang, K. C. (2013) The role of hydrolases in bacterial cell-wall growth., *Current Opinion in Microbiology*, 16 (6), pp. 760–766.

Lerner, T. R., Lovering, A. L., Bui, N. K., Uchida, K., Aizawa, S., Vollmer, W., *et al.* (2012) Specialized peptidoglycan hydrolases sculpt the intra-bacterial niche of predatory *Bdellovibrio* and increase population fitness., *PLoS Pathogens*, 8 (2), pp. e1002524. DOI:10.1371/journal.ppat.1002524.

Lobanovska, M. and Pilla, G. (2017) Penicillin's discovery and antibiotic resistance: lessons for the future?, *The Yale Journal of Biology and Medicine*, 90 (1), pp. 135–145. Available at: https://www.ncbi.nlm.nih.gov/pmc/articles/PMC5369031/pdf/yjbm_90_1_135.pdf.

Łusiak-Szelachowska, M., Zaczek, M., Weber-Dąbrowska, B., Międzybrodzki, R., Kłak, M., Fortuna, W., *et al.* (2014) Phage neutralization by sera of patients receiving phage therapy., *Viral Immunology*, 27 (6), pp. 295–304. DOI:10.1089/vim.2013.0128.

Madigan, M. T., Martinko, J. M., Bender, K. S., Buckley, D. H. and Stahl, D. A. (2015) *Brock Biology of Microorganisms*. 14th ed. Boston: Pearson.

Magnet, S., Bellais, S., Dubost, L., Fourgeaud, M., Mainardi, J.-L., Petit-Frère, S., *et al.* (2007) Identification of the L,D-transpeptidases responsible for attachment of the Braun lipoprotein to *Escherichia coli* peptidoglycan., *Journal of Bacteriology*, 189 (10), pp. 3927–3931. DOI:10.1128/JB.00084-07.

Magnet, S., Dubost, L., Marie, A., Arthur, M. and Gutmann, L. (2008) Identification of the L,D-transpeptidases for peptidoglycan cross-linking in *Escherichia coli.*, *Journal of Bacteriology*, 190 (13), pp. 4782–4785. DOI:10.1128/JB.00025-08.

Mahmoud, K. K. and Koval, S. F. (2010) Characterization of type IV pili in the life cycle of the predator bacterium *Bdellovibrio*., *Microbiology*, 156 (Pt 4), pp. 1040–1051. DOI:10.1099/mic.0.036137-0.

Mainardi, J. L., Legrand, R., Arthur, M., Schoot, B., van Heijenoort, J. and Gutmann, L. (2000) Novel mechanism of beta-lactam resistance due to bypass of DD-transpeptidation in *Enterococcus faecium*., *The Journal of Biological Chemistry*, 275 (22), pp. 16490–16496.

Mainardi, J.-L., Fourgeaud, M., Hugonnet, J.-E., Dubost, L., Brouard, J.-P., Ouazzani, J., *et al.* (2005) A novel peptidoglycan cross-linking enzyme for a beta-lactam-resistant transpeptidation pathway., *The Journal of Biological Chemistry*, 280 (46), pp. 38146–38152.

Matin, A. and Rittenberg, S. C. (1972) Kinetics of deoxyribonucleic acid destruction and synthesis during growth of *Bdellovibrio bacteriovorus* strain 109D on *Pseudomonas putida* and *Escherichia coli.*, *Journal of Bacteriology*, 111 (3), pp. 664–673. Available at: https://jb.asm.org/content/jb/111/3/664.full.pdf.

McBride, M. J. (2001) Bacterial gliding motility: multiple mechanisms for cell movement over surfaces., *Annual Review of Microbiology*, 55, pp. 49–75.

Medina, A. A., Shanks, R. M. and Kadouri, D. E. (2008) Development of a novel system for isolating genes involved in predator-prey interactions using host independent derivatives of *Bdellovibrio bacteriovorus* 109J., *BMC Microbiology*, 8, pp. 33. DOI:10.1186/1471-2180-8-33.

Mohammadi, T., Karczmarek, A., Crouvoisier, M., Bouhss, A., Mengin-Lecreulx, D. and den Blaauwen, T. (2007) The essential peptidoglycan glycosyltransferase MurG forms a complex with proteins involved in lateral envelope growth as well as with proteins involved in cell division in *Escherichia coli.*, *Molecular Microbiology*, 65 (4), pp. 1106–1121.

Morgan, D. J., Okeke, I. N., Laxminarayan, R., Perencevich, E. N. and Weisenberg, S. (2011) Non-prescription antimicrobial use worldwide: a systematic review., *The Lancet Infectious Diseases*, 11 (9), pp. 692–701.

Moscoso, J. A., Mikkelsen, H., Heeb, S., Williams, P. and Filloux, A. (2011) The *Pseudomonas aeruginosa* sensor RetS switches type III and type VI secretion via c-di-GMP signalling., *Environmental Microbiology*, 13 (12), pp. 3128–3138.

Munita, J. M. and Arias, C. A. (2016) Mechanisms of antibiotic resistance., *Microbiology Spectrum*, 4 (2). DOI:10.1128/microbiolspec.VMBF-0016-2015.

Nan, B., Mauriello, E. M. F., Sun, I.-H., Wong, A. and Zusman, D. R. (2010) A multi-protein complex from *Myxococcus xanthus* required for bacterial gliding motility., *Molecular Microbiology*, 76 (6), pp. 1539–1554.

Nan, B., Chen, J., Neu, J. C., Berry, R. M., Oster, G. and Zusman, D. R. (2011) Myxobacteria gliding motility requires cytoskeleton rotation powered by proton motive force., *Proceedings of the National Academy of Sciences of the United States of America*, 108 (6), pp. 2498–2503.

Ozawa, S., Clark, S., Portnoy, A., Grewal, S., Stack, M. L., Sinha, A., *et al.* (2017) Estimated economic impact of vaccinations in 73 low- and middle-income countries, 2001-2020., *Bulletin of the World Health Organization*, 95 (9), pp. 629–638.

Paterson, D. L. and Bonomo, R. A. (2005) Extended-spectrum beta-lactamases: a clinical update., *Clinical Microbiology Reviews*, 18 (4), pp. 657–686. DOI:10.1128/CMR.18.4.657-686.2005.

Paul, R., Weiser, S., Amiot, N. C., Chan, C., Schirmer, T., Giese, B., *et al.* (2004) Cell cycle-dependent dynamic localization of a bacterial response regulator with a novel di-guanylate cyclase output domain., *Genes & Development*, 18 (6), pp. 715–727.

Pechère, J. C. (2001) Patients' interviews and misuse of antibiotics., *Clinical Infectious Diseases*, 33 (Suppl 3), pp. S170–3.

Pei, J. and Grishin, N. V. (2014) PROMALS3D: multiple protein sequence alignment enhanced with evolutionary and three-dimensional structural information., *Methods in Molecular Biology*, 1079, pp. 263–271. DOI:10.1007/978-1-62703-646-7_17.

Petersen, T. N., Brunak, S., von Heijne, G. and Nielsen, H. (2011) SignalP 4.0: discriminating signal peptides from transmembrane regions., *Nature Methods*, 8 (10), pp. 785–786.

Piddock, L. J. V. (2006) Multidrug-resistance efflux pumps - not just for resistance., *Nature Reviews Microbiology*, 4 (8), pp. 629–636.

Poehlsgaard, J. and Douthwaite, S. (2005) The bacterial ribosome as a target for antibiotics., *Nature Reviews Microbiology*, 3 (11), pp. 870–881.

Pogue, C. B., Zhou, T. and Nan, B. (2017) PlpA, a PilZ-like protein, regulates directed motility of the bacterium *Myxococcus xanthus.*, *Molecular Microbiology*, 107 (2), pp. 214-228.

Poole, K. (2007) Efflux pumps as antimicrobial resistance mechanisms., *Annals of Medicine*, 39 (3), pp. 162–176.

Power, E. (2006) Impact of antibiotic restrictions: the pharmaceutical perspective., *Clinical Microbiology and Infection*, 12 (Suppl 5), pp. 25–34.

Queenan, A. M. and Bush, K. (2007) Carbapenemases: the versatile beta-lactamases., *Clinical Microbiology Reviews*, 20 (3), pp. 440–58. DOI:10.1128/CMR.00001-07.

Quinn, J. P., Dudek, E. J., DiVincenzo, C. A., Lucks, D. A. and Lerner, S. A. (1986) Emergence of resistance to imipenem during therapy for *Pseudomonas aeruginosa* infections., *The Journal of Infectious Diseases*, 154 (2), pp. 289–294.

Rasko, D. A. and Sperandio, V. (2010) Anti-virulence strategies to combat bacteria-mediated disease., *Nature Reviews Drug Discovery*, 9 (2), pp. 117–128.

Rendulic, S., Jagtap, P., Rosinus, A., Eppinger, M., Baar, C., Lanz, C., *et al.* (2004) A predator unmasked: life cycle of *Bdellovibrio bacteriovorus* from a genomic perspective., *Science*, 303 (5658), pp. 689–692.

Reyrat, J. M., Pelicic, V., Gicquel, B. and Rappuoli, R. (1998) Counterselectable markers: untapped tools for bacterial genetics and pathogenesis., *Infection and Immunity*, 66 (9), pp. 4011–4017. Available at: https://www.ncbi.nlm.nih.gov/pmc/articles/PMC108478/pdf/ii004011.pdf.

Rice, L. (2008) Federal funding for the study of antimicrobial resistance in nosocomial pathogens: no ESKAPE, *The Journal of Infectious Diseases*, 197 (8), pp. 1079–1081.

Rittenberg, S. C. and Shilo, M. (1970) Early host damage in the infection cycle of *Bdellovibrio bacteriovorus.*, *Journal of Bacteriology*, 102 (1), pp. 149–160. Available at: https://jb.asm.org/content/jb/102/1/149.full.pdf.

Roberts, M. C. (2005) Update on acquired tetracycline resistance genes., *FEMS Microbiology Letters*, 245 (2), pp. 195–203. DOI:10.1016/j.femsle.2005.02.034.

Rodríguez-Rubio, L., Gerstmans, H., Thorpe, S., Mesnage, S., Lavigne, R. and Briers, Y. (2016) DUF3380 Domain from a *Salmonella* phage endolysin shows potent N-acetylmuramidase activity., *Applied and Environmental Microbiology*, 82 (16), pp. 4975–4981. DOI:10.1128/AEM.00446-16.

Rogers, M., Ekaterinaki, N., Nimmo, E. and Sherratt, D. (1986) Analysis of Tn7 transposition., *Molecular and General Genetics,* 205 (3), pp. 550–556.

Römling, U., Galperin, M. Y. and Gomelsky, M. (2013) Cyclic di-GMP: the first 25 years of a universal bacterial second messenger., *Microbiology and Molecular Biology Reviews*, 77 (1), pp. 1–52. DOI:10.1128/MMBR.00043-12.

Rotem, O., Nesper, J., Borovok, I., Gorovits, R., Kolot, M., Pasternak, Z., *et al.* (2016) An extended cyclic di-GMP network in the predatory bacterium *Bdellovibrio bacteriovorus*., *Journal of Bacteriology*, 198 (1), pp. 127–137. DOI:10.1128/JB.00422-15.

Ruby, E. G., McCabe, J. B. and Barke, J. I. (1985) Uptake of intact nucleoside monophosphates by *Bdellovibrio bacteriovorus* 109J., *Journal of Bacteriology*, 163 (3), pp. 1087–1094. Available at: https://jb.asm.org/content/jb/163/3/1087.full.pdf.

Russell, A. B., Peterson, S. B. and Mougous, J. D. (2014) Type VI secretion system effectors: poisons with a purpose., *Nature Reviews Microbiology*, 12 (2), pp. 137–148.

Salmond, G. P. C. and Fineran, P. C. (2015) A century of the phage: past, present and future., *Nature Reviews Microbiology*, 13 (12), pp. 777–786.

Sanchez-Pescador, R., Brown, J. T., Roberts, M. and Urdea, M. S. (1988) Homology of the TetM with translational elongation factors: implications for potential modes of *tetM*-conferred tetracycline resistance., *Nucleic Acids Research*, 16 (3), pp. 1218.

Sanders, A. N. and Pavelka, M. S. (2013) Phenotypic analysis of *Eschericia coli* mutants lacking L,D-transpeptidases., *Microbiology*, 159 (Pt 9), pp. 1842–1852. DOI:10.1099/mic.0.069211-0.

Schäfer, A., Tauch, A., Jäger, W., Kalinowski, J., Thierbach, G. and Pühler, A. (1994) Small mobilizable multi-purpose cloning vectors derived from the *Escherichia coli* plasmids pK18 and pK19: selection of defined deletions in the chromosome of *Corynebacterium glutamicum*., *Gene*, 145 (1), pp. 69–73.

Schindelin, J., Arganda-Carreras, I., Frise, E., Kaynig, V., Longair, M., Pietzsch, T., *et al.* (2012) Fiji: an open-source platform for biological-image analysis., *Nature Methods*, 9 (7), pp. 676–682.

Schooley, R. T., Biswas, B., Gill, J. J., Hernandez-Morales, A., Lancaster, J., Lessor, L., *et al.* (2017) Development and use of personalized bacteriophage-based therapeutic cocktails to treat a patient with a disseminated resistant *Acinetobacter baumannii* infection., *Antimicrobial Agents and Chemotherapy*, 61 (10), e00954-17. DOI:10.1128/AAC.00954-17.

Schwarz, U., Asmus, A. and Frank, H. (1969) Autolytic enzymes and cell division of *Escherichia coli*, *Journal of Molecular Biology*, 41 (3), pp. 419–429.

Schwudke, D., Linscheid, M., Strauch, E., Appel, B., Zahringer, U., Moll, H., *et al.* (2003) The obligate predatory *Bdellovibrio bacteriovorus* possesses a neutral lipid A containing alpha-D-mannoses that replace phosphate residues: similarities and differences between the lipid As and the lipopolysaccharides of the wild type strain *B. bacteriovorus* HD100 and its host-independent derivative HI100., *The Journal of Biological Chemistry*, 278 (30), pp. 27502–27512.

Seidler, R. J. and Starr, M. P. (1969) Isolation and characterization of host-independent *Bdellovibrios*., *Journal of Bacteriology*, 100 (2), pp. 769–785. Available at: https://www.ncbi.nlm.nih.gov/pmc/articles/PMC250157/pdf/jbacter00385-0249.pdf.

Sham, L.-T., Butler, E. K., Lebar, M. D., Kahne, D., Bernhardt, T. G. and Ruiz, N. (2014) MurJ is the flippase of lipid-linked precursors for peptidoglycan biogenesis., *Science*, 345 (6193), pp. 220–222.

Shatzkes, K., Chae, R., Tang, C., Ramirez, G. C., Mukherjee, S., Tsenova, L., *et al.* (2015) Examining the safety of respiratory and intravenous inoculation of *Bdellovibrio bacteriovorus* and *Micavibrio aeruginosavorus* in a mouse model., *Scientific Reports*, 5, pp. 12899. DOI:10.1038/srep12899.

Shatzkes, K., Singleton, E., Tang, C., Zuena, M., Shukla, S., Gupta, S., *et al.* (2016) Predatory bacteria attenuate *Klebsiella pneumoniae* burden in rat lungs., *mBio*, 7 (6), pp. e01847-16. DOI:10.1128/mBio.01847-16.

Shilo, M. (1969) Morphological and physiological aspects of the interaction of *Bdellovibrio* with host bacteria., *Current Topics in Microbiology and Immunology*, 50, pp. 174–204. Available at: https://link.springer.com/chapter/10.1007/978-3-642-46169-9_6.

Silhavy, T. J., Kahne, D. and Walker, S. (2010) The bacterial cell envelope., *Cold Spring Harbor Perspectives in Biology*, 2 (5), pp. a000414. DOI:10.1101/cshperspect.a000414.

Simm, R., Morr, M., Kader, A., Nimtz, M. and Römling, U. (2004) GGDEF and EAL domains inversely regulate cyclic di-GMP levels and transition from sessility to motility., *Molecular Microbiology*, 53 (4), pp. 1123–1134.

Simon, R., Priefer, U. and Pühler, A. (1983) A broad host range mobilization system for *in vivo* genetic engineering: transposon mutagenesis in Gram negative bacteria, *Nature Biotechnology*, 1 (9), pp. 784–791.

Skotnicka, D., Petters, T., Heering, J., Hoppert, M., Kaever, V. and Søgaard-Andersen, L. (2015) Cyclic di-GMP regulates type IV pilus-dependent motility

in *Myxococcus xanthus*., *Journal of Bacteriology*, 198 (1), pp. 77–90. DOI:10.1128/JB.00281-15.

Smith, R. and Coast, J. (2013) The true cost of antimicrobial resistance., *BMJ*, 346, pp. f1493.

Sockett, R. E. (2009) Predatory lifestyle of *Bdellovibrio bacteriovorus*., *Annual Review of Microbiology*, 63, pp. 523–539.

Sonnhammer, E. L., Eddy, S. R. and Durbin, R. (1997) Pfam: a comprehensive database of protein domain families based on seed alignments., *Proteins*: *Structure, Function, and Bioinformatics*, 28 (3), pp. 405–420.

Spidlova, P., Stojkova, P., Dankova, V., Senitkova, I., Santic, M., Pinkas, D., *et al.* (2018) *Francisella tularensis* D-Ala D-Ala carboxypeptidase DacD is involved in intracellular replication and it is necessary for bacterial cell wall integrity., *Frontiers in Cellular and Infection Microbiology*, 8, pp. 111. DOI:10.3389/fcimb.2018.00111.

Steinmetz, M., Le Coq, D., Djemia, H. B. and Gay, P. (1983) Analyse génétique de *sacB*, gène de structure d'une enzyme secrétée, la lévane-saccharase de *Bacillus subtilis* Marburg, *Molecular and General Genetics*, 191 (1), pp. 138–144.

Stolp, H. and Starr, M. P. (1963) *Bdellovibrio bacteriovorus* gen. et sp. n., a predatory, ectoparasitic, and bacteriolytic microorganism., *Antonie Van Leeuwenhoek*, 29 (1), pp. 217–248.

Strasfeld, L. and Chou, S. (2010) Antiviral drug resistance: mechanisms and clinical implications., *Infectious Disease Clinics of North America*, 24 (2), pp. 413–437.

Summers, W. C. (1999) *Felix d'Herelle and the origins of molecular biology.* 1st ed. New Haven: Yale University Press.

Summers, W. C. (2012) The strange history of phage therapy., *Bacteriophage*, 2 (2), pp. 130–133.

Sun, J., Deng, Z. and Yan, A. (2014) Bacterial multidrug efflux pumps: mechanisms, physiology and pharmacological exploitations., *Biochemical and Biophysical Research Communications*, 453 (2), pp. 254–267.

Sycuro, L. K., Pincus, Z., Gutierrez, K. D., Biboy, J., Stern, C. A., Vollmer, W., *et al.* (2010) Peptidoglycan crosslinking relaxation promotes *Helicobacter pylori*'s helical shape and stomach colonization., *Cell*, 141 (5), pp. 822–833.

Sycuro, L. K., Wyckoff, T. J., Biboy, J., Born, P., Pincus, Z., Vollmer, W., *et al.* (2012) Multiple peptidoglycan modification networks modulate *Helicobacter pylori's* cell shape, motility, and colonization potential., *PLoS Pathogens*, 8 (3), pp. e1002603. DOI:10.1371/journal.ppat.1002603.

Sycuro, L. K., Rule, C. S., Petersen, T. W., Wyckoff, T. J., Sessler, T., Nagarkar, D. B., *et al.* (2013) Flow cytometry-based enrichment for cell shape mutants identifies multiple genes that influence *Helicobacter pylori* morphology., *Molecular Microbiology*, 90 (4), pp. 869–883.

Taylor, A. J. (2013) The role of Bd3100 in *Bdellovibrio bacteriovorus*. *University of Nottingham undergraduate project report.*

The Business Times. (2018). *Superbugs win another round as Big Pharma exits antibiotics* [online] Available at: https://www.businesstimes.com.sg/companies-markets/superbugs-win-another-round-as-big-pharma-exits-antibiotics [Accessed 6/7/18].

The World Health Organisation. (2017a). *Global priority list of antibiotic-resistant bacteria to guide research, discovery, and development of new antibiotics* [online] Available at: https://www.who.int/medicines/publications/WHO-PPL-Short_Summary_25Feb-ET_NM_WHO.pdf?ua=1 [Accessed: 8/7/18].

The World Health Organisation (2017b) *Global tuberculosis report* [online] Available at: http://www.who.int/tb/publications/global_report/gtbr2017_main_text.pdf [Accessed 8/7/18].

Tomasz, A. and Munoz, R. (1995) Beta-lactam antibiotic resistance in Gram-positive bacterial pathogens of the upper respiratory tract: a brief overview of mechanisms., *Microbial Drug Resistance*, 1 (2), pp. 103–109. DOI:10.1089/mdr.1995.1.103.

Totsika, M. (2016) Benefits and challenges of antivirulence antimicrobials at the dawn of the post-antibiotic era, *Drug Delivery Letters*, 6 (1), pp. 30–37.

Twort, F. W. (1915) An investigation on the nature of ultra-microscopic viruses., *The Lancet*, 186 (4814), pp. 1241–1243.

Typas, A., Banzhaf, M., Gross, C. A. and Vollmer, W. (2012) From the regulation of peptidoglycan synthesis to bacterial growth and morphology., *Nature Reviews Microbiology*, 10 (2), pp. 123–136.

Van Boeckel, T. P., Brower, C., Gilbert, M., Grenfell, B. T., Levin, S. A., Robinson, T. P., *et al.* (2015) Global trends in antimicrobial use in food

animals., *Proceedings of the National Academy of Sciences of the United States of America*, 112 (18), pp. 5649–5654.

van den Ent, F., Johnson, C. M., Persons, L., de Boer, P. and Löwe, J. (2010) Bacterial actin MreB assembles in complex with cell shape protein RodZ., *The EMBO Journal*, 29 (6), pp. 1081–1090.

van Teeffelen, S., Wang, S., Furchtgott, L., Huang, K. C., Wingreen, N. S., Shaevitz, J. W., *et al.* (2011) The bacterial actin MreB rotates, and rotation depends on cell-wall assembly., *Proceedings of the National Academy of Sciences of the United States of America*, 108 (38), pp. 15822–15827.

Ventola, C. L. (2015) The antibiotic resistance crisis: part 1: causes and threats., *Pharmacy and Therapeutics,* 40 (4), pp. 277–283.

Vollmer, W., Blanot, D. and de Pedro, M. A. (2008) Peptidoglycan structure and architecture., *FEMS Microbiology Reviews*, 32 (2), pp. 149–167. DOI:10.1111/j.1574-6976.2007.00094.x.

Waksman, S. A. (1947) What is an antibiotic or an antibiotic substance? *Mycologia*, 39 (5), pp. 565–569.

Wang, I. N., Smith, D. L. and Young, R. (2000) Holins: the protein clocks of bacteriophage infections., *Annual Review of Microbiology*, 54, pp. 799–825.

Wegener, H. C. (2003) Antibiotics in animal feed and their role in resistance development, *Current Opinion in Microbiology*, 6 (5), pp. 439–445.

Wiederhold, N. P. (2017) Antifungal resistance: current trends and future strategies to combat., *Infection and Drug Resistance*, 10, pp. 249–259. DOI:10.2147/IDR.S124918.

Wielders, C. L. C., Fluit, A. C., Brisse, S., Verhoef, J. and Schmitz, F. J. (2002) *mecA* gene is widely disseminated in *Staphylococcus aureus* population., *Journal of Clinical Microbiology*, 40 (11), pp. 3970–3975. DOI:10.1128/JCM.40.11.3970-3975.2002.

Willis, A. R., Moore, C., Mazon-Moya, M., Krokowski, S., Lambert, C., Till, R., *et al.* (2016) Injections of predatory bacteria work alongside host immune cells to treat *Shigella* infection in zebrafish larvae., *Current Biology*, 26 (24), pp. 3343–3351.

Young, K. D. (2006) The selective value of bacterial shape., *Microbiology and Molecular Biology Reviews*, 70 (3), pp. 660–703. DOI:10.1128/MMBR.00001-06.

Young, K. D. (2007) Bacterial morphology: why have different shapes?, *Current Opinion in Microbiology*, 10 (6), pp. 596–600.

Zhang, Y. (2008) I-TASSER server for protein 3D structure prediction., *BMC Bioinformatics*, 9 (40). DOI:10.1186/1471-2105-9-40.